UNCLASSIFIED

Contract No. AT(30-1)-1432

Report No. NYO 6013

# ELECTROCHEMISTRY OF MOLTEN SALTS

by

Earl H. Roland

G. M. Pound



Period Covered:

June 1, 1954 to June 1, 1956

Metals Research Laboratory
Carnegie Institute of Technology
Pittsburgh, Pennsylvania

June 1, 1956

UNCLASSIFIED

## DISCLAIMER

Report No. NYO 6013

DISTRIBUTION LIST

No Standard Distribution

Copies on request to Carnegie Institute of Technology

Total Distribution 30 Copies

ABSTRACT

A new back-emf method for measuring the thermodynamic emf of molten salt cells of the type $M/MCl_2$ in molten salt solvent/$Cl_2$ is presented. Decomposition potentials are measured in the course of the thermodynamic emf determination. The systems $PbCl_2$ - $ZrCl_2$, LiCl - KCl eutectic, LiCl - KCl - $NdCl_3$, $MgCl_2$ in LiCl - KCl and NaCl, $SnCl_2$, KCl, and $PbCl_2$ and $ZnCl_2$ in LiCl - KCl eutectic. The thermodynamic emf's obtained by the back-emf method are in good agreement with values calculated from independent thermochemical data. Thus Raoult's law is thought to apply in these simple systems to within a factor of two in the activity coefficient.

TABLE OF CONTENTS

## LIST OF TABLES

LIST OF FIGURES

## HISTORICAL INTRODUCTION

In recent years there has been much interest in molten salt electrolysis as a method for winning metals from there compounds. Perhaps the two best known examples are the production of Al from fluoride melts containing $Al_2O_3$ and the electrowinning of Mg from molten $MgCl_2$.

Prior to the early 1790's the only source of current for experimental investigation was the electrophorous machine which delivered small currents at large potentials. Of course, such a source of current is not useful in electrolytic measurements. In 1791 Galvani introduced a better source of current, and this was the beginning of the science of electrochemistry. Volta (1792) showed that an electric current flowed between two different metals when placed in an electrolytic solution. Electrolytic cells of this type are termed galvanic cells. Volta also introduced an electromotive series of the metals, where the metal higher in the series would cause a positive current to flow in the electrolyte when coupled to a metal lower in the series. Ritter (1798) showed experimentally that Volta's series was the same as that of the ability of one metal to displace another from solution.

Prior to 1800 the potentials of the cells used were limited to approximately 1 volt and polarization effects prevented the deposition of many metals from aqueous solutions. At this time Volta's pile was introduced and higher potentials were now available to the experimenter. Nicholson and Carlisle (1800), for the first time, decomposed water into $H_2$ and $O_2$. Ritter recognized that at one electrode an oxidizing reaction was proceeding and a reduction at the other. In 1808 Davy prepared Na by electrolysis of molten NaOH.

Ohm's law and Faraday's law resulted from the study of the physical

laws governing the flow of current in the electrolyte and the external metallic circuit and the relation between the electric and chemical phenomena. Faraday's laws (1834) state that the quantity of material deposited is proportional to the current passed, and, for a constant amount of current passed, the quantity of material deposited is proportional to the equivalent weights of the metal deposited. At this same time it was shown that oxidation occurs at the anode and reduction at the cathode.

The galvanic cells used up to this time were very unstable (potential was not constant), and in 1836 the Daniell cell was introduced which gave a much more constant potential. Poggendorf (1841) introduced a comparison method (the fore-runner of the modern potentiometer) for accurate potential measurements, and in 1843 the Wheatstone bridge for resistance measurements came upon the scene.

Both Bunsen and Faraday produced Mg through the electrolysis of molten $MgCl_2$. Bunsen and St. Claire Deville in 1854 prepared Al by electrolysis of molten $NaCl-AlCl_3$ mixtures. In 1855 Matthiessen prepared Ca electrolytically and Bunsen and Matthiessen electrolyzed molten LiCl in order to prepare Li metal. Matthiessen (1886) prepared Na by the electrolysis of molten NaCl. Kohlrausch (1876) showed that salt conductivity is entirely ionic, and in 1887 the dissociation theory for salts in solution was introduced. Lebeau (1898) prepared Be by the electrolysis of Be salts of the alkali halides.

In recent years the list of metals produced by molten salt electrolysis has expanded rapidly. In the atomic energy field, uranium, zirconium, and hafnium have been produced electrolytically. In other fields boron, beryllium, titanium and many others have been produced by the electrolysis of molten salts.

Kortüm and Bockris[1], and Drossbach[2] have written excellent reviews on molten salt electrolysis. The electrolysis of molten salts differs markedly from that in aqueous solutions. The main differences lie in the high reactivity of the constituents, large solubilities of the metals in some of their molten salts and the high temperatures at which the reactions are occurring. The current yield is always low because the amount of metal deposited on the electrode is decreased due to the solubility of the metal in the molten salt phase and diffusion of this metal (in solution) to the anode where it combines with the evolved gas to reform the metal salt.

The current yield can be increased by preventing the solution and back-diffusion of the deposited metal. Cubicciotti[13] has shown that the metal solubility in the molten salt phase can be decreased by decreasing the temperature and by the addition of a second salt in which the metal is sparingly soluble. The back diffusion can be minimized by dividing the cell into electrode compartments by a porous diaphragm.

Single electrode potentials cannot be measured experimentally, only total cell potentials. The reversible single potentials in aqueous solutions have been evaluated by referring them to an arbitrary zero of potential for one of the electrodes (e.g., the hydrogen electrode, and the calomel electrode). This same approach has been attempted in molten salt cells and proven unsuccessful. In a Daniell cell of the type $M_A/M_ACl_2//M_BCl_2/M_B$, single electrode potentials can be approximated by giving to one of the electrodes an emf value of zero (e.g., $M_BCl_2/M_B$). However, the diffusion potential between solutions A and B cannot be readily evaluated and the resulting single electrode potentials measured in this way are not exactly additive.

The decomposition potential is defined as the minimum applied potential necessary for continuous electrodeposition and is evaluated by extrapolating the current-voltage relationships to zero current. The decomposition potential gives the actual applied potential necessary to make an electrolytic separation.

According to Kortüm and Bockris[1] for each value of electrolyzing current the applied voltage is comprised of the following potentials: -

$$E = E_A - E_B + \Sigma\eta + IR$$

where $E_A$ and $E_B$ are the two respective reversible single electrode potentials for the ions deposited, $\Sigma\eta$ is defined as the summation of the overpotentials, and IR is the potential drop through the solution due to the ohmic resistance. Thus it can be seen that the decomposition potential is dependent upon irreversible reactions and because of this has no very simple physical significance.

The term $\Sigma\eta$ contains three types of over-potentials which are activation over-potentials, concentration over-potential, and ohmic over-potential. The activation over-potential is related to the rate controlling reaction at the electrode and has the form $\eta = a + b \log i$ (the Tafel equation). The concentration over-potential is related to the concentration gradient of the reacting ions from the bulk of the solution to the electrode surface. The ohmic over-potential is caused by the potential drop through the electrolytic bath and any resistive films on the electrodes. The activation over-potential decays exponentially with time upon the removal of electrolysis current, ohmic over-potential disappears instantly, and the concentration over-potential decays slowly but follows no simple law[1].

If the over-potentials are zero, then the decomposition potential is the same as the thermodynamic potential, but in general, this is not the case. For aqueous solutions, the overvoltage decreases[1] rapidly with increasing temperature. In molten salts, the electrode reactions proceed rapidly at the elevated temperatures and the related over-voltages are usually small. The data on decomposition potentials and emf's of Daniell cells and cells of the type $M/MCl_2/Cl_2$ has been summarized by Kortüm and Bockris[1], Dresbach[2], and Conway[3].

The more promising electrolysis baths are mixtures of chlorides, fluorides containing the oxide of the metal to be deposited, or in some cases mixtures of the halides (e.g., chlorides and fluorides). The decomposition potentials of the alkali chlorides and fluorides are the largest known and these salts are very suitable for use as molten salt solvents in electrolysis cells.

Purpose of Present Work

Both the decomposition potential and the thermodynamic emf are of interest in planning an electrolytic separation or extraction operation It has been shown that the decomposition potential is the minimum applied potential necessary for continuous electrodeposition. The thermodynamic emf is a measure of reversible work and is given by the Gibbs free energy function $\Delta F$. Therefore the difference between the decomposition potential and the reversible cell potential measures the irreversible electrode phenomena, which is designated as over-potential.

The classical, reversible cell method has been used for measuring the thermodynamic emf for a number of molten salt cells of the type $M/MCl_2/Cl_2$[1]. This method has also been applied (unsuccessfully) to a number of other salts, chiefly salts of the more electropositive metals (results summarized in Kortüm and Bockris[1], and Conway[3]). In this

method it is difficult to ensure reversible electrodes, the measuring of potentials is time-consuming and tedious, and careful purification of the salt is necessary.

This study was designed to present a method by which the decomposition potential and the thermodynamic emf could be evaluated in one series of measurements. This new method, the back-emf method, has the advantages that the metal and gas electrodes are produced by electrodeposition, the molten salt is given a preliminary electrolytic purification step, and the experimental procedure is shorter in duration and experimentally less exacting. Also the decomposition potential is obtained in the course of the thermodynamic emf determination. Actually, it will be shown that in the present systems the decomposition potential should equal the thermodynamic cell emf. However, it will appear that the thermodynamic cell emf as obtained by the new back-emf method is a much more reliable value.

## DISCUSSION OF MEASURING METHODS

Thermodynamic emf's for cells of the type $M/MCl_2$ in solution/$Cl_2$ can be measured by two methods, the classical reversible cell method and the present back-emf method. Decomposition potentials are obtained in the course of the over-potential decay measurements. It will be shown that in the present systems the decomposition potential should equal the thermodynamic cell emf. However, it will appear that the back-emf method is more reliable for determination of thermodynamic cell emf.

The apparatus for the classical, reversible cell method consists of two reversible electrodes, a metal electrode and a gas (e.g., chlorine) electrode, immersed in the molten metal chloride. The scheme can be represented by the cell $M/MCl_2$ in solution/$Cl_2$ (graphite), where the cathode is the pure metal and the anode is a graphite rod with the gas bubbling over it. The resulting cell emf is measured by means of a potentiometer and, if the criteria of reversibility are met, gives the thermodynamic value.

The new back-emf method is closely related to the standard procedure for determining decomposition potential. Figure 1 is a schematic representation of the current-voltage relationship and the value for applied potential at zero electrolyzing current represents the experimental value for the decomposition potential. The significance of the decomposition potential has been discussed in the Introduction. The initial portion of the curve is due to the electrolysis of minor impurities and/or redox reactions. The linear steeply ascending portion is due to the electrolysis of the most readily electrolyzable solute. The slope of this portion of the curve is equal to the reciprocal of the cell resistance. Extrapolation

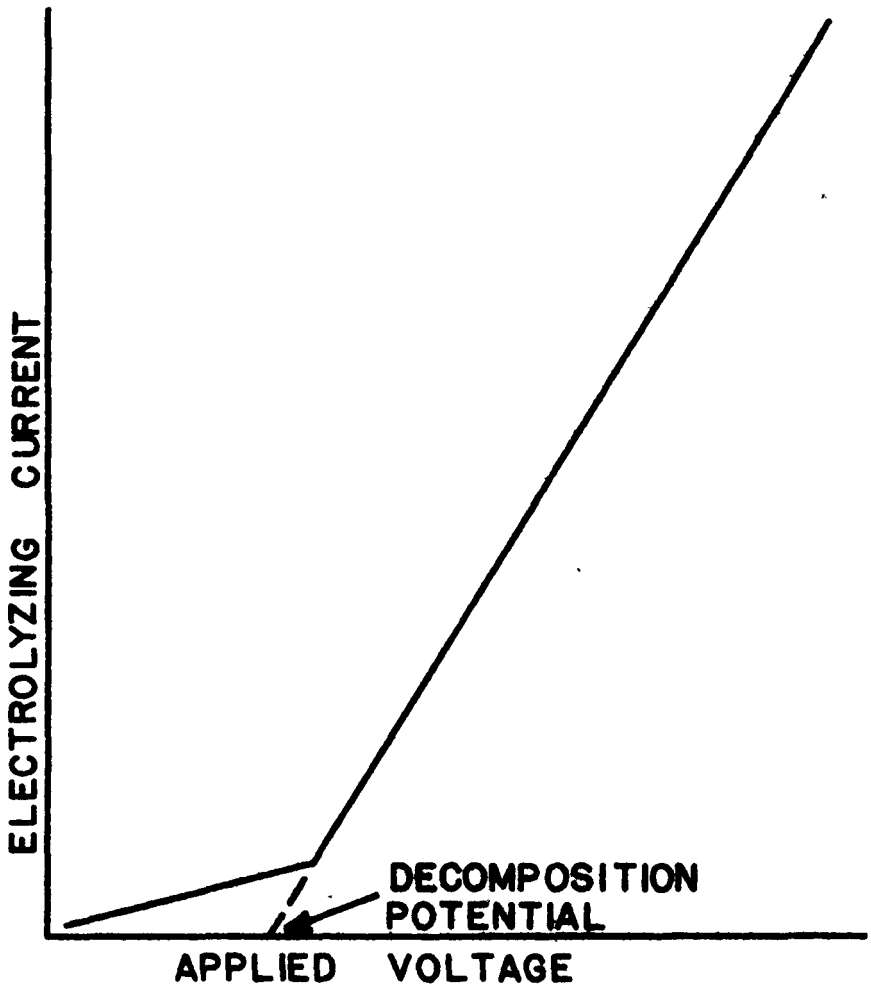


TYPICAL CURVE FOR ELECTROLYZING CURRENT VS APPLIED POTENTIAL

FIGURE 1

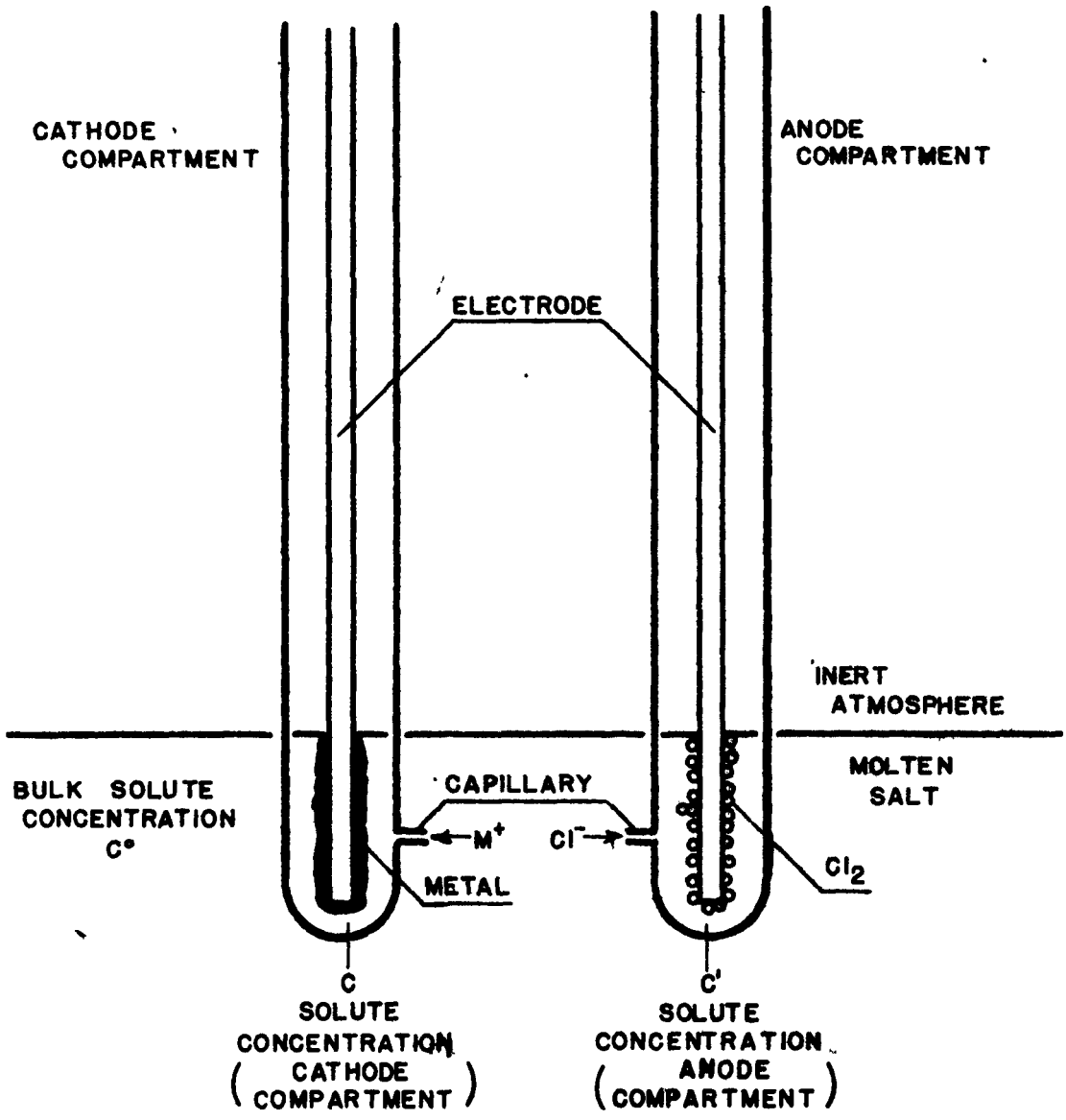


SCHEMATIC DIAGRAM OF ELECTROLYSIS IN A DIVIDED CELL

Figure 2

to zero current eliminates the IR drop and gives the applied potential that is just sufficient for electrolysis to begin, e.g., the decomposition potential. In the present systems, where it is demonstrated that the activation over-potential is linearly dependent on electrolyzing current, the decomposition potential should approximate to the thermodynamic cell emf.

During electrolysis, as material, metal on the cathode and chlorine on the anode, is deposited a cell of the type $M/MCl_2/Cl_2$ is produced. This cell exhibits a potential which opposes the applied voltage. As indicated in Figure 2, a schematic sketch of the electrolysis cell, the cell is comprised of three main portions:-

1) the anode compartment where the $Cl^-$ ion is consumed as chlorine is evolved.
2) the cathode compartment where the $M^{++}$ ion is depleted as the metal is deposited.

and 3) the connecting reservoir or middle compartment where the concentration of the solute remains essentially constant.

The electrode compartments are separated from the reservoir by a porous diaphragm or capillary. The entire system is blanketed with purified argon to prevent contamination of the melt by air or water vapor. The concentration of the solute salt in the electrode compartments is less than that in the reservoir, which remains at the initial concentration, due to ionic depletion during electrolysis.

First let us consider the relationship between cell potential and solute concentration in the electrode compartments. The cell potential is a function of the concentration of the solute in the electrode compartments which is related directly to the electrolyzing current or the

current density. For any point on the applied voltage-electrolyzing current curve (figure 1), the concentration of the solute in the electrode compartments is a steady-state value determined by the rate of depletion due to electrodeposition and rate of replenishment of the solute by diffusion from the reservoir into the electrode compartments.

The cell potential is related to the solute concentration by means of the equation:-

$$(1) \quad E = E^{o} - \frac{RT}{nF} \ln \frac{a_{M^{++}} \, a^{2}_{Cl^{-}}}{a_{M} \quad a_{Cl_2}}$$

where for the cell $M/MCl_2$ in solution/$Cl_2$ the electrode reactions are:-

$$M = M^{++} + 2e$$

and

$$Cl_2 + 2e = 2Cl^{-} \ ,$$

and the overall reaction is

$$M + Cl_2 = M^{++} + 2Cl^{-} \ .$$

$a_M = a_{Cl_2} = 1$ because both the metal and the chlorine are in their standard states of pure metal and pure chlorine gas at one atmosphere pressure. Also in the present systems where the anion is entirely chloride, it is convenient to take the standard state of the solute as the pure molten condition where the mole fraction of the anion that is chloride $C_{Cl^-} = 1$ and the mole fraction of the cation that is solute metal $C_{M^{++}} = 1$. In this standard state of both $M^{++}$ and $Cl^-$, $a_{M^{++}} = 1$ and $a_{Cl^-} = 1$ and the individual activity coefficients $\gamma_{M^{++}} = \gamma_{Cl^-} = 1$. In these systems $C_{Cl^-} = 1$ always, and the activity ratio in equation (1) becomes $Q = \gamma_{M^{++}} \cdot \gamma^{2}_{Cl^-} \cdot C_{M^{++}} = \gamma C_{M^{++}}$ in the instance of a bivalent solute cation.

Equation (1) can be written to give

$$(2) \quad E = E^{o} - \frac{RT}{nF} \ln \gamma - \frac{RT}{nF} \ln C_{M^{++}} \ .$$

At each electrolysis characterized by a specific value for the electrolyzing current I the solute concentration in an electrode compartment can be written, neglecting transference of solute, as

(3) $C_{M^{++}} = C_t = C_o - \underbrace{\frac{VIt}{nFv_c}}_{\text{material deposited}} + \underbrace{\frac{Jt}{v_c}}_{\text{material diffused into compartment from reservoir}}$

where $C_o$ = initial or reservoir concentration, mole fraction of cation that is solute cation, mole fraction of solute salt.

$t$ = time of electrolysis.

$v_c$ = volume of compartment, cc.

$V$ = volume in cc containing 1 mole of cations, molar volume of salt mixture.

$A$ = cross-sectional area of connecting capillary.

and $J$ = solute diffusion current through connecting capillary.

Actually, in the present systems where the anion is entirely chloride, there is no impoverishment of the anode compartment with respect to chloride ion concentration. Accordingly, the concentration in equation (13) refers to solute cation concentrations. Evaluating the diffusion term by applying Fick's law of diffusion.

(4) $J = -AD\frac{dc}{dx}$

to the electrolysis scheme pictured in figure 2, where x is the length of the connecting capillary.

(5) $J = AD\left[\frac{C_o - C_t}{x}\right]$

Accordingly equation (3) becomes

(6) $C_t = C_o - \frac{VIt}{nFv_c} + \frac{AD}{v_c}\left[\frac{C_o - C_t}{x}\right]$ ;

For steady state conditions, the concentration is invariant with time and

$$(7) \quad \left(\frac{dc}{dt}\right)_I = 0 = -\frac{VI}{nFv_c} + \frac{ADC_o}{xv_c} - \frac{AD}{xv_c} C_t$$

or

$$(8) \quad C_t = C_o - \frac{xV}{nFAD} I$$

Letting $\beta = \frac{xV}{nFAD}$ equation (8) becomes

$$(9) \quad C_t = C_o - \beta I$$

and placing this result into equation (2)

$$(10) \quad E_a = E^o - \frac{RT}{nF} \ln \gamma - \frac{RT}{nF} \ln (C_o - \beta I)$$

Applying Taylors expansion about I = 0 for the term $\ln (C_o - \beta I)$ it can be shown that

$$(11) \quad \ln (C_o - \beta I) = \ln C_o - \frac{\beta I}{C_o} - \frac{\beta^2 I^2}{C_o^2} ,$$

and neglecting terms having powers greater than 1 equation (10) becomes

$$(12) \quad E_a = E^o - \frac{RT}{nF} \ln \gamma - \frac{RT}{nF} \ln C_o + \frac{RT\beta}{nFC_o} I$$

Letting $\alpha = RT\beta / nFC_o$ and $a_o = \gamma C_o$

equation (12) may be expressed as

$$(13) \quad E_a = E^o - \frac{RT}{nF} \ln a_o + \alpha I$$

Equation (13), which expresses the effect of cation depletion in the cathode compartment on cell emf, says that for values of current near zero the cell potential defined as the value $E_a$ is a linear function of the electrolyzing current I. At zero current, equation (13) is the same as equation (1) which is the definition for thermodynamic emf. Thus, neglecting activation over-potentials for the moment, $E_{ao}$, the value for cell potential at zero current is the thermodynamic emf for the cell $M/MCl_2$ (in molten salt solvent)/$Cl_2$ at the initial concentration $C_o$. The term $\alpha I$ in equation (13) arises entirely from depletion of solute

cations in the cathode compartment. Assuming no activation over-potentials, it is possible to compute the diffusion coefficient D of the solute cation from the slope of the plot $E_a$ versus I, and the calculated D's are equal to $10^{-2}$ - $10^{-3}$ $cm^2/sec$. The D values are high, probably due to convection in the capillary.

The effect of activation over-potential (usually no more than 20 millivolts) is best considered in connection with analysis of the back-emf data. However, in anticipation of the results, we may point out that the activation over-potential is essentially linear with electrolyzing current I. Accordingly, equation (13) may be modified to take this factor into account by replacing $\alpha$ by $\alpha'$ where $\alpha' = \alpha + \alpha''$ Here $\alpha$ relates to diffusion of solute cation through the capillary as previously derived, and $\alpha''$ is a factor expressing the dependency of activation over-potential on I. Therefore, extrapolation of $E_a$ to I = 0 gives the thermodynamic cell emf.

The determination of thermodynamic emf's from the back-emf method consists of a three-step analysis of the electrolysis data and is shown schematically in figure 3. In part A the decay of the cell potential as a function of time is given. At 1) steady-state electrolysis is occurring, and it is characterized by specific values for voltage and electrolyzing current. At 2) the applied potential is removed, and 3) is the decay curve for the cell potential.

In part B, the values of cell potential from part A are plotted as a function of the square root of the time, giving a linear relationship.

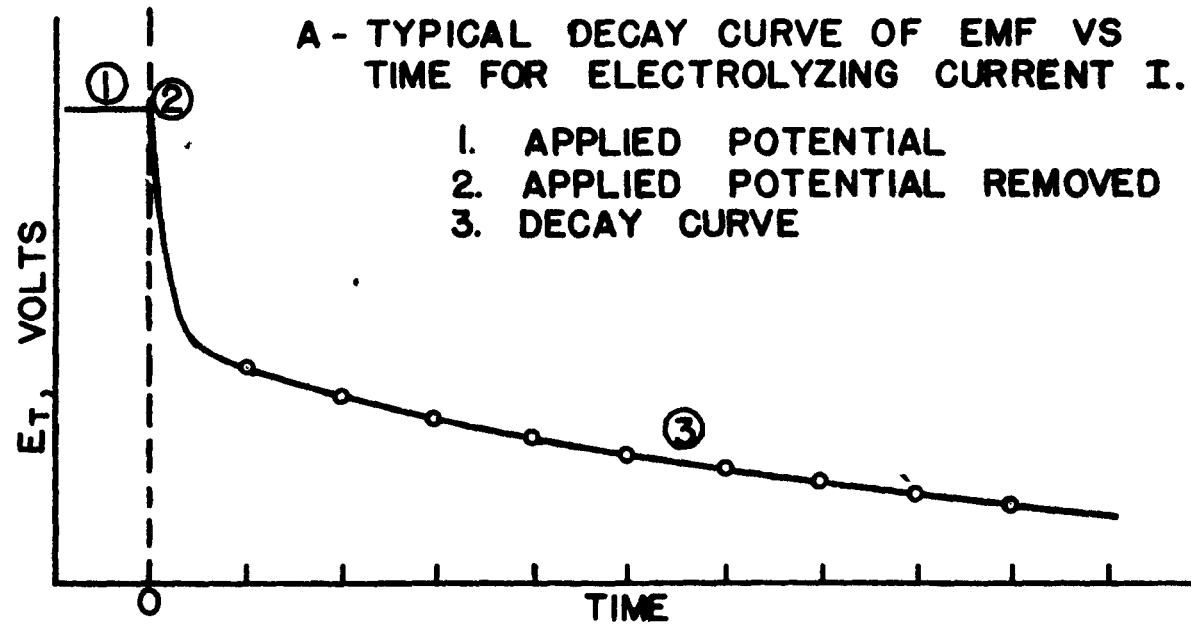
A - TYPICAL DECAY CURVE OF EMF VS TIME FOR ELECTROLYZING CURRENT I.
1. APPLIED POTENTIAL
2. APPLIED POTENTIAL REMOVED
3. DECAY CURVE
① ② ③
$E_T$, VOLTS
0
TIME

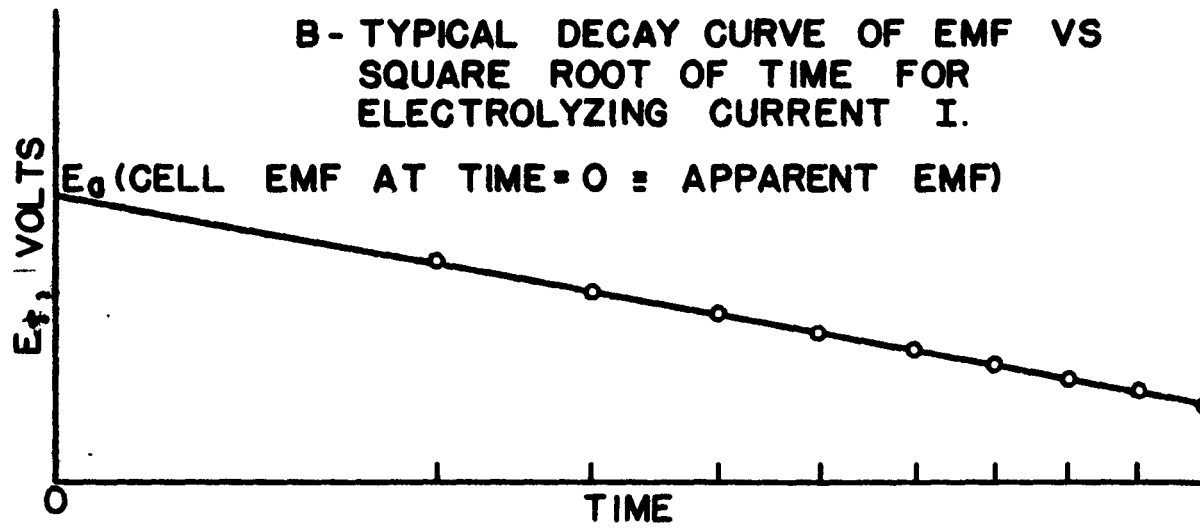
B - TYPICAL DECAY CURVE OF EMF VS SQUARE ROOT OF TIME FOR ELECTROLYZING CURRENT I.
$E_a$ (CELL EMF AT TIME = 0 ≡ APPARENT EMF)
$E_a$, VOLTS
0
TIME

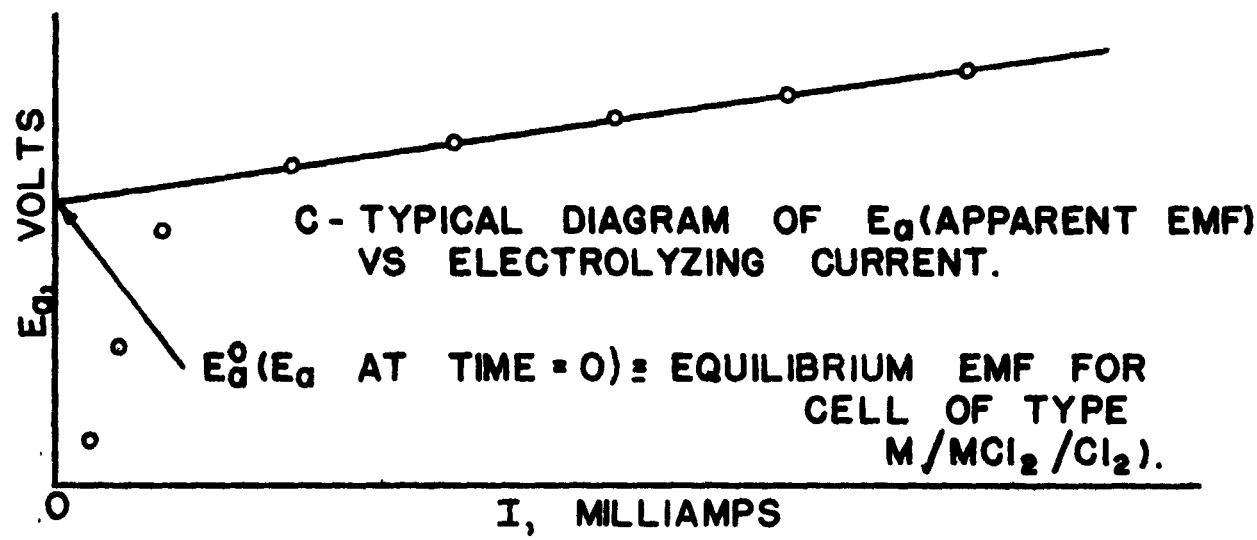
C - TYPICAL DIAGRAM OF $E_a$ (APPARENT EMF) VS ELECTROLYZING CURRENT.
$E_a^0$ ($E_a$ AT TIME = 0) ≡ EQUILIBRIUM EMF FOR CELL OF TYPE M/$MCl_2$/$Cl_2$).
$E_a$, VOLTS
0
I, MILLIAMPS



Figure 3

The decay of cell potential arises from three sources: 1) decay of activation over-potential at the chlorine anode, 2) further decay of cell potential due to diffusion of chlorine out of the anode compartment, and 3) diffusion of solute cation from the reservoir through the capillary and back into the cathode compartment. Local concentration polarization at the cathode is thought to decay too rapidly to be identified in the present decay curves. Also, it is believed that there is no appreciable activation over-potential at the cathode. This explanation of the decay curve is supported by the following evidence:

1) The early portion (first 30 seconds) of the decay curves, while dependent on electrolyzing current and temperature of the chloride systems, are almost independent of solute or solute concentration.

2) If chlorine is bubbled through the anode compartment in measurements on pure salts (e.g. $PbCl_2$), the decay will stop within several minutes and the observed cell emf is the thermodynamic equilibrium emf.

3) As will be indicated in the following, the slope of apparent cell emf $E_a$ versus electrolyzing current I is affected by capillary dimensions approximately as predicted by equation (13).

4) Inasmuch as the plot of $E_a$ versus I is linear, the dependence of activation over-potential on electrolyzing current must be linear.

The value $E_a$ for time equal to zero is the potential of the cell $M/MCl_2/Cl_2$ at the instant that the applied potential is removed and is a function of the electrolyzing current as previously shown. This value ($E_a$) is not the true thermodynamic emf but rather an apparent emf which differs from the thermodynamic emf due to the depletion of the solute cation in the cathode compartment and presence of over-potentials. The apparent emf ($E_a$) versus electrolyzing current relationship is shown

in part C. The value for $E_a$ at zero electrolyzing current ($E_{a_0}$) has been shown to be the true thermodynamic emf for the cell $H/HCl_2$ in molten salt solvent/$Cl_2$ at the initial concentration of the solute cation $C_o$.

When thermodynamic cell emf's are being measured, it is necessary that the condition of reversibility be met. A value may be reproducible and still not represent a reversible value. A practical test for reversibility is to displace the cell conditions from equilibrium in one direction and then in the other. If the emf returns to the same value after each displacement, the emf is considered to represent reversible conditions.

In the present study, the displacements from equilibrium were obtained by manually changing the setting of the recorder such that the potential of the combined potentiometer was either greater than or less than the cell potential. This method was used for two different cases:

1) Where the rate of decay of cell emf was zero (using a pure molten salt, e.g. $PbCl_2$ and bubbling chlorine over the anode).
and 2) Where the cell emf was still decreasing with time, e.g. for $PbCl_2$ - LiCl - KCl and LiCl - KCl - $NdCl_3$. In the first case, for $PbCl_2$, the emf returned to the thermodynamic value (e.g., the same as measured by Wachter and Hildebrand[20]) after the potential of the measuring potentiometers had been displaced about 2 to 3 mv. In the second case after the potential of the measuring potentiometers had been displaced about 2 to 3 mv from the trace value, the cell potential always returned to the value of the emf expected if the rate of decay of cell emf were not changed by the slight flow of current through the cell. The conclusion to be drawn from the above study is that the chlorine and the metal electrodes behave reversibly, at least within ± 0.5 mv.

## EXPERIMENTAL PROCEDURE

In measuring potentials associated with electrolysis of molten salts it is necessary that:-

1) The molten salt be free of water.
2) The melt be blanketed with an inert gas to prevent contamination from the atmosphere.
3) There be no back-diffusion of the electrolysis products (e.g., diffusion of the metal to the anode, there to react with the chlorine to reform the metal chloride).
4) The cell materials be inert with respect to the molten salts and the electrolysis products.
5) No thermal emf's be present.

The salts used were C.P. grades which contained water of crystallization, and it was therefore necessary to pre-dry these salts. Many of the metal chlorides are hygroscopic and this retained moisture (upon heating the wet salt in air) reacts with the oxygen present to form either oxides or oxychlorides. Water-free chlorides can be obtained by several different methods. One is to start with a water free oxide which is converted to the chloride by reacting the oxide with dry HCl gas at an elevated temperature(7).

The hydrated salts can be vacuum dried. In this treatment the hydrated salt is heated in a vacuum of the order of $10^{-4}$ mm of Hg pressure at a temperature below the melting point of the salt. The drying time depends upon the salt to be dried and the water content of the salt and must be determined for each individual salt. It is necessary in this treatment that the drying chamber be flushed with a dry gas prior to heating and evacuation to eliminate the residual oxygen present at the small pressures and prevent oxide or oxychloride formation. The water

vapor is condensed in the liquid nitrogen freeze-out trap, thus maintaining a concentration gradient and ensuring almost complete removal of water from the hydrated salt (see figure 4).

In addition, the salts are subjected to a pre-electrolysis purification stage. The molten salts contain small amounts of minor impurities which are deposited in the initial electrolysis period. At the start of electrolysis, for a given small electrolyzing current of the order of 10-20 ma, the applied voltage is in the range of 1 to 2 volts below the decomposition potential, and rises continuously until the applied voltage reaches a steady value. At this point, the applied potential is usually greater than the decomposition potential of the major solute salt. This pre-electrolysis step eliminates the minor impurities and any residual water from the drying stage and also saturates the electrode compartments with metal and chlorine respectively.

Figure 5 is a schematic sketch of the experimental electrolysis cell. The cell is comprised of three main parts, the cell container which holds the molten salt, the cooling head assembly, and the electrode compartment assembly. The cell is a closed-end 45 mm pyrex, McDanel, vycor, or alumina tube 15 inches long. The main requirement of the container material is that it will not react with the molten salt. Molten mixtures of the alkali halides melted in the above containers have been analyzed and show negligible amounts of dissolved oxides (as either $SiO_2$ or $Al_2O_3$). Molten fluorides exhibit no pickup of $Al_2O_3$ or $SiO_2$ when melted in alumina and McDanel tubes up to temperatures of 800°C.

The cooling head assembly is of stainless steel and is a "tapered ground joint" type. The lower part is water cooled and sealed to the cell container by means of apiezon wax. The upper portion, which is

# SCHEMATIC SKETCH OF VACUUM DRYING APPARATUS

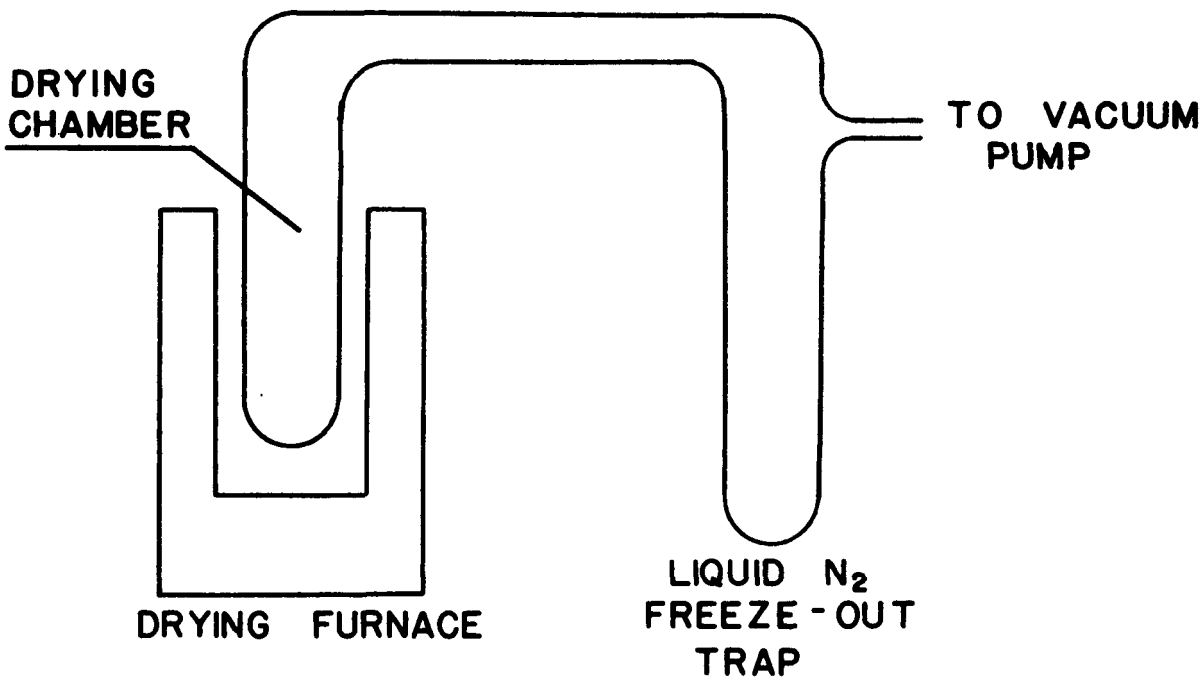


Figure 4

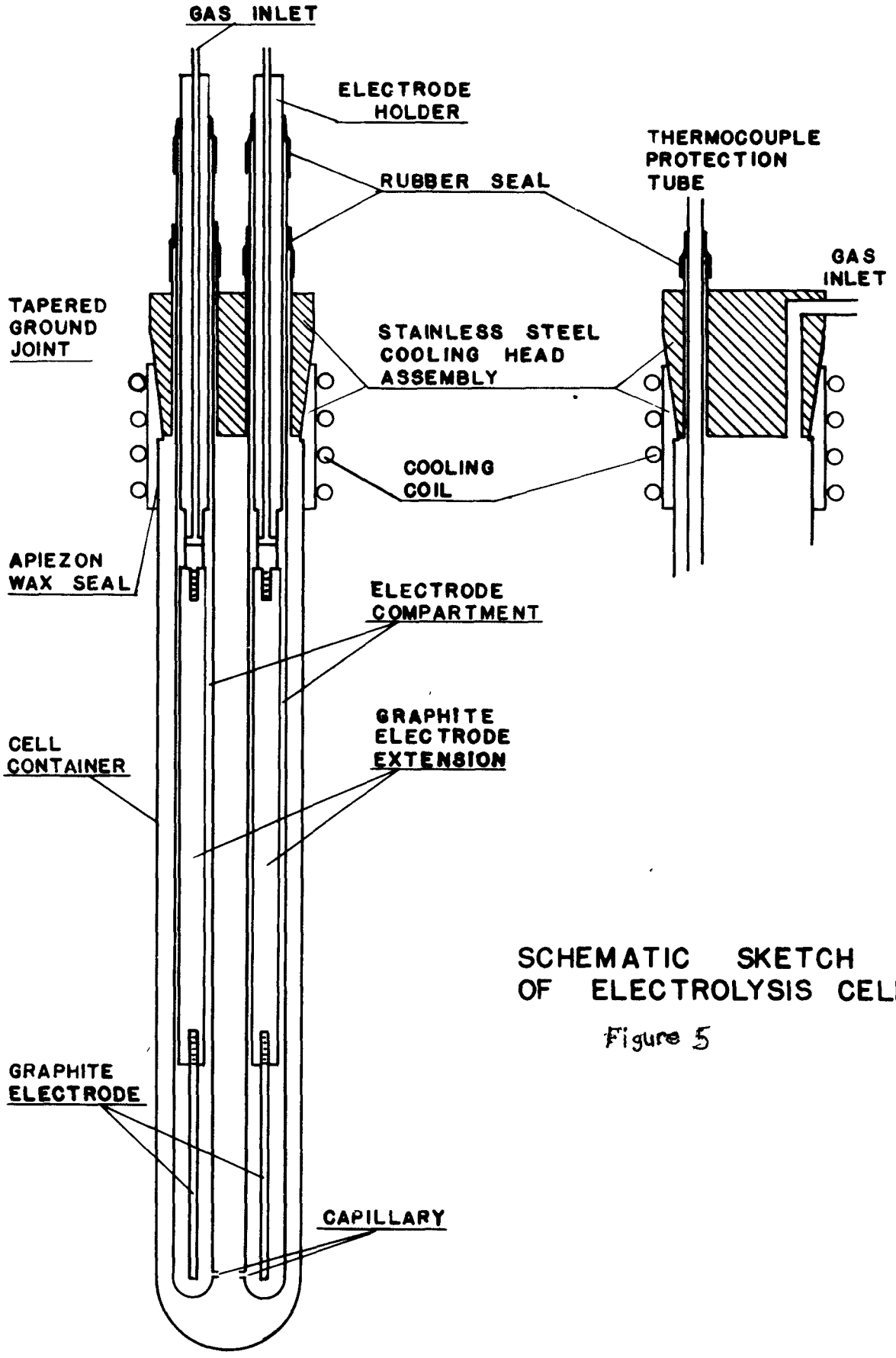


SCHEMATIC SKETCH OF ELECTROLYSIS CELL

Figure 5

tapered to fit into the lower part, has openings for the insertion of the two electrode compartments and the thermocouple tube. There is also an opening for admittance of the argon atmosphere. A vacuum tight seal between the two parts is made by means of silicone stopcock grease on the tapered joint. A vacuum seal is made between the cooling head assembly and the electrode compartments and thermocouple tube with rubber tubing (see figure 5).

The electrode assembly is made from 13 mm closed-end pyrex, porcelin, or alumina tubes 19 inches long. In order to prevent back-diffusion of the electrolysis products, the electrode compartments are separated from the reservoir by a short length of capillary (see Figure 5). The capillary must be long enough to prevent back-diffusion and yet short enough that the cell resistance is not too large. The water-cooled electrode head is used for making electrical contact with the electrode and also as a means of admitting an inert atmosphere to the electrode compartments.

Each graphite electrode is made from a 3/8" graphite rod 12 inches in length, tapped with 6-32 thread at both ends. Into one end is screwed a 1/8" graphite electrode which extends into the molten salt. The other end screws onto the electrode head. The entire unit is placed in the electrode compartment tube and a gas-tight seal is made by means of rubber tubing (see figure 5).

This type of gas seal permits an easy and rapid method for changing compartments if necessary and also for raising and lowering the electrode compartments into and out of the molten salt bath without removing the inert atmosphere. It also allows any gas to be bubbled through the melt and permits the purging of the cell with an inert gas for

melting under an inert atmosphere. With the external manifold arrangement, a vacuum can be applied for a vacuum degassing treatment on the molten salt.

In order to prevent contamination from the air a dry inert atmosphere must be provided. In the present study dry purified argon is used. The drying and purification train is sketched in figure 6. Seybolt and Burke[68] describe several methods for removing hydrogen, oxygen, and nitrogen from helium and argon. The impure gas is passed over calcium turnings at 600-650°C in one tube furnace and then through another at 350°C. The first furnace removes all gaseous impurities but hydrogen, and the second furnace (at 350°C) removes the hydrogen, since Ca hydride is stable at this temperature. Oxygen and nitrogen can be removed by passing the gas over Ti chips or powder at 850°C Zr chips can be used to remove the oxygen and hydrogen. In this work the argon was passed over Ti chips at 850°C to remove the oxygen and nitrogen, after the gas had first passed through a $P_2O_5$ drying tube to remove the water vapor.

The vapor pressure of many of the molten salts at electrolysis temperatures is great enough that if the inert atmosphere were to be circulated through the cell the salt vapor would be swept out along with the inert gas. For this reason a static cell atmosphere was maintained. The gas train is shown in figure 6 where the cell manifold is pictured. The stopcock arrangement permits the flushing of the cell with inert gas, the bubbling of any gas through the molten salt, and the application of a vacuum. This by-pass system also prevents the back-diffusion of the chlorine gas into the cathode compartment.

# SCHEMATIC SKETCH OF PURIFICATION TRAIN AND CELL MANIFOLD

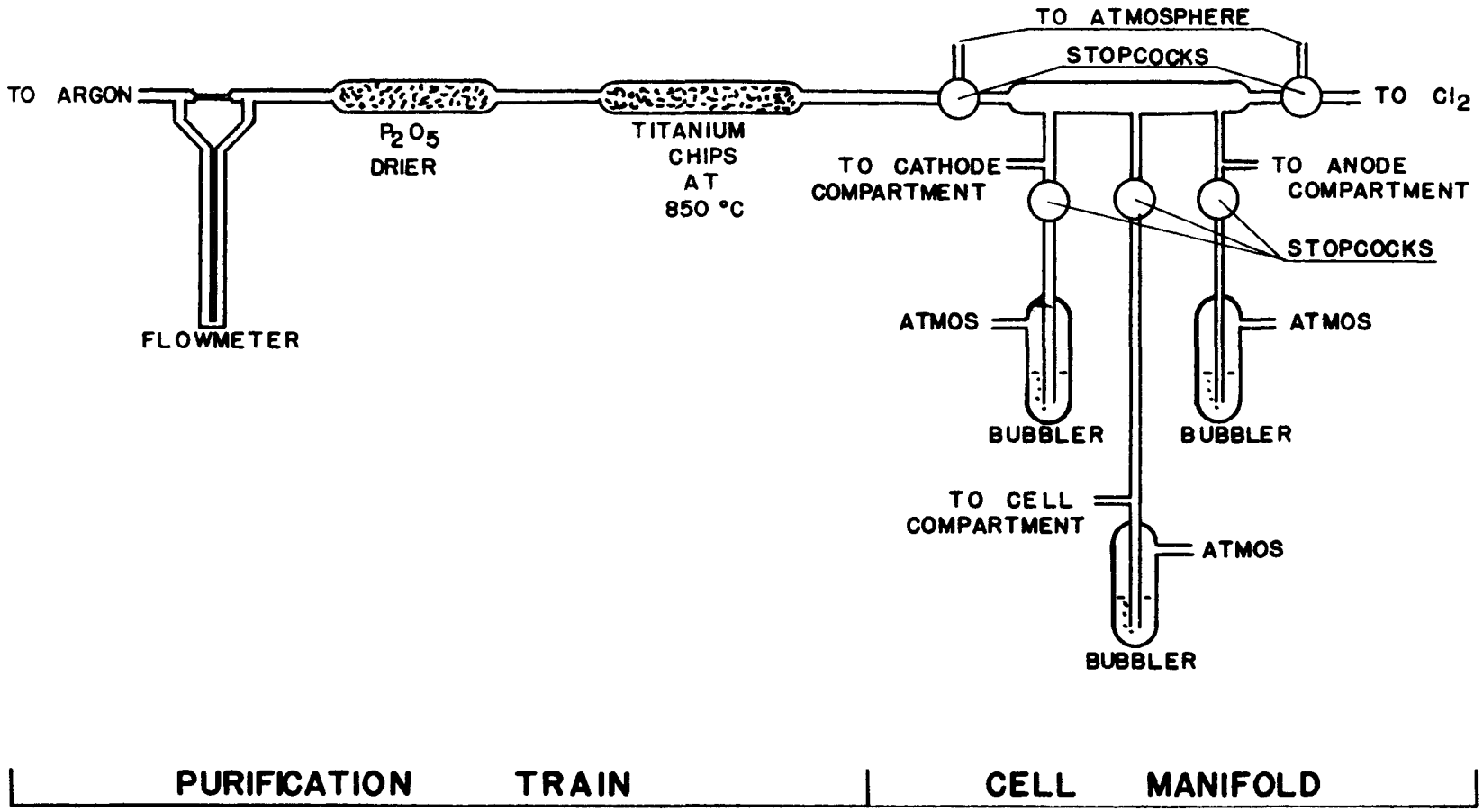


Figure 6

In analyzing the back-emf decay curve it is necessary that a potentiometric measuring circuit be used and that an accurate curve of cell emf versus time be recorded for a time interval of 30 to 40 seconds after the applied voltage is removed. Since the decomposition potentials of the molten halides vary from 0 to 6 volts and the electrolysis should be carried out over a range of applied voltages up to 10 volts, a potentiometric instrument with a 10 volt range was constructed. The overall instrument is a combination of three potentiometers:-

1) a 0-10 volt potentiometer in steps of 1 volt.
2) a Leeds and Northrup type K-2 potentiometer which can be continuously varied over its full range of 1.5 volts.

and 3) a modified Brown Electronik Potentiometer with full scale spans of:-

a. 0-10 mv or 0.01 volts
b. 0-100 mv or 0.10 volts
c. 0-200 mv or 0.20 volts
d. 0-500 mv or 0.50 volts
e. 0-1000 mv or 1.00 volts

The wiring diagram of the instrument is shown in figure 7.

This instrument is quite flexible in operation. Any applied potential from zero to 11.5 volts can be read to ± 0.0001 volts and recorded versus time. The 0-10 volt potentiometer and the Leeds and Northrup type K-2 potentiometer are adjusted until the difference between the potential to be measured and the sum of the two above potentiometers is less than the range of the Brown Recorder. The applied potential is then the sum of the values read from the three potentiometers. The Brown Recorder actually functions as a recording galvanometer. If the

Figure 7

# SCHEMATIC WIRING DIAGRAM

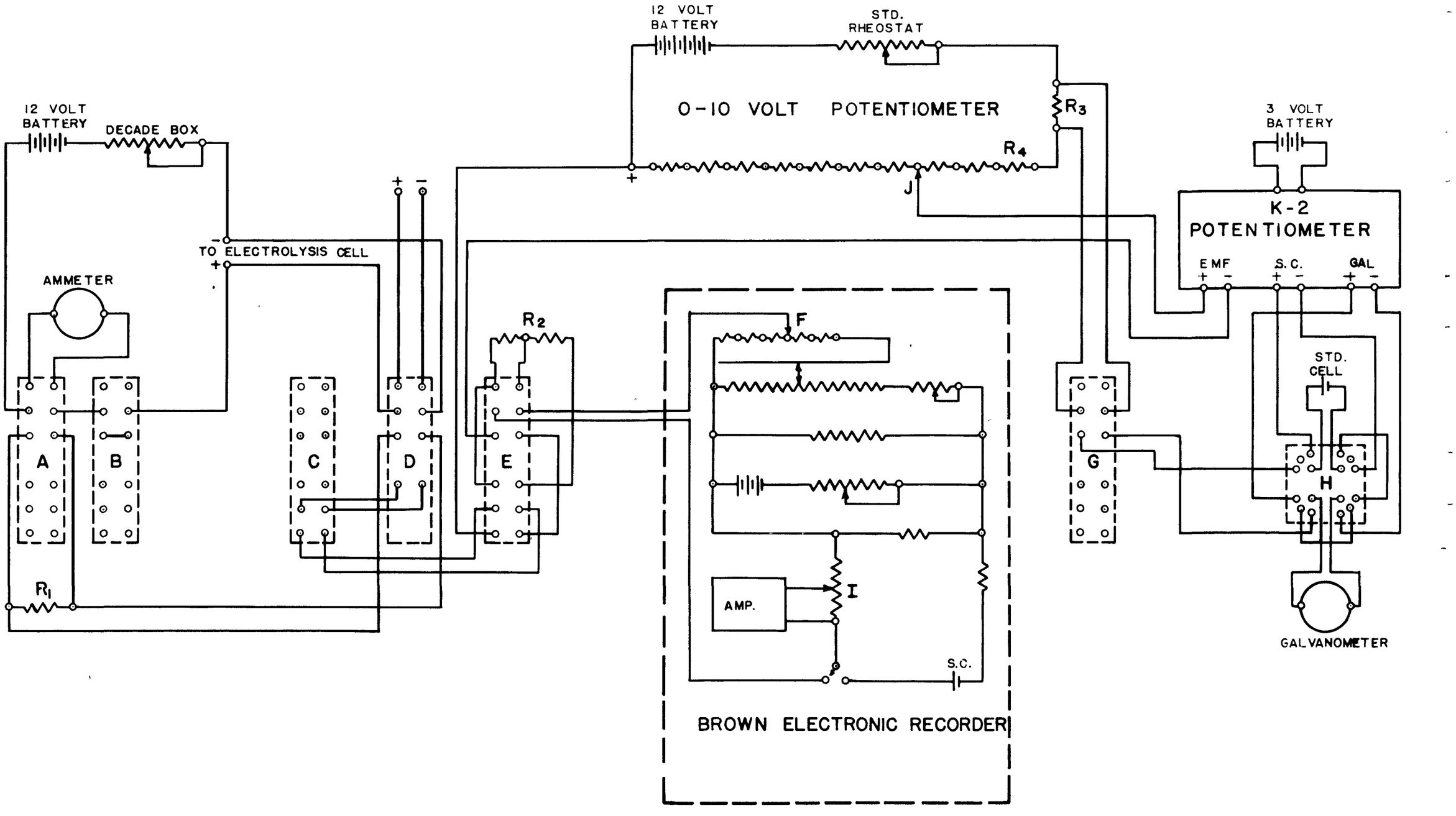

emf being measured is changing with time, this change with time is recorded. In measuring the decay curve (figure 3, part B) the K-2 and the 0-10 volt potentiometer are adjusted such that the entire decay curve can be recorded with just one setting of the potentiometers. If the 0-100 mv range is not large enough to record the decay curve, one of the larger ranges can be used.

Using the 0-10 mv range on the Brown Electronik, 0 setting on the 0-10 volt potentiometer, and adjusting the K-2 until the Brown Electronik reading is on scale, the instrument can be used to record thermocouple emf's and thereby cell temperatures. If switch A is in the down position the potential drop across a known standard resistor can be recorded, and with proper calibration, the electrolyzing current recorded.

The Brown Electronik has two chart speeds, 24 inches per minute and 24 inches per hour, which can be changed by a switch mounted on the panel board which activates a solenoid in the drive mechanism The 24 inches per minute chart speed is used only when recording the decay curve (figure 3, part B). The total elapsed time for the cell emf decay curve is 37.5 seconds, or 15 inches of chart.

Due to the fact that this circuit is a true potentiometric one, there is no current drain on the cell when potentials are being measured. The Brown Electronik needs $10^{-8}$ amp to drive the pen full scale in one second. Thus $10^{-8}$ amp is the maximum current drain possible, and this only for very small intervals of time.

The heating furnace is a 3 inch diameter by 24 inch long alundum tube wound with nichrome wire. Surrounding this tube is 6 inches of silocel powder insulation. The upper temperature limit of the nichrome winding is 1000°C. The temperature is controlled by a Celect-Ray controller

to within ± 0.5°C at 500°C.

The free energy of formation of $CCl_4$ is given by Kubaschewski and Evans(5) to be

$$\Delta F = -26{,}500 - 5.16\ T \log T + 49.32\ T$$

At the temperature corresponding to $\Delta F^{\circ} = 0$ the carbon and chlorine will no longer react to form $CCl_4$ and graphite will serve as an inert electrode with respect to chlorine. The temperature at which $\Delta F^{\circ} = 0$ is 497°C, such that above this temperature graphite can be utilized as electrode material. In the present study, 1/8" diameter by 12" long "spectographic" grade graphite rods served as electrodes for the electrolysis of molten chlorides.

For electrolysis studies of fused salt mixtures, the pre-dried salts were carefully weighed to give the desired composition and then introduced into the electrolysis cell. The entire cell is then assembled, but the electrode compartments are not lowered into the salt. The stopcocks on the gas manifold are turned such that the dried argon is forced down the electrode compartments, through the capillary into the cell container, and thence out through the gas outlet in the cooling head assembly through bubbling bottles into the atmosphere. In this manner the cell is purged of air. When the cell is purged, the stopcocks in the manifold are turned such that the inert gas flow bypasses the cell and electrode compartments ensuring a static atmosphere in the electrolysis cell. The salt mixture is then fused under the dry inert gas blanket. After the salt is molten, the electrode compartments are lowered into the bath and the electrolyzing current turned on and adjusted until 5 to 10 milliamps of current are flowing through the cell. The applied voltage, however, does not correspond to the value for the steady state

E versus I curve but exhibits a value too low by ½ to 2 volts for a salt with a decomposition potential of about 3 volts. This corresponds to the decomposition of minor impurities that are present in the bath. As the minor impurities are removed by electrolysis, the applied potential increases steadily to the steady-state value characterized by a particular applied voltage and electrolyzing current, and this steady-state electrolysis corresponds to the decomposition of the most readily electrolyzable salt in the melt. This initial period when the applied potential is steadily increasing to the steady-state value constitutes the pre-electrolysis purification stage.

After the applied potential has reached the steady-state electrolysis conditions, the thermodynamic emf for the cell $M/MCl_2$ (in solution)$/Cl_2$ is measured by the back-emf method. Also, the decomposition potential is measured. For each steady-state electrolysis level of applied potential and electrolyzing current the following information is recorded:-

1) Applied potential.

2) Electrolyzing current I.

3) Decay curve of cell emf ($E_t$ versus time).

4) Apparent emf ($E_a$), the value at t = 0 for the plot of $E_t$ versus $\sqrt{t}$.

5) The temperature and initial concentration of the molten salt.

From these data, two separate sets of information can be derived:

1) The decomposition potential from the plot of applied potential versus electrolyzing current (see figure 1) extrapolated to the intercept at I = 0.

and 2) The thermodynamic emf ($E_{ac}$) of the cell $M/MCl_2$ (in solution)$/Cl_2$ at the initial concentration $C_o$, which is evaluated by the back-emf method as pictured in figure 3.

## CALCULATION OF THEORETICAL CELL EMF

The free energies of formation and the heats of fusion of many of the metal chlorides have been compiled by Quill[4], Kubaschewski and Evans[5], and Kellogg[12]. These three sources of thermodynamic data are used here for the calculation of the theoretical cell emf's.

Using these data for the free energy of formation and free energy of fusion, and assuming ideal solution behavior, the theoretical cell emf can be calculated by the following method.

The free energy of formation as a function of temperature is given in two ways:-

1) Quill[4] tabulates the quantity $\frac{\Delta F^\circ - \Delta H^\circ_{298}}{T}$ as a function of the temperature together with the value of $\Delta H^\circ_{298}$,

where $\Delta F^\circ$ = standard free energy of formation

$T$ = $^\circ K$

$\Delta H^\circ_{298}$ = standard heat of reaction at $298^\circ K$.

2) Kubaschewski and Evans[5] fit the free energy versus temperature data to an empirical equation of the type

$$\Delta F^\circ = A + BT \log T + CT$$

where A, B, and C are empirical constants. This is not the only empirical equation which could be used but is representative of the empirical approach (Kellogg[12], for instance uses a different equation). These equations are only valid over the temperature range of the empirical fit.

The first reaction to be considered is the formation of the compound from its elements where the reaction is written:-

$$M + Cl_2 = MCl_2$$

In the above reaction, the products and reactants are in their standard states of pure metal and metal chloride, either in the solid or liquid state, and $Cl_2$ gas at one atmosphere pressure. The value for the free energy of formation must be such that all of the components, metal, chlorine, and metal chloride are in their equilibrium state at the corresponding temperatures. For example, the previous equation could have been written as:-

$$M(l) + Cl_{2(g)} = MCl_{2(s)}$$

where l = liquid or molten

g = gas at 1 atmosphere pressure

s = solid

for temperatures above the melting point of the metal and below the melting point of the chloride. In the present study, solute electrolyses was conducted on the molten salts at temperatures below the melting points of the solute salts. Thus the salts are in the liquid state, and therefore the free energy of supercooling must be taken into account in the calculation of emf's from thermodynamic data. This supercooling effect is corrected for by taking into account the free energy of melting at the actual electrolysis temperature. The reaction to be considered here is then that of the solid to liquid transition:-

$$MCl_2(s) = MCl_2(l)$$

where the free energy of fusion is given by

$$\Delta F_f = \Delta H_f - T\Delta S_f \ .$$

Making the basic assumption that $\Delta H_f$ and $\Delta S_f$ are independent of temperature over the range of temperature between the melting point and the electrolysis temperature, $\Delta S_f$ can be evaluated by setting $\Delta F=0$ at the equilibrium melting temperature. Assuming $\Delta H_f$ to be independent of temperature,

the free energy of fusion, at temperatures below the melting point, can be estimated by the equation

$$\Delta F_f = \Delta H_f \left(1 - \frac{T}{T_M}\right)$$

With the exception of pure substances, the metal chlorides represent a mixture of salts in a single phase and the component salts are therefore not at unit activity. In any calculation of the emf for molten salt systems the free energy of mixing must be taken into account. It would be best to calculate the free energy of mixing from the activities of the salt constituents. Since the information is not known except for a few simple systems, the free energy of mixing must therefore be estimated. The simplest method is to assume ideal solution behavior (i.e., the solute obeys Raoult's Law). The relationship for this computation is

$$\overline{\Delta F_M} = \overline{F} - F^o = RT \ln a$$

and for ideal solution behavior assumption

$$\overline{\Delta F_M} = RT \ln N = 4.576\ T \log N$$

where $\overline{F}$ = partial molar free energy

$F^o$ = free energy at standard state of N = 1

a = activity of metal chloride in solution

N = mol fraction of metal chloride in solution

The units for all the free energy values are calories per mole.

In summary, for calculating the theoretical emf's the following reactions are considered to have taken place:-

1) $M_{(s)} + Cl_{2(g)} = MCl_{2(s)}$

and $\Delta F^\circ = A + BT \log T + CT = \Delta F_1$

or $\frac{\Delta F^\circ - \Delta H^\circ_{298}}{T}$ = tabulated value.

2) $MCl_{2(s)} = MCl_{2(l)}$

and $\Delta F_2 = \Delta H_f - T\Delta S_f = \Delta H_f \left(1 - \frac{T}{T_{MP}}\right)$

3) Assuming ideal solution behavior for

$$MCl_{2(l,N=1)} = MCl_{2(l,N)}$$

$\overline{\Delta F_3} = 4.576\ T \log N$.

In the above reaction, the standard states are the pure metal and metal chlorides in either the solid or liquid phase and chlorine gas at 1 atmosphere pressure. The total free energy change is equal to $\Delta F_T = (\Delta F_1) + (\Delta F_2) + (\overline{\Delta F_3})$ which corresponds to the cell $M/MCl_2/Cl_2$ and the cell reactions,

$M = M^{++} + 2e$

and $Cl_2 + 2e = 2Cl^-$, where the overall reaction is

$M + Cl_2 = M^{++} + 2Cl^-$.

For reversible cells:-

$$\Delta F_T = -n\mathcal{F}E$$

$$E = -\frac{\Delta F_T}{n\mathcal{F}}$$

Since $\Delta F_T$ is actually negative in value, E is positive, which is in agreement with equation 13, page 13.

Two sample calculations will be given to show the use of the free energy of formation data. The two examples will be those for LiCl and KCl at 500°C in LiCl - KCl eutectic where the eutectic composition is 0.48 mol fraction of KCl and 0.52 mol fraction of LiCl.

The first calculation will be based on data taken from "Metallurgical Thermochemistry" by Kubaschewski and Evans[5].

1) $K_{(l)} + \frac{1}{2} Cl_{2(g)} = KCl_{(s)}$

$\Delta F_1 = -104{,}900 + 24.0\,T \pm 1000$ cal.

and $\Delta F_1$ is valid for the range 298 - 1043°K.

2) $KCl_{(s)} = KCl_{(l)}$

$\Delta F_2 = 6{,}700 - T\Delta S$

where $\Delta H_2 = 6{,}700 \pm 200$ cal/mol.

At $T = 1043°K$, the melting point of KCl

$\Delta F_2 = 0$

and $0 = 6700 - 1043\ \Delta S$

or $\Delta S = 6.4$ cal/mol deg.

and thus

$\Delta F_2 = 6700 - 6.4T$.

3) $KCl_{(N=1)} = KCl_{(N)}$

$\overline{\Delta F}_3 = 4.576\ T \log N$ , and for N = 0.42 mol fraction

$\overline{\Delta F}_3 = -1.725\ T$ , where the overall reaction is now

$KCl_{(N)} = K_{(l)} + 1/2\ Cl_{2(g)}$ .

Therefore, $-\Delta F_T = -(\Delta F_1 + \Delta F_2 + \overline{\Delta F}_3)$

$-\Delta F_T = +104{,}900 - 24.0T - 6700 + 6.4T + 1.72T$

$-\Delta F_T = 98{,}200 - 15.9T$

$-\Delta F_T = 98{,}200 - 15.9\ (773)$

$-\Delta F_T = 85{,}909$ .

For a galvanic cell,

$\Delta F_T = -n\mathcal{F}E$

or $E = -\frac{\Delta F_T}{n\mathcal{F}}$

where $n = 1$

and $\mathcal{F} = 23{,}020$ cal./volt.

giving $E = + 85{,}909/23{,}020 = + 3.735$ volts

As an estimate of the limits of accuracy of the calculated value

$$\Delta E = \frac{\pm 1000 + \pm 200}{n\mathcal{F}} = \pm \frac{1200}{23020}$$

$$\Delta E = \pm 0.052 \text{ volts.}$$

For the calculation of the theoretical cell emf of LiCl, the thermochemical data is taken from "Chemistry and Metallurgy of Miscellaneous Materials: Thermodynamics" by Quill[4].

1) $Li_{(l)} + 1/2\ Cl_{2(g)} = LiCl_{(s)}$

$$\frac{\Delta F_1 - \Delta H^{\circ}_{298}}{T} = 18.37 \quad \text{at } 500^{\circ}C.$$

$$\Delta H^{\circ}_{298} = - 97{,}700 \pm 2000 \text{ cal.}$$

or $\Delta F_1 = - 97{,}700 + 18.37T.$

2) $LiCl_{(s)} = LiCl_{(l)}$

$\Delta F_2 = 3200 - 3.6T$

3) $LiCl_{(N=1)} = LiCl_{(N)}$

$\overline{\Delta F}_3 = 4.576\ T \log N$

where $N = 0.52.$

$\overline{\Delta F}_3 = 4.576\ T \log 0.52$

$\overline{\Delta F}_3 = - 1.30\ T$

$-\Delta F_T = - (\Delta F_1 + \Delta F_2 + \Delta F_3)$

$= 97{,}700 - 18.37\ T - 3200 + 3.6\ T + 1.3\ T$

$= + 94{,}500 - 13.47\ T$

$= 94{,}500 - 13.47\ (773)$

$-\Delta F_T = 84{,}088$ cal.

and $E = \frac{\Delta F_T}{n\mathcal{F}}$

$$E = + \frac{84,088}{23,020}$$

$$E = + 3.655 \text{ volts}$$

and $\Delta E = \pm 2000/23020 = \pm 0.087$ volts.

The activity of the solute is defined by the equation:

$$\Delta F = \Delta F' - \Delta F^{o} = RT \ln \frac{a'}{a^{o}} = 4.576\ T \log \frac{a'}{a^{o}}$$

where $\Delta F'_{a} = - nFE$

and $\Delta F^{o} = - nFE^{o}$ .

$E^{o}$ can be calculated from thermochemical data by taking into account only the free energy of formation and the super-cooling effect. (Steps 1 and 2 of the previous calculations for theoretical cell emf's). Thus the activity ratio may be obtained from:-

$$\Delta F = -nF\ (E - E^{o}) = RT \ln \frac{a_{MCl_2}}{a^{o}} .$$

$a^{o} = 1$, therefore

$$- nF\ (E - E^{o}) = RT \ln a_{MCl_2}$$

or $$\ln a_{MCl_2} = - \frac{(23020)\ n}{RT} \quad (E - E^{o})$$

and $$a_{MCl_2} = \exp \left[ - \frac{23020\ n}{RT} \quad (E - E^{o}) \right]$$

Since $\gamma = \frac{a}{N}$ the activity coefficient is also known.

Values of theoretical thermodynamic emf's, experimental decomposition potentials, and experimental thermodynamic emf's are tabulated in Table I through IV.

## DISCUSSION OF RESULTS

In this section the experimental results of the electrolysis studies on some molten salt systems are given. The data are reported as the decomposition potential and the thermodynamic cell emf obtained by the back-emf method. Where possible, the experimental values are compared with thermodynamic emf's measured by the classical method and with the theoretical cell emf calculated from thermochemical data. In most cases, where the activities of the components of the molten salt mixtures are not known, the free energy of mixing is approximated by assuming the solutes obey Raoult's law and $\overline{\Delta F}_M = - RT \ln N$.

The systems studied were:-

1) $PbCl_2 - ZnCl_2$ for mole fractions of $PbCl_2$ equal to 1, 0.855, and 0.688 for temperatures between 500°C and 600°C. The thermodynamic cell emf values are compared with the experimental results of Wachter and Hildebrand[20] (measured by the classical method) and with calculated theoretical cell emf.

2) LiCl - KCl eutectic compositions (45 wt. % LiCl, 55 wt. % KCl) for temperatures between 500°C and 600°C. The results of this study aid in the interpretation of ternary mixtures (e.g., solute chlorides in the LiCl - KCl eutectic solvent).

3) $LiCl - KCl - PbCl_2$ .

4) $LiCl - KCl - ZnCl_2$ .

5) $LiCl - KCl - MgCl_2$ .

6) $NaCl - MgCl_2$ .

7) $LiCl - KCl - NdCl_3$ .

8) NaF - KF - LiF eutectic.

## The Electrolysis of the $PbCl_2$ - $ZnCl_2$ System

Electrolysis measurements were made for a series of compositions of $PbCl_2$ at various temperatures as listed below:-

1) 1.0 mole fraction of $PbCl_2$ at 518°C, 535°C, 550°C.

2) 0.855 mole fraction of $PbCl_2$ at 519°C, 533°C, 567°C.

3) 0.688 mole fraction of $PbCl_2$ at 516°C, 535°C.

The measured emf represents the value for the cell $Pb/PbCl_2$ in $ZnCl_2/Cl_2$ (graphite). This system was studied extensively by Wachter and Hildebrand[20] and their results are summarized in figure 8. Electrolysis data are presented for the decomposition potential and for thermodynamic emf measured by the back-emf method. Figures 9 to 24 are the experimental curves of cell emf versus electrolyzing current for the back-emf method and electrolyzing current versus applied potential for the decomposition potential determination. The results are tabulated in Table I along with the corresponding values from Wachter and Hildebrand's determination at the same compositions and temperatures. The two sets of data, Wachter and Hildebrand's and the values for thermodynamic emf's from this study, are compared in figure 8 .

The values for the thermodynamic cell emf measured by the "back-emf" method are in excellent agreement with those of Wachter and Hildebrand, while the values for the decomposition potential are quite erratic. The experimental data for the back-emf method ($E_a$ vs. I) for $PbCl_2$ - $ZnCl_2$ are presented in figures 9, 11, 13, 15, 17, 19, 21, 23. The curves for pure $PbCl_2$ (N = 1) show only a single line which is characteristic of the decomposition of $PbCl_2$. However, the curves for the $PbCl_2$ - $ZnCl_2$ mixtures exhibit two distinct horizontal lines. The lower curve corresponds to the decomposition of $PbCl_2$ and the higher curve represents the

decomposition of the $ZnCl_2$. The liquid metal phase is an alloy for the higher curve. This value for the decomposition of $ZnCl_2$ does not represent the thermodynamic value for the cell $Zn/ZnCl_2/Cl_2$, for there is a depolarization due to the alloying of Zn with the Pb.

The decomposition potential plots are given in figures 10, 12, 14, 16, 18, 20, 22, 24. These curves show that there is only a single "break" which corresponds to the decomposition potential of $PbCl_2$. Only in cases where the limiting current density has been reached will the decomposition potential curve (V vs. I) exhibit more than one "break".

For electrolysis, it is necessary that the current be carried by ions and that ions be deposited at the electrodes. It is not necessary, however, that the current carrying ion be deposited. Using the conductivity of molten salts as a qualitative measure of the degree of ionization of the salt, it is seen that $ZnCl_2$ has few ions in the molten state. Attempts to electrolyze pure zinc chloride failed because of inability to attain a sufficiently high current density to sustain deposition.

The electrolysis study of the $PbCl_2$ - $ZnCl_2$ studied by the decomposition potential method and by the back-emf method has shown:-

1) The cell emf, as measured by the new back-emf method, is the thermodynamic reversible potential of cells of the type $Pb/PbCl_2/Cl_2$.

2) The decomposition potential, which theoretically should be the same as the equilibrium cell emf in the present systems, shows no agreement with the equilibrium cell emf. This indicates that the back-emf method is much more accurate than the decomposition potential technique for determining thermodynamic cell emf.

TABLE I

Summary of the Electrolysis Data For the $PbCl_2$-$ZnCl_2$ System

| Solute | Mole Fraction | Temp. °C | Solvent | $E_{ao}$ | Theo. emf* | D.P. |
|---|---|---|---|---|---|---|
| $PbCl_2$ | 1.000 | 518 | | 1.261 | 1 2616 | 1.269 |
| $PbCl_2$ | 1.000 | 535 | | 1.253 | 1. 2518 | 1.279 |
| $PbCl_2$ | 1.000 | 550 | | 1.242 | 1.2420 | 1.258 |
| $PbCl_2$ | 0.855 | 519 | $PbCl_2$-$ZnCl_2$ | 1.269<br>1.281 | 1. 2685 | 1.289 |
| $PbCl_2$ | 0.855 | 533 | $PbCl_2$-$ZnCl_2$ | 1.259<br>1.271 | 1.2596 | 1.250 |
| $PbCl_2$ | 0.855 | 567 | $PbCl_2$-$ZnCl_2$ | 1.238<br>1.249 | 1.2380 | 1.200 |
| $PbCl_2$ | 0.688 | 516 | $PbCl_2$-$ZnCl_2$ | 1.280<br>1.293 | 1.2810 | 1.309 |
| $PbCl_2$ | 0.688 | 535 | $PbCl_2$-$ZnCl_2$ | 1.271<br>1.282 | 1.2698 | 1.311 |

* From the best curve through Wachter and Hildebrand data.

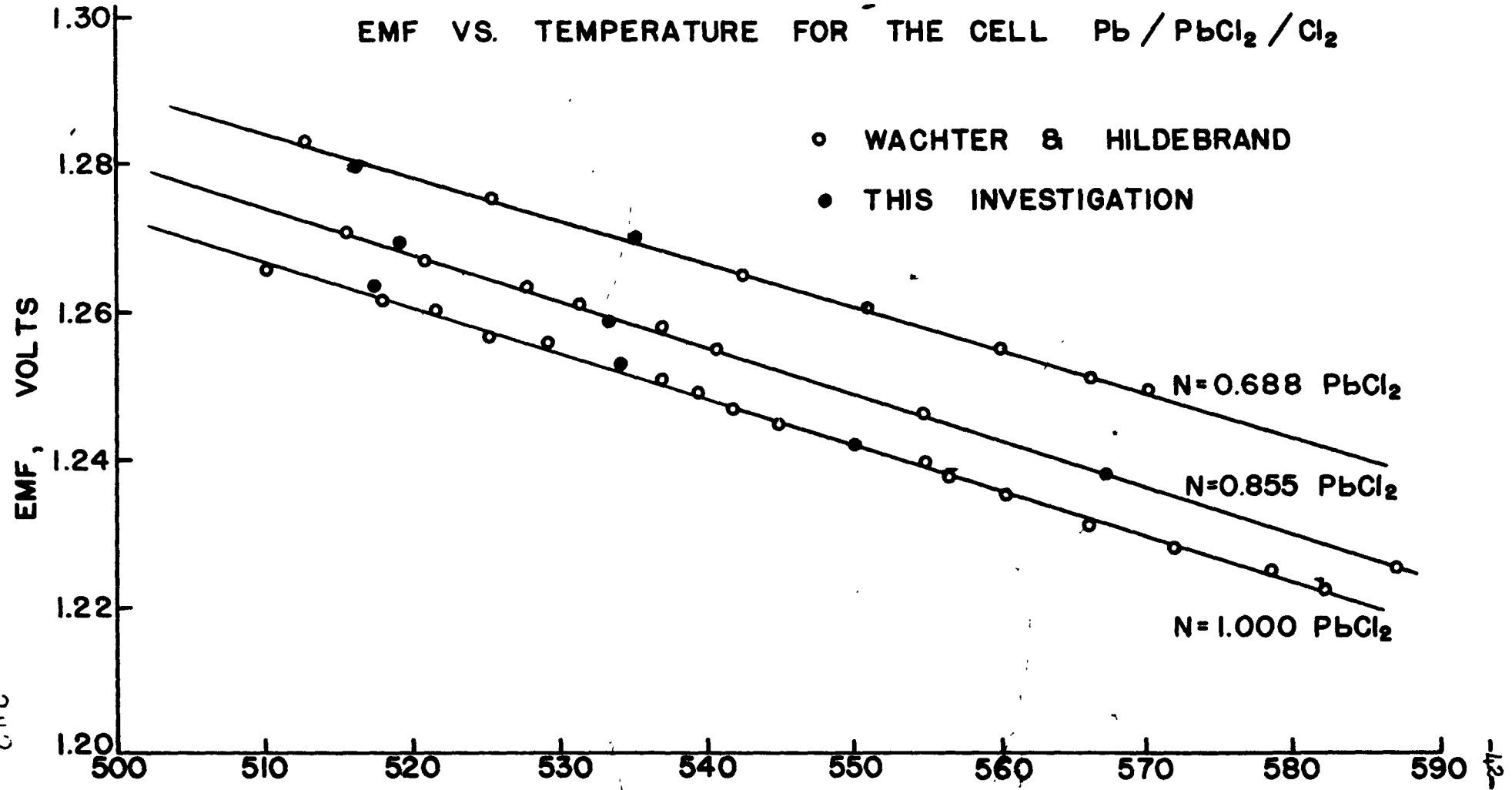
EMF VS. TEMPERATURE FOR THE CELL Pb / PbCl2 / Cl2
WACHTER & HILDEBRAND
THIS INVESTIGATION
N=0.688 PbCl2
N=0.855 PbCl2
N=1.000 PbCl2
EMF, VOLTS
1.30
1.28
1.26
1.24
1.22
1.20
500
510
520
530
540
550
560
570
580
590
TEMPERATURE, °C

Figure 8

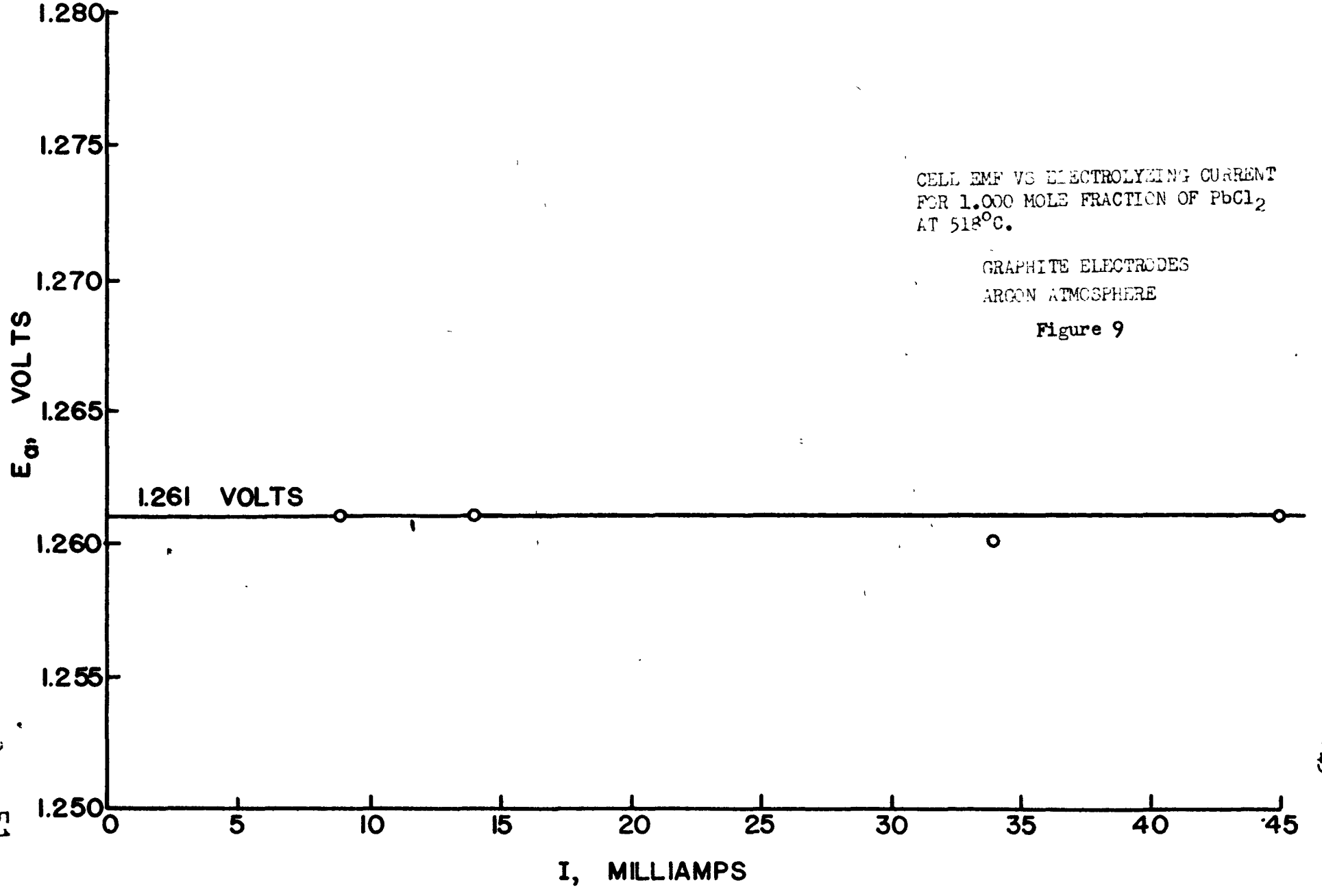


CELL EMF VS ELECTROLYZING CURRENT FOR 1.000 MOLE FRACTION OF $PbCl_2$ AT 518°C.

GRAPHITE ELECTRODES

ARGON ATMOSPHERE

**Figure 9**

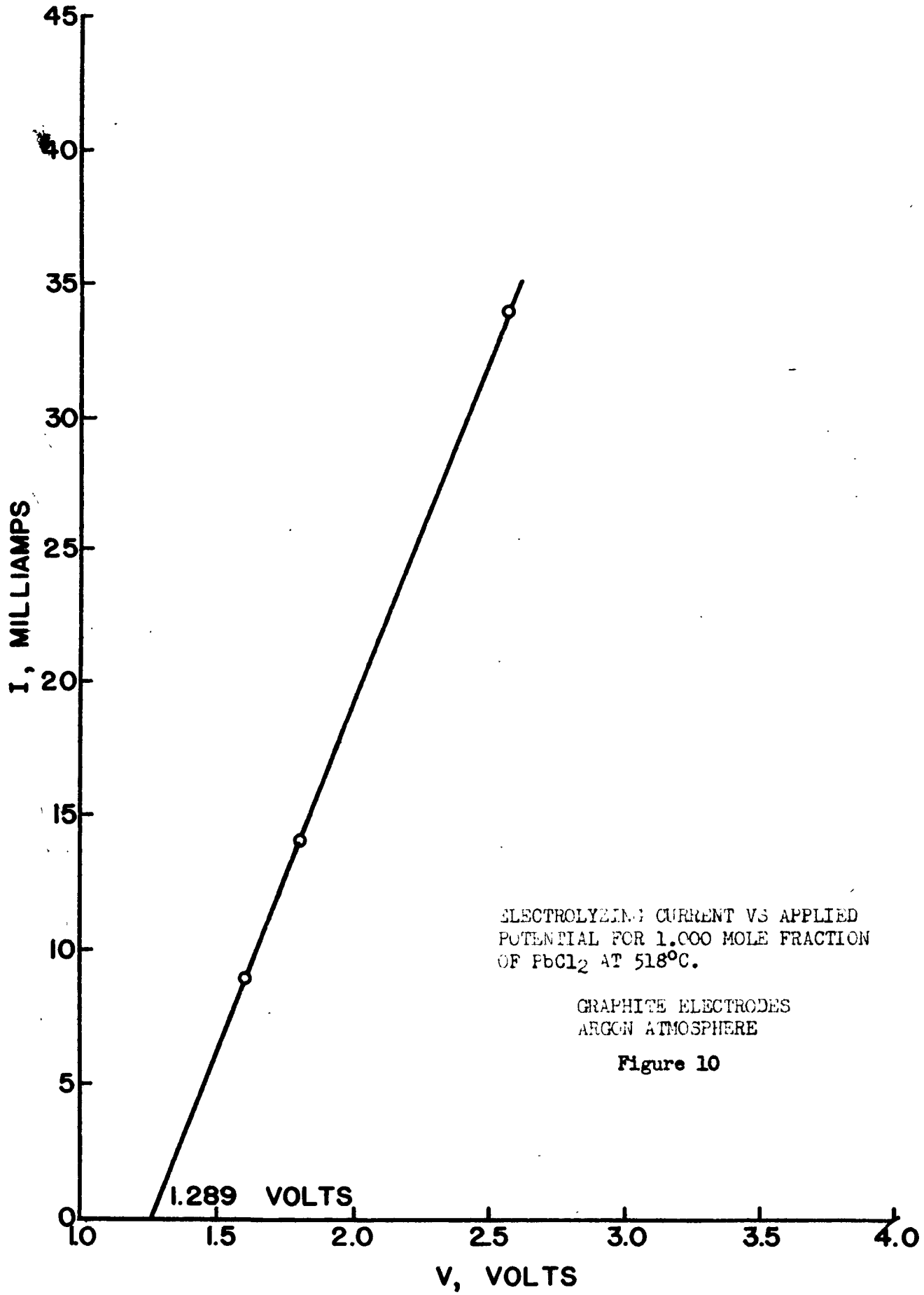


ELECTROLYZING CURRENT VS APPLIED POTENTIAL FOR 1.000 MOLE FRACTION OF $PbCl_2$ AT 518°C.

GRAPHITE ELECTRODES
ARGON ATMOSPHERE

**Figure 10**

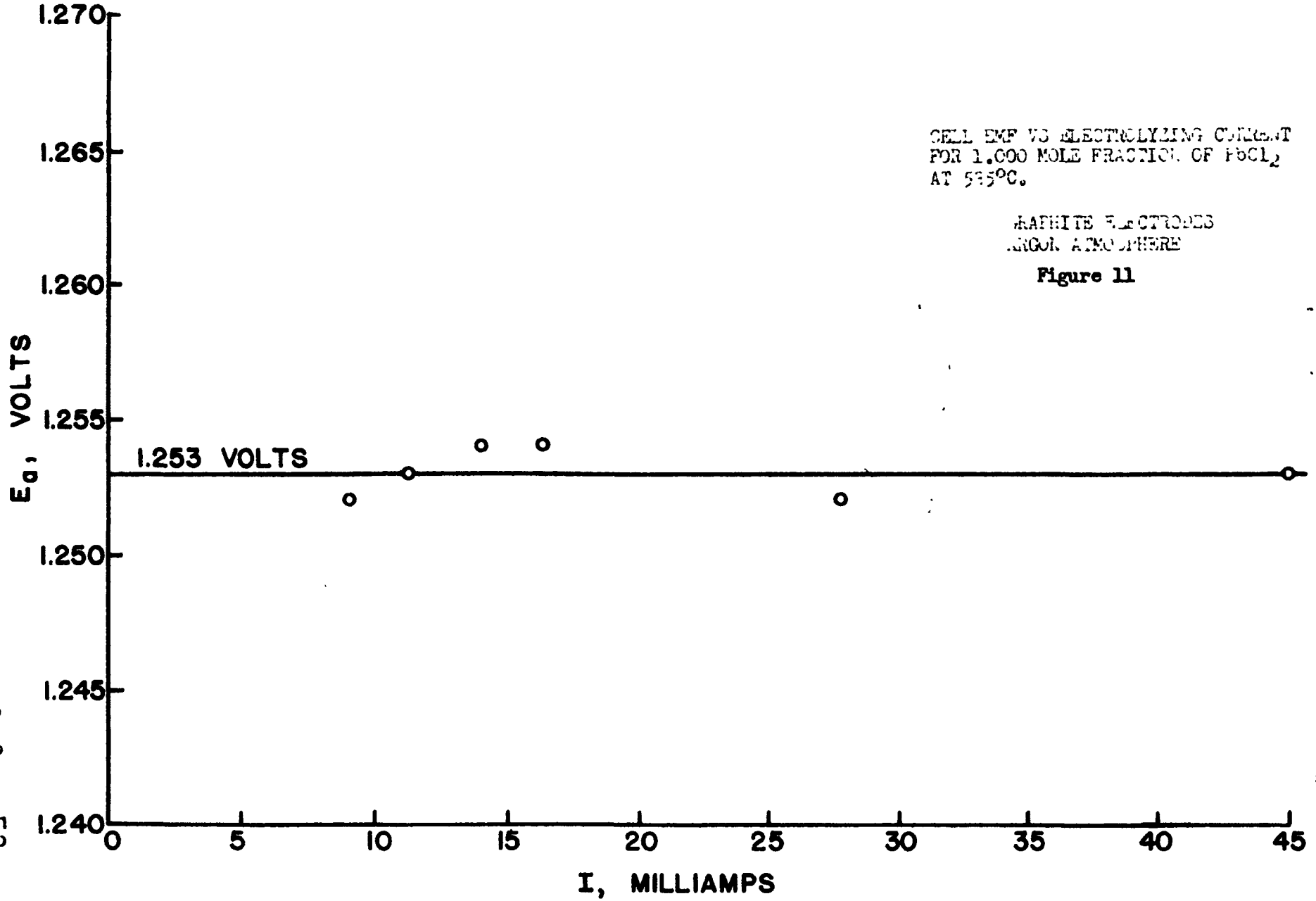


CELL EMF VS ELECTROLYZING CURRENT FOR 1.000 MOLE FRACTION OF $PbCl_2$ AT 535°C.

GRAPHITE ELECTRODES
ARGON ATMOSPHERE

**Figure 11**

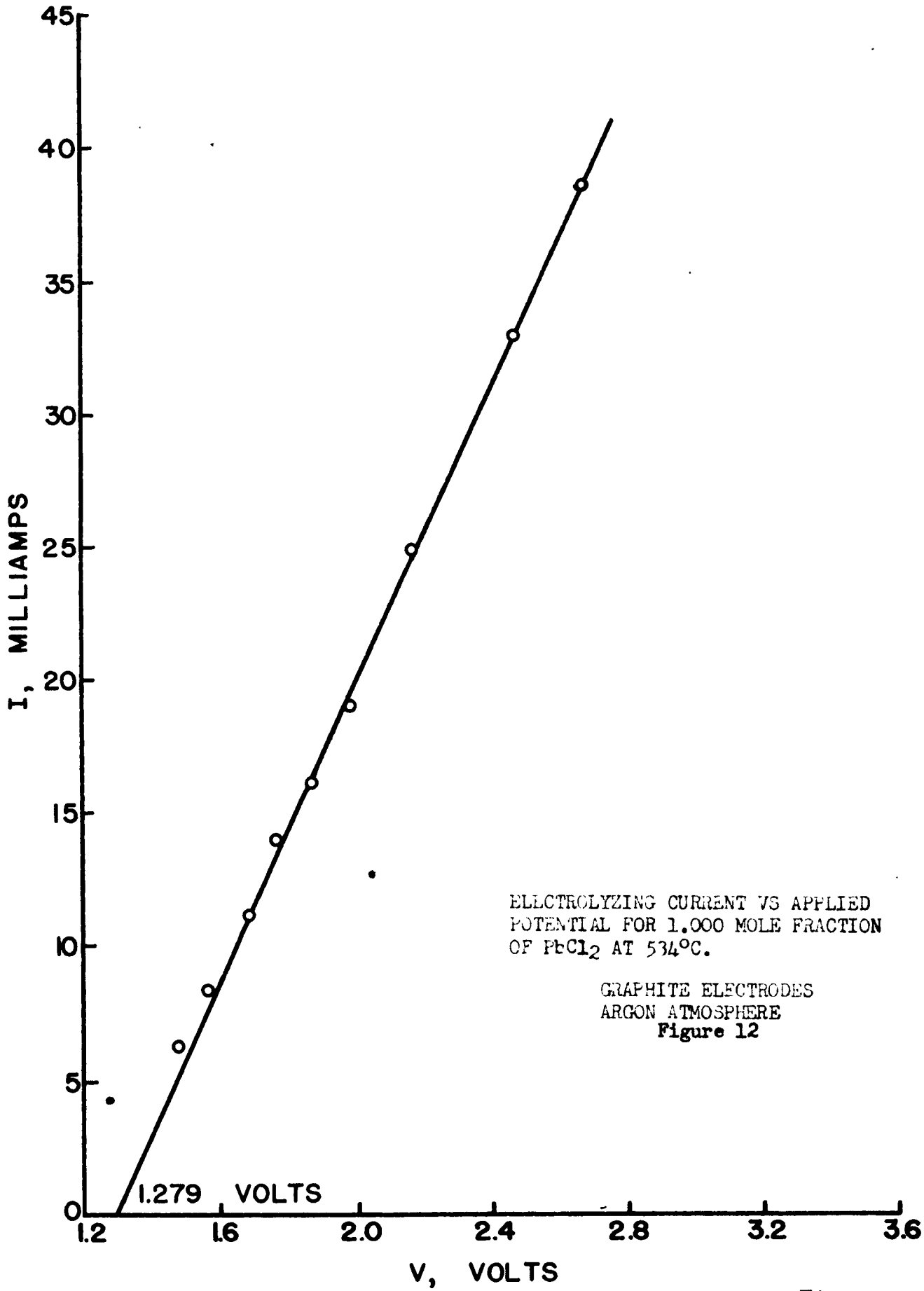


ELECTROLYZING CURRENT VS APPLIED POTENTIAL FOR 1.000 MOLE FRACTION OF $PbCl_2$ AT 534°C.

GRAPHITE ELECTRODES
ARGON ATMOSPHERE
**Figure 12**

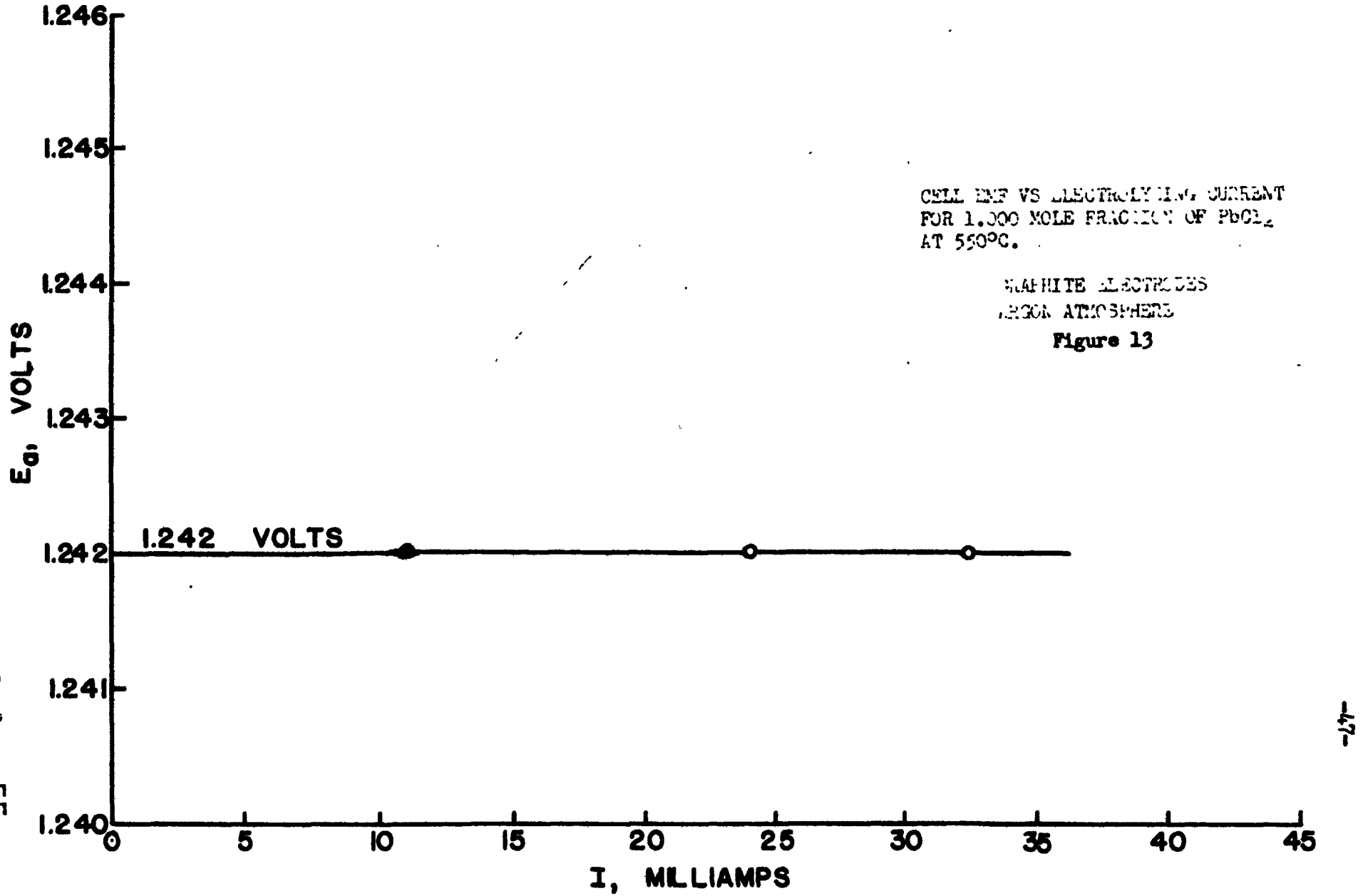


CELL EMF VS ELECTROLYZING CURRENT FOR 1.000 MOLE FRACTION OF $PbCl_2$ AT 550°C.

GRAPHITE ELECTRODES
ARGON ATMOSPHERE

**Figure 13**

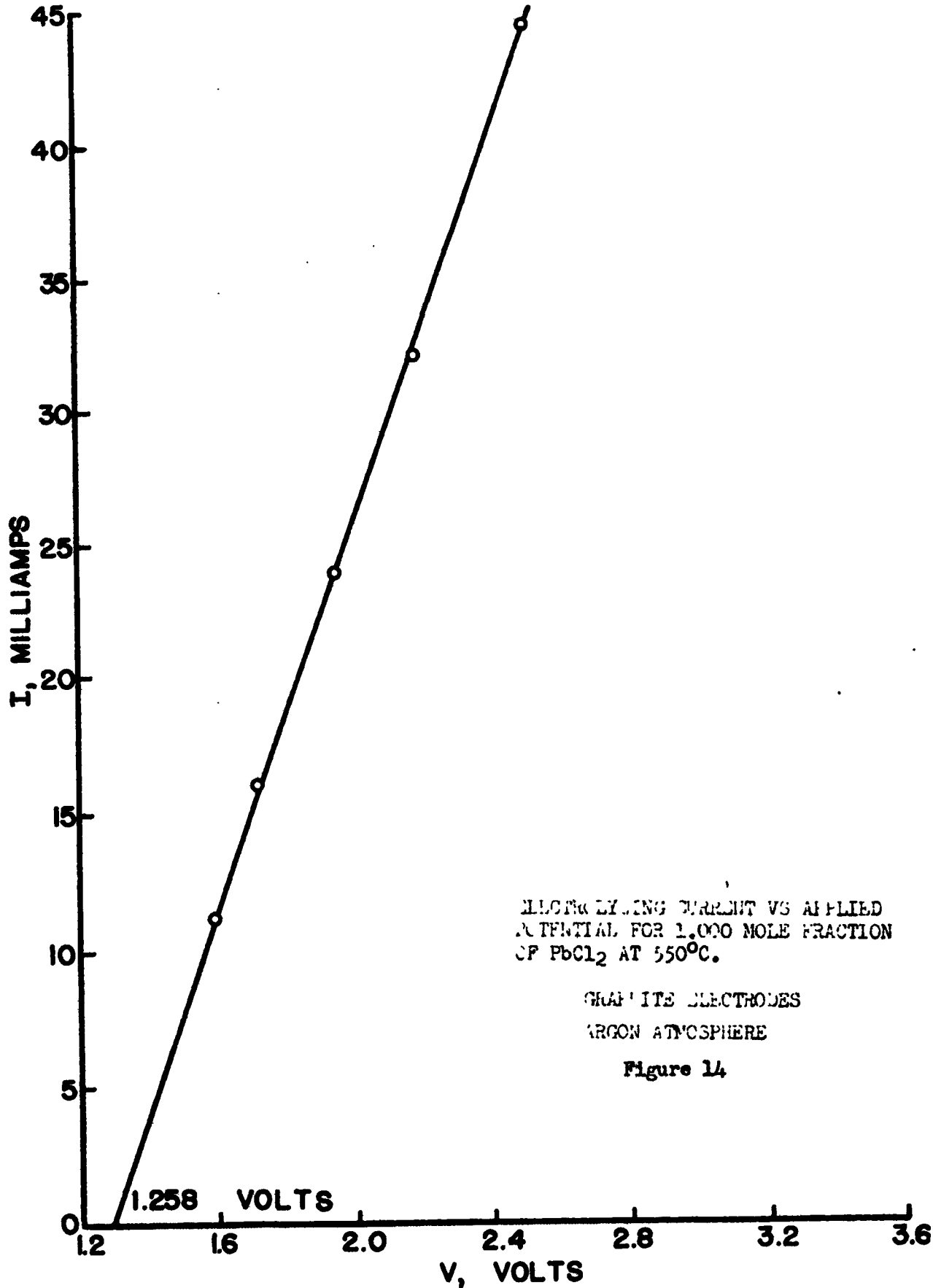


ELECTROLYZING CURRENT VS APPLIED POTENTIAL FOR 1.000 MOLE FRACTION OF $PbCl_2$ AT 550°C.

GRAPHITE ELECTRODES

ARGON ATMOSPHERE

**Figure 14**

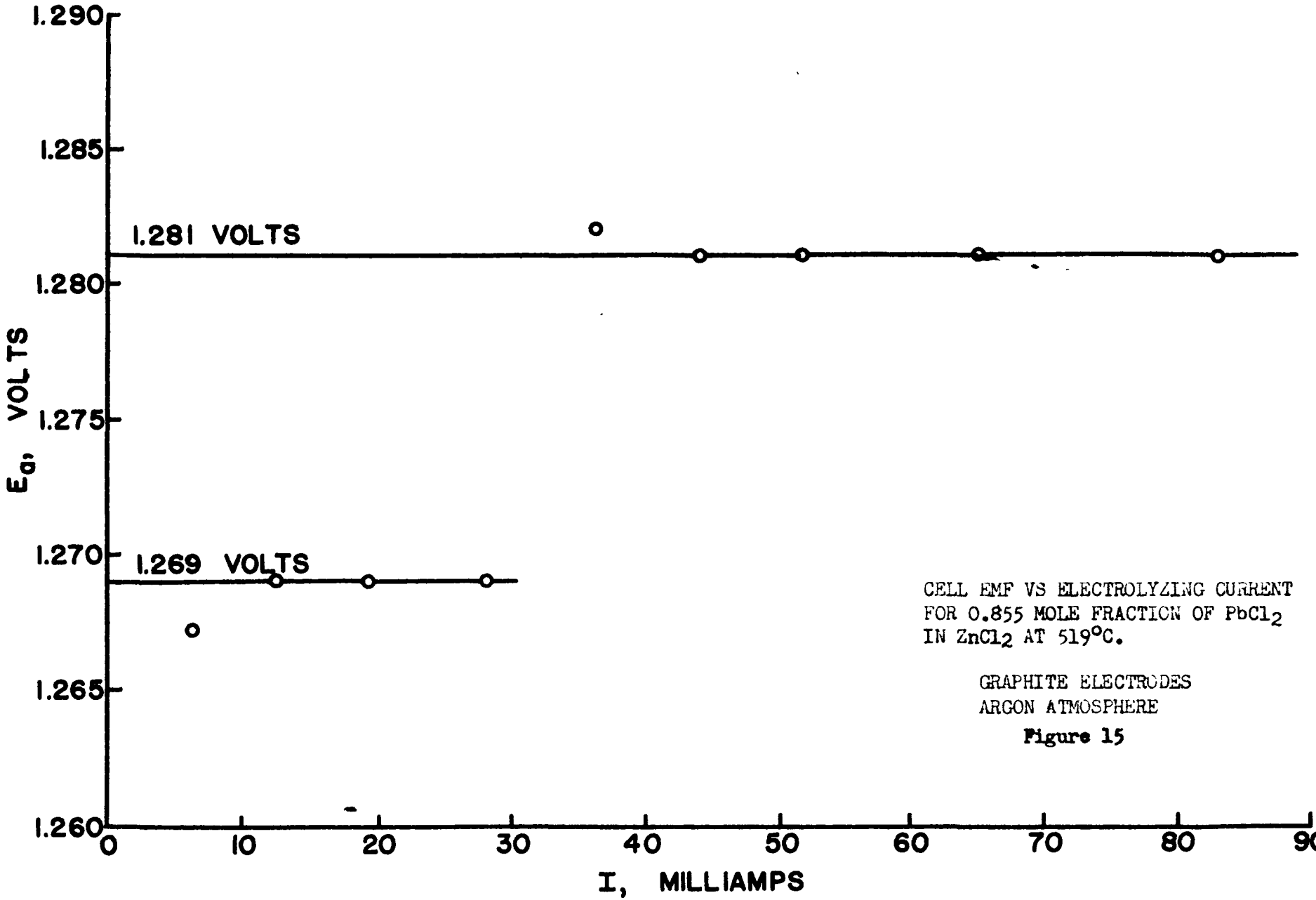


CELL EMF VS ELECTROLYZING CURRENT FOR 0.855 MOLE FRACTION OF $PbCl_2$ IN $ZnCl_2$ AT 519°C.

GRAPHITE ELECTRODES
ARGON ATMOSPHERE

**Figure 15**

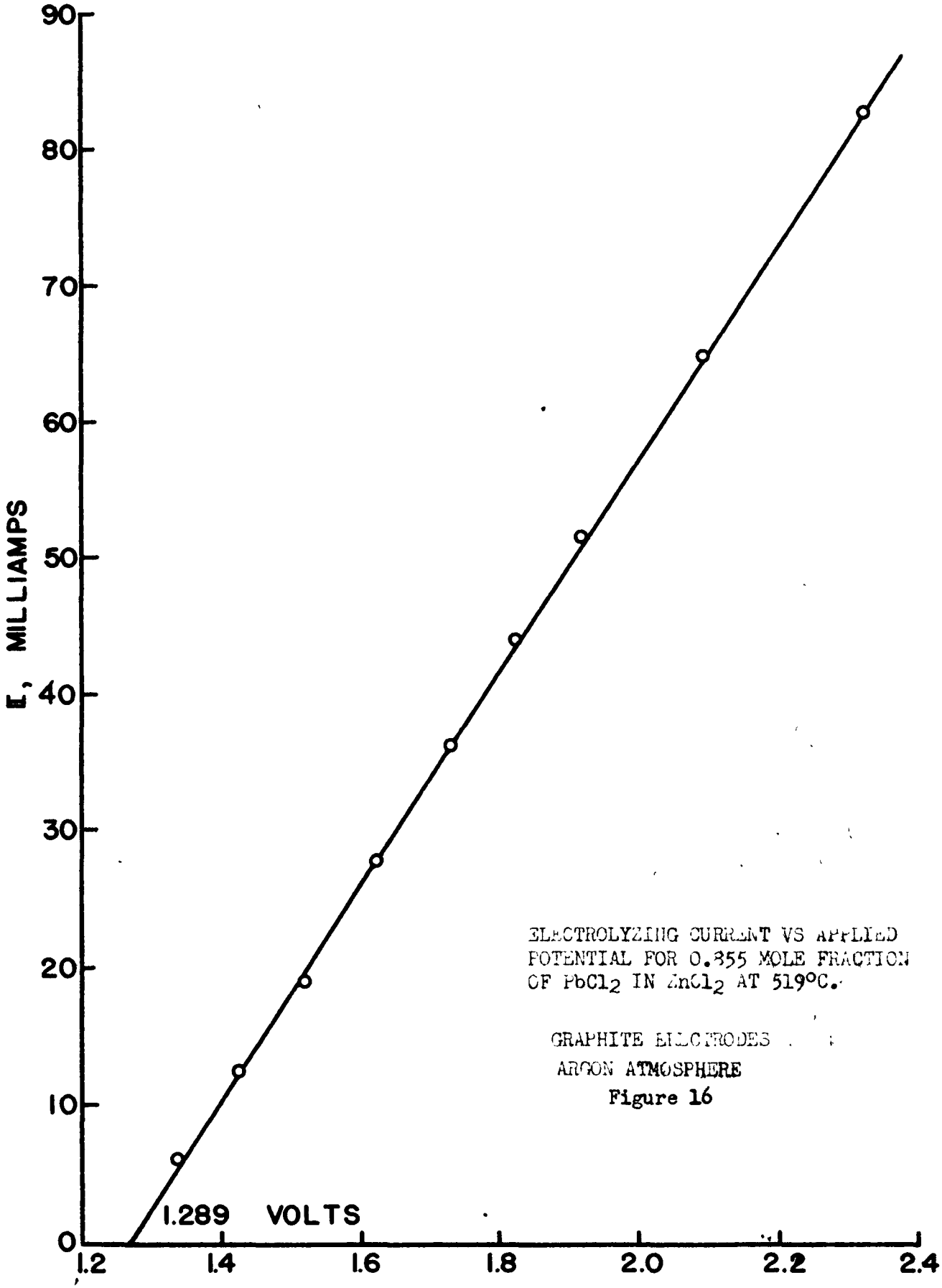


ELECTROLYZING CURRENT VS APPLIED POTENTIAL FOR 0.355 MOLE FRACTION OF $PbCl_2$ IN $ZnCl_2$ AT 519°C.

GRAPHITE ELECTRODES

ARGON ATMOSPHERE

**Figure 16**

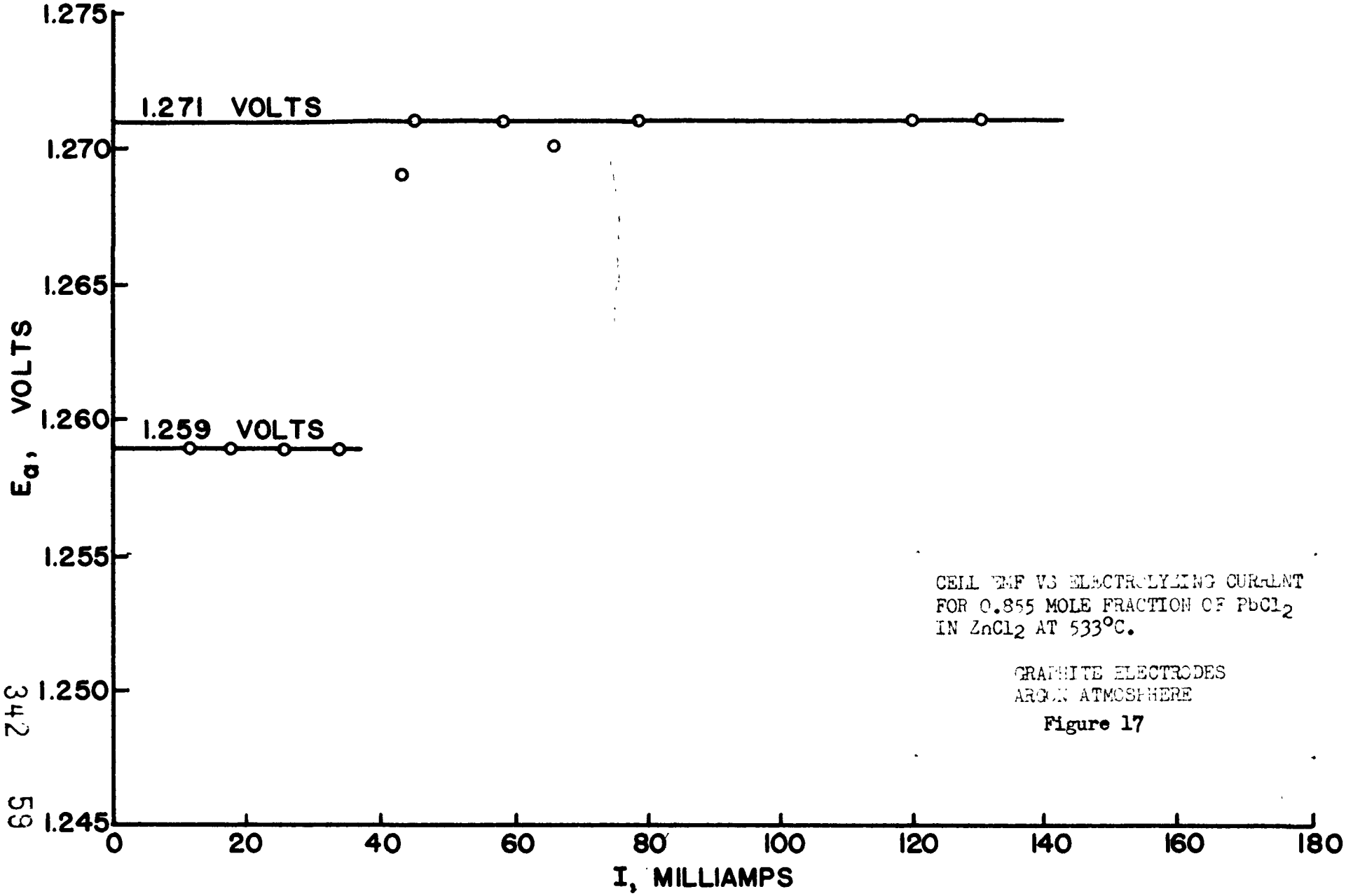


CELL EMF VS ELECTROLYZING CURRENT FOR 0.855 MOLE FRACTION OF $PbCl_2$ IN $ZnCl_2$ AT 533°C.

GRAPHITE ELECTRODES
ARGON ATMOSPHERE

**Figure 17**

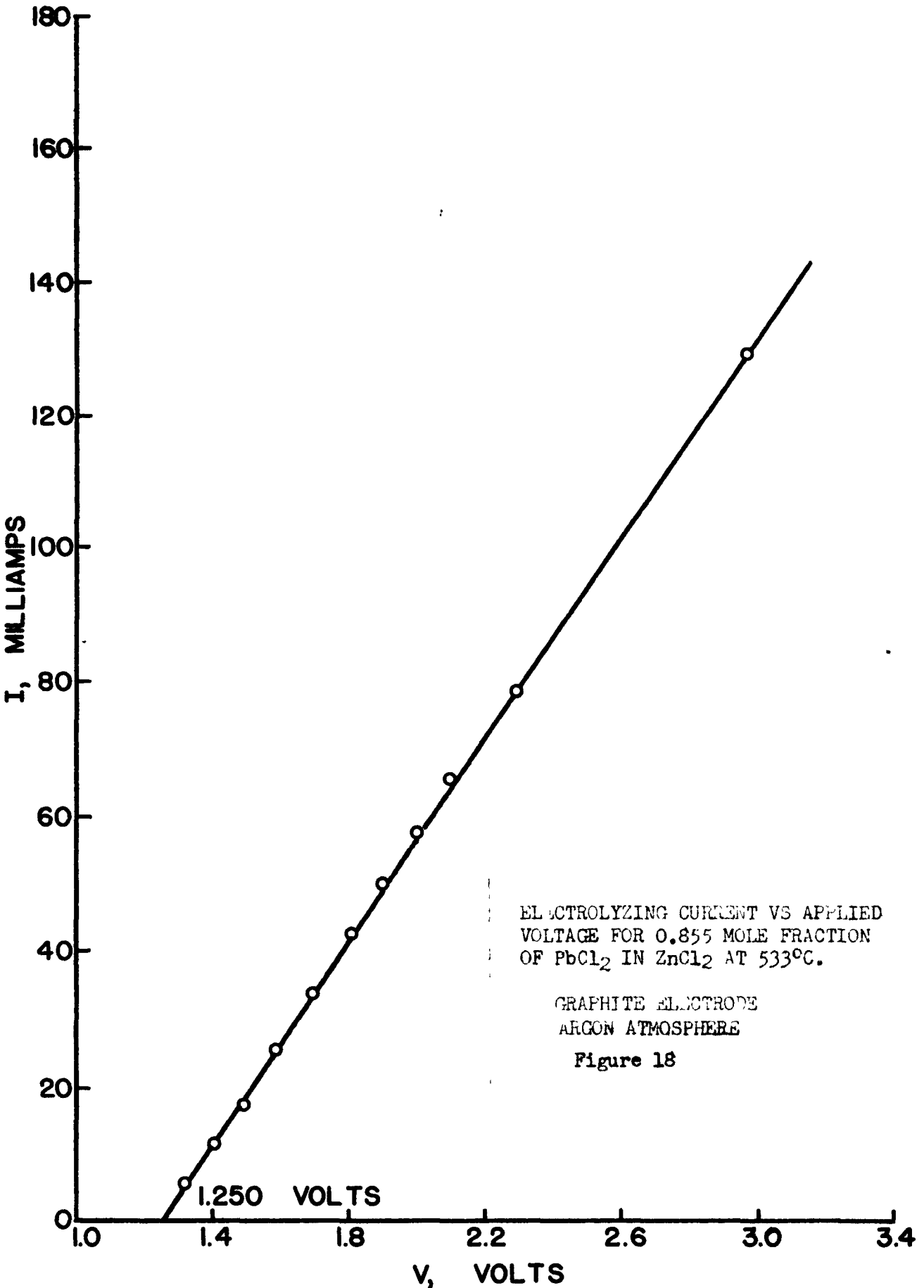


ELECTROLYZING CURRENT VS APPLIED VOLTAGE FOR 0.855 MOLE FRACTION OF $PbCl_2$ IN $ZnCl_2$ AT 533°C.

GRAPHITE ELECTRODE
ARGON ATMOSPHERE

**Figure 18**

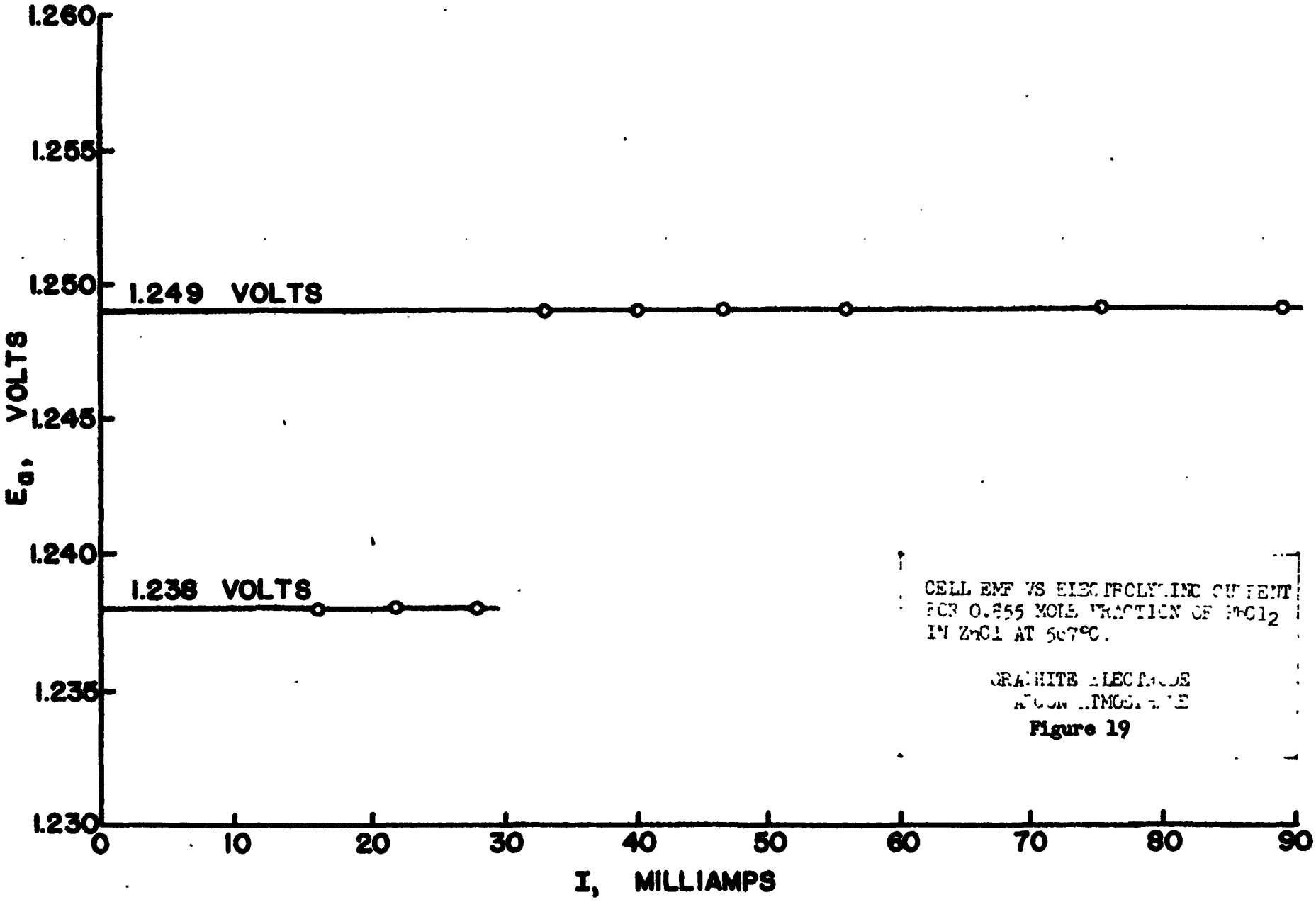


CELL EMF VS ELECTROLYTIC CURRENT FOR 0.855 MOLE FRACTION OF $PbCl_2$ IN ZnCl AT 507°C.

GRAPHITE ELECTRODE
ARGON ATMOSPHERE

**Figure 19**

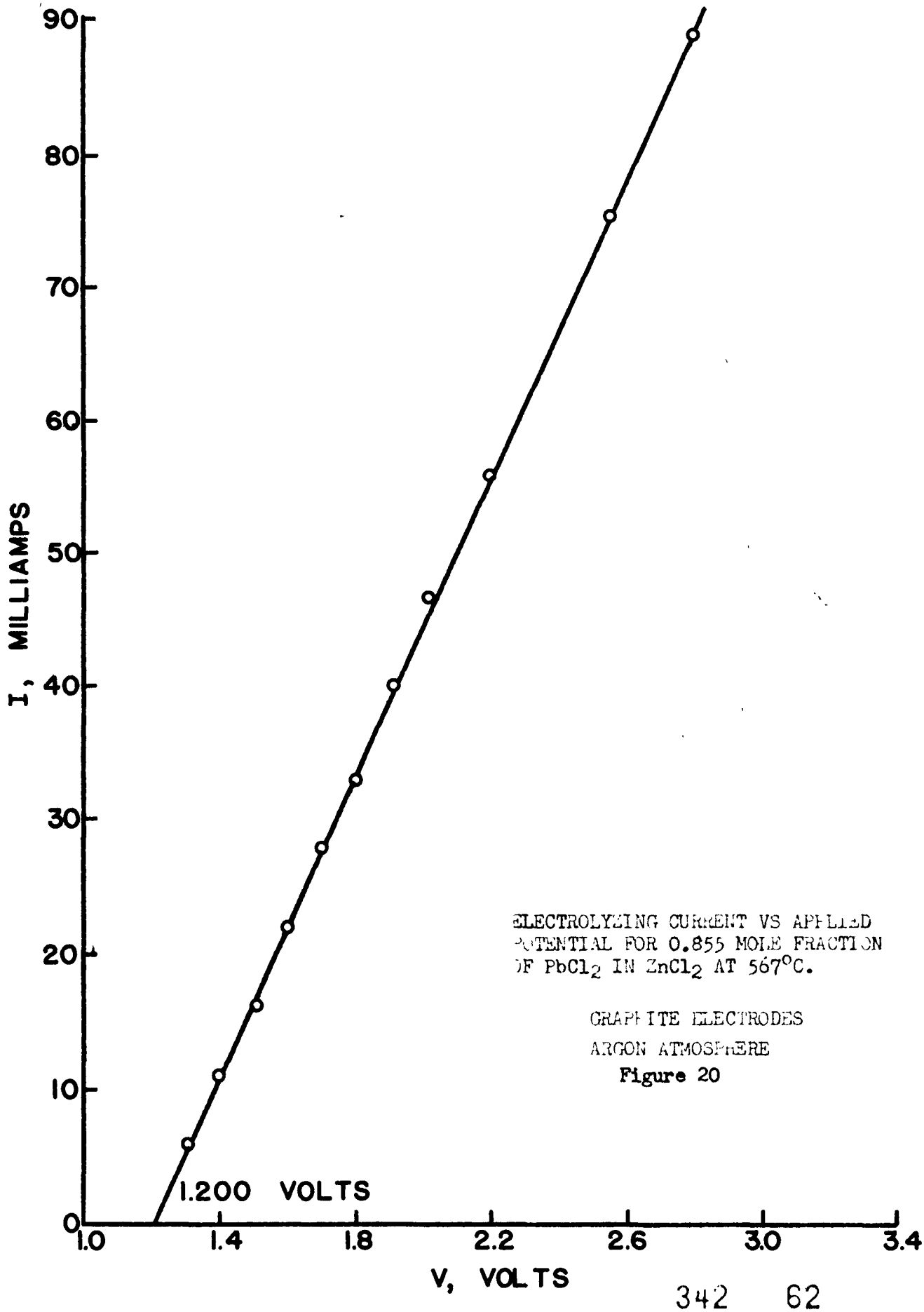


ELECTROLYZING CURRENT VS APPLIED POTENTIAL FOR 0.855 MOLE FRACTION OF $PbCl_2$ IN $ZnCl_2$ AT 567°C.

GRAPHITE ELECTRODES
ARGON ATMOSPHERE

**Figure 20**

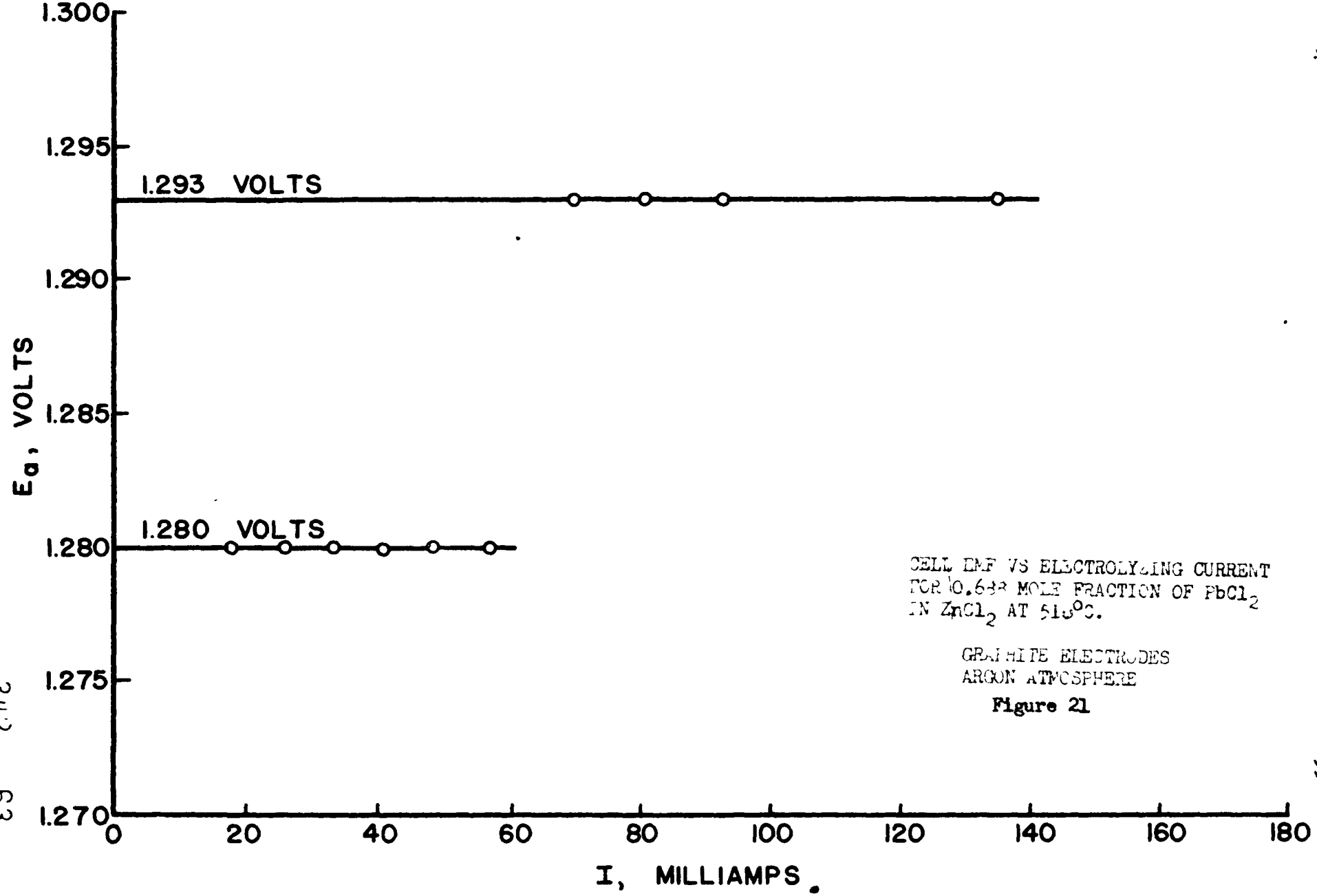


CELL EMF VS ELECTROLYZING CURRENT FOR 0.68 MOLE FRACTION OF $PbCl_2$ IN $ZnCl_2$ AT 515°C.

GRAPHITE ELECTRODES
ARGON ATMOSPHERE

**Figure 21**

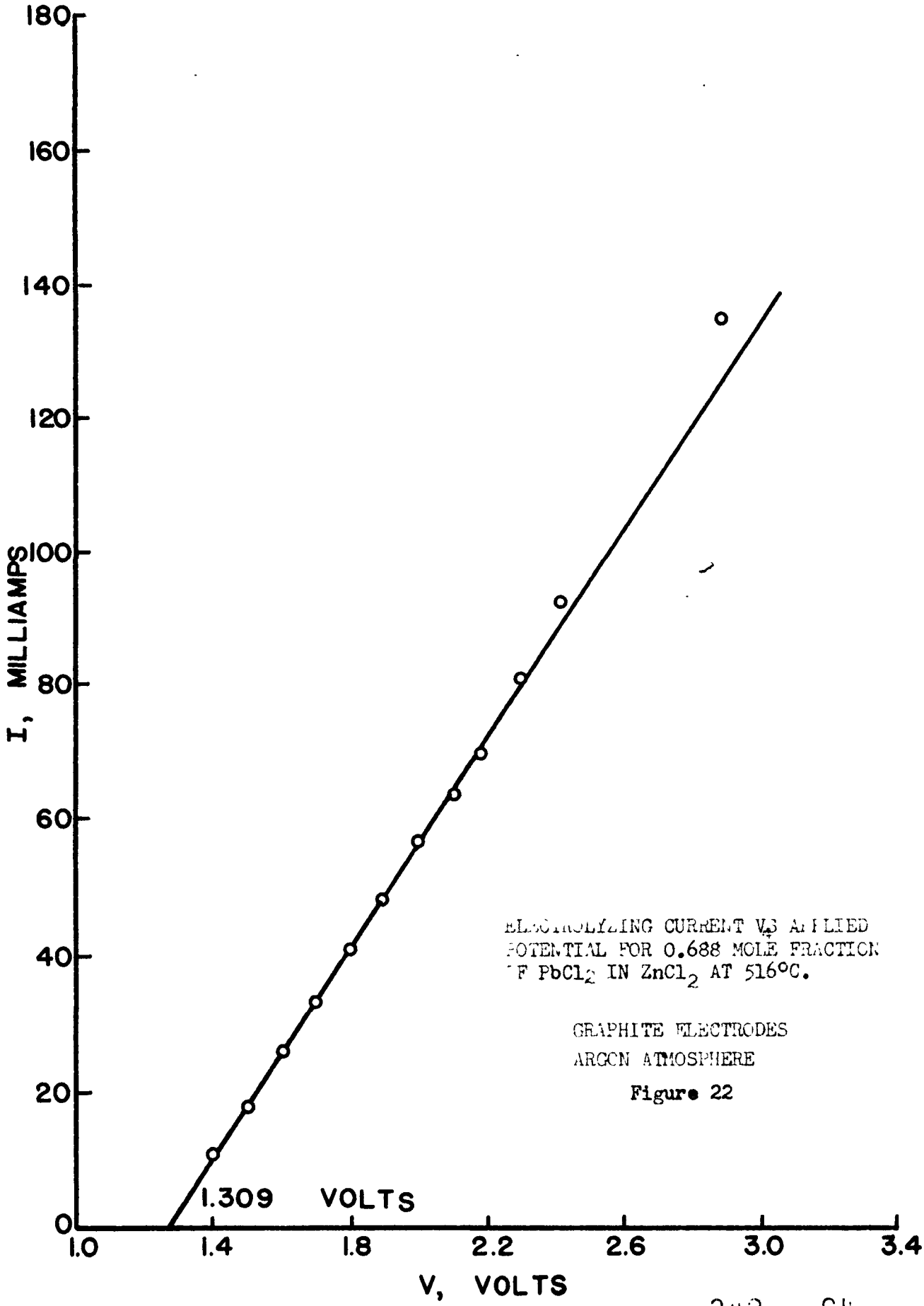


ELECTROLYZING CURRENT VS APPLIED POTENTIAL FOR 0.688 MOLE FRACTION OF $PbCl_2$ IN $ZnCl_2$ AT 516°C.

GRAPHITE ELECTRODES
ARGON ATMOSPHERE

**Figure 22**

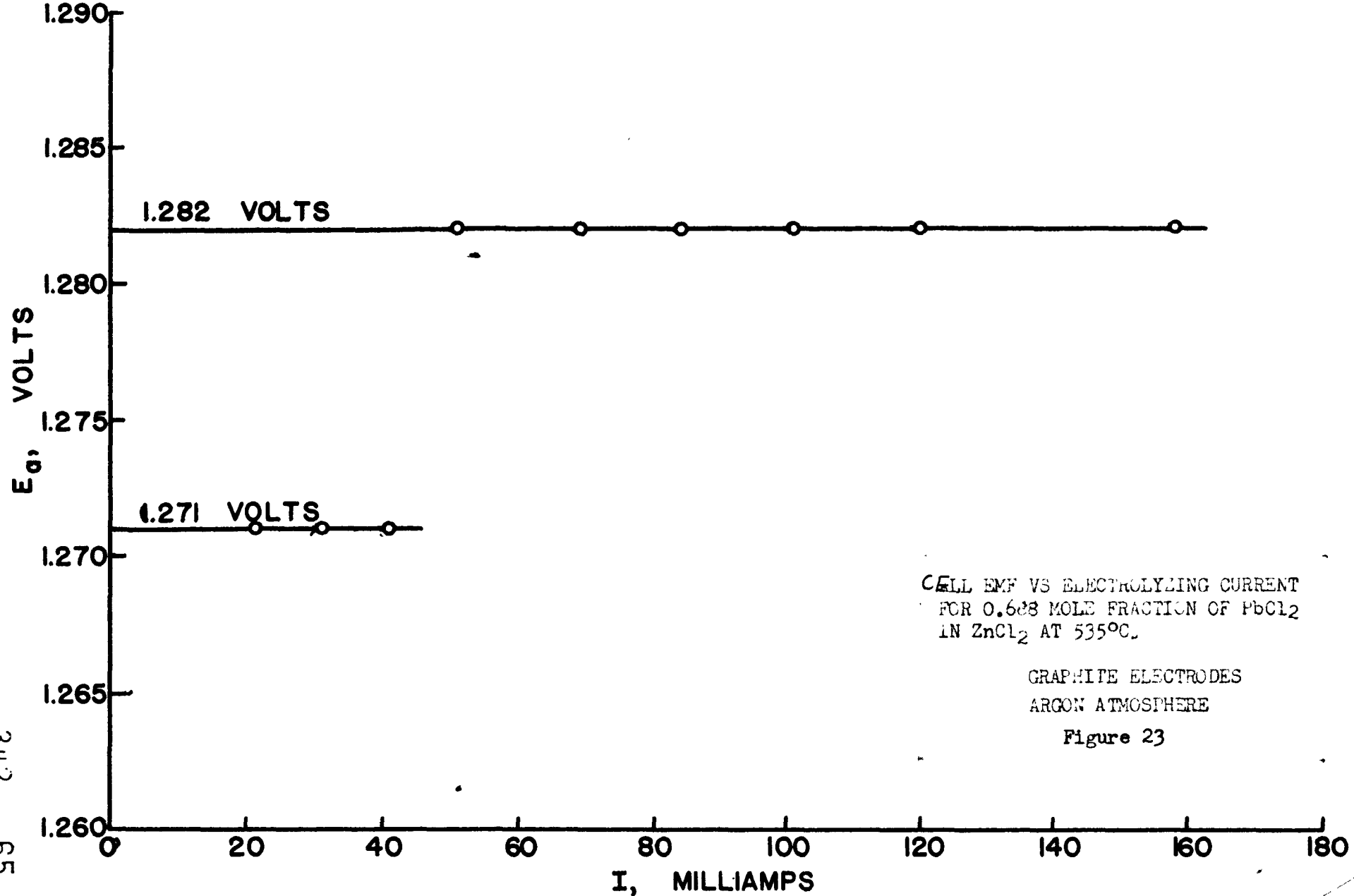


CELL EMF VS ELECTROLYZING CURRENT FOR 0.608 MOLE FRACTION OF $PbCl_2$ IN $ZnCl_2$ AT 535°C.

GRAPHITE ELECTRODES
ARGON ATMOSPHERE

Figure 23

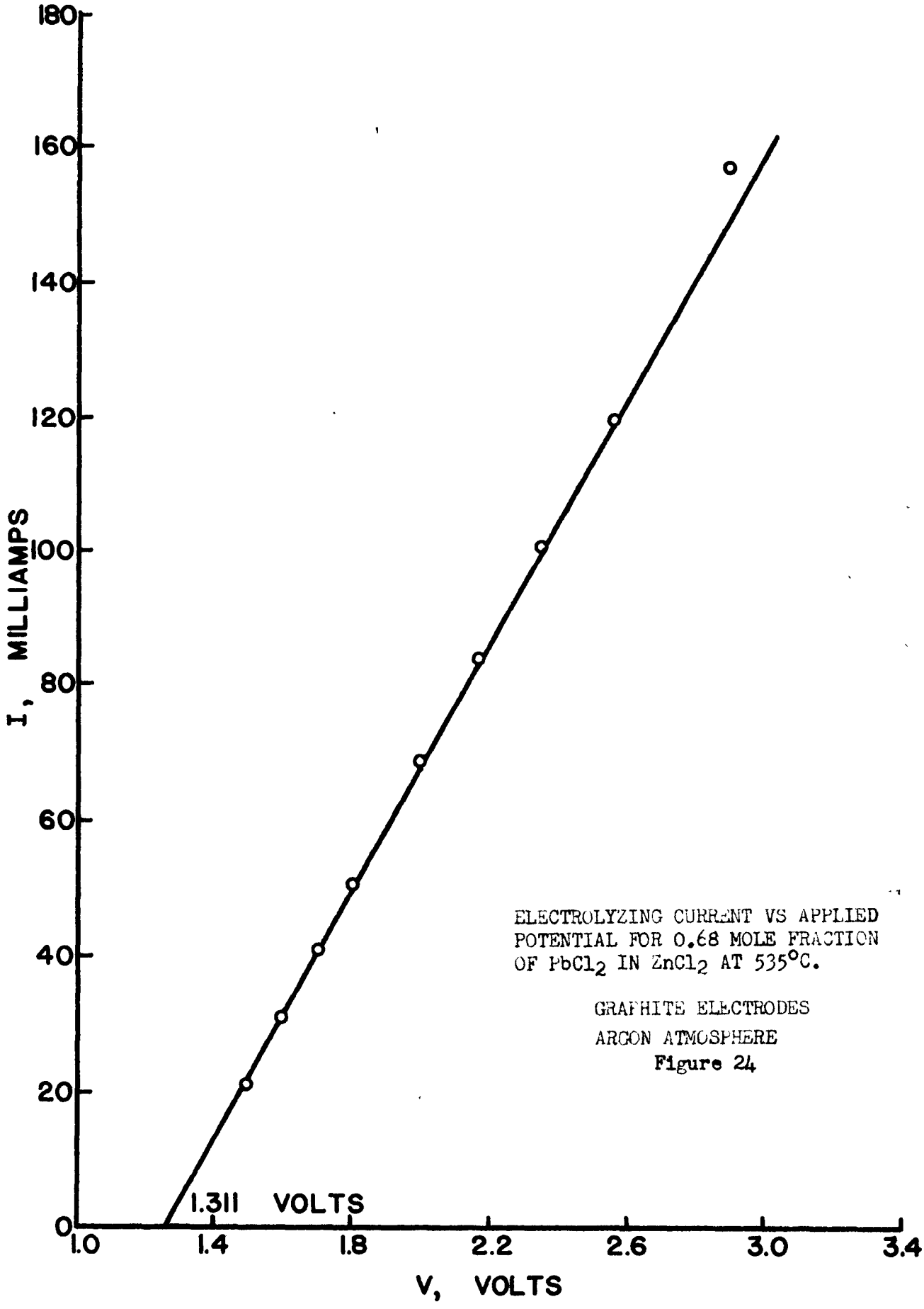


ELECTROLYZING CURRENT VS APPLIED POTENTIAL FOR 0.68 MOLE FRACTION OF $PbCl_2$ IN $ZnCl_2$ AT 535°C.

GRAPHITE ELECTRODES

ARGON ATMOSPHERE

**Figure 24**

3) In order that measurements be made by the new back-emf method, the ionic conductivity must be great enough to ensure a sufficient current density to give a rate of deposition greater than the rate of loss through solution, vaporization, etc.

4) There is a characteristic "break" in the cell emf versus electrolyzing current plot corresponding to each cationic species present.

Electrolysis of LiCl - KCl Eutectic

The eutectic mixture of LiCl - KCl (0.42 mol fraction KCl and 0.58 mol fraction of LiCl) has many properties which make it an excellent molten salt solvent. These properties are:-

1) Low eutectic melting point of 355°C.

2) Large theoretical decomposition potential of the component salts, LiCl and KCl.

3) Large ionic conductivity, which increases the sensitivity of both the decomposition potential measurement and the back-emf analysis.

4) Many of the metal chlorides exhibit an appreciable solubility in the molten eutectic.

5) The addition of LiCl and KCl to a metal chloride decreases the solubility of the metal in its molten salt, thereby increasing the current efficiency.

6) Low vapor pressure of the eutectic mixture.

This solvent was used in much of the present work. Accordingly, it was thought desirable to give it particular study. The variables studied were the decomposition potential and the thermodynamic emf as a function of temperature for the range 500°C to 600°C. Since graphite is attacked by both molten Li and K, an iron rod was used as the cathode while graphite served as the anode.

The experimental results are tabulated in Table II and thermodynamic emf's are compared with the calculated thermodynamic emf's in figure 25. Decomposition potential curves are given in figures 27, 29, 31 and the curves of cell emf versus electrolyzing current in figures 26, 28, 30.

The decomposition potentials are in poor agreement with thermodynamic emf's. Figure 30 shows "breaks" characteristic for the deposition of lithium ion as well as for potassium ion. In the electrolysis of the eutectic of LiCl - KCl, the decomposition potentials of the two salts are close together. Thus it is possible that for the experiments at 513°C and 557°C the applied potential was above the decomposition potential of both salt components and the lower break was missed completely. There is a double break in the $E_a$ versus I curve for 567°C, but the value corresponding to the decomposition of KCl is less than the calculated theoretical value because the potassium was not in its standard pure state but in solution in the lithium. It can be concluded that the measured values are, in general, those for the eutectic and no attempt will be made to correlate the measured values with the deposition of either cation. The experimental and thermodynamic emf's fall within the calculated emf band as given by figure 25.

The conclusions that can be drawn from experimental work on the molten LiCl - KCl eutectic are:-

1) The measured thermodynamic emf's show reasonable agreement with calculated thermodynamic emf's.

2) The decay curve fits the empirical relationship $E_{..} = E_a - k\, t^{1}/2$.

Electrolysis of LiCl - KCl - $NdCl_3$

The electrolysis of LiCl - KCl eutectic containing $NdCl_3$ was studied at 513°C and 586°C and for contents up to 0.03 mol fraction

TABLE II

Summary of the Electrolysis Data for LiCl-KCl Eutectic, 0.42 Mol Fraction KCl and 0.58 Mol Fraction LiCl

| $E_{ao}$ | Theo. emf (LiCl) | D.P. | Temp. |
|---|---|---|---|
| 3.6080 | 3.647 ± .087 volts | 3.55 | 513°C |
| 3.5835 | 3.620 ± .087 | 3.64 | 557 |
| 3.5820<br>3.5750 | 3.614 ± .087 | 3.64 | 567 |

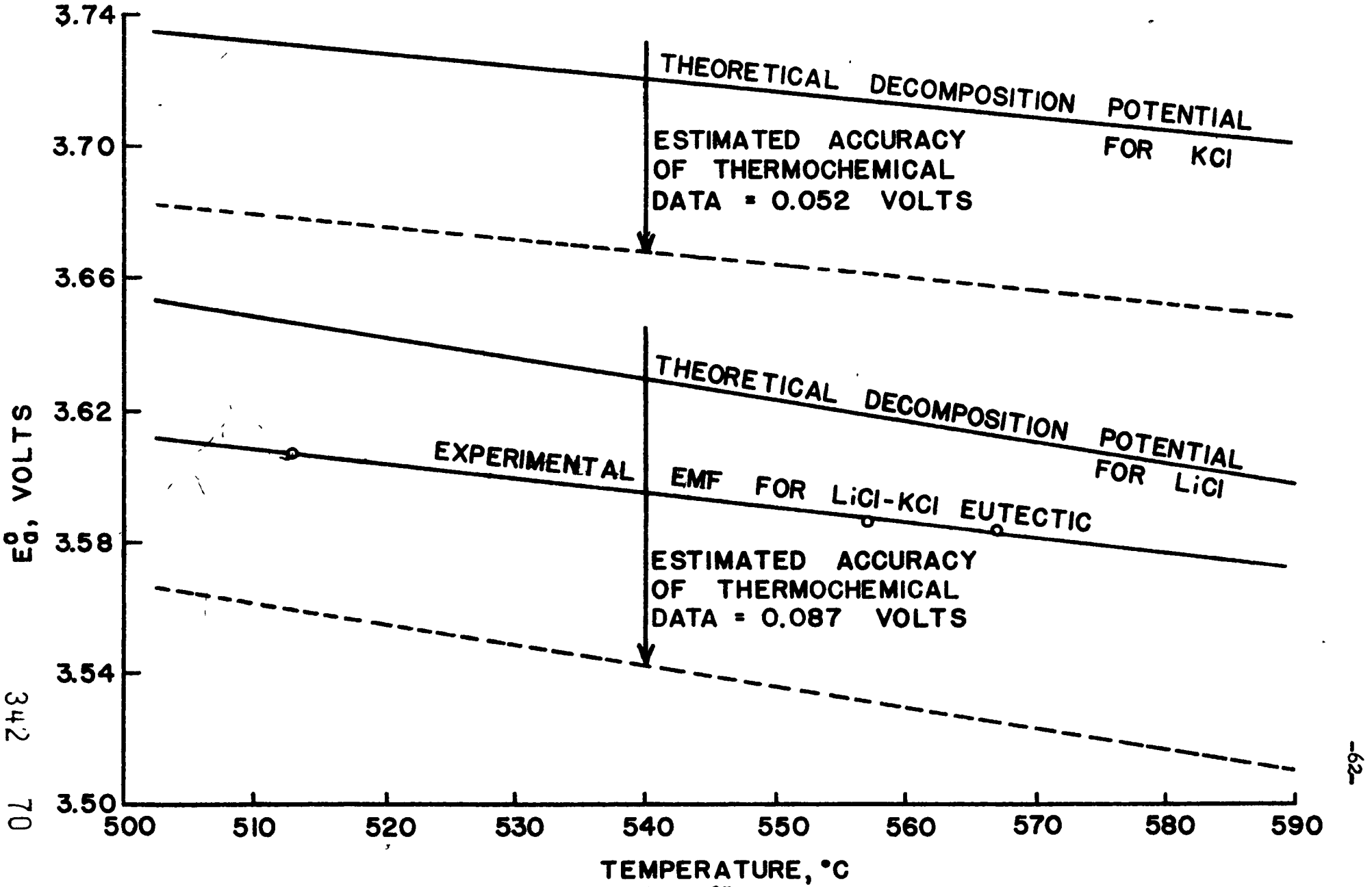


Figure 25

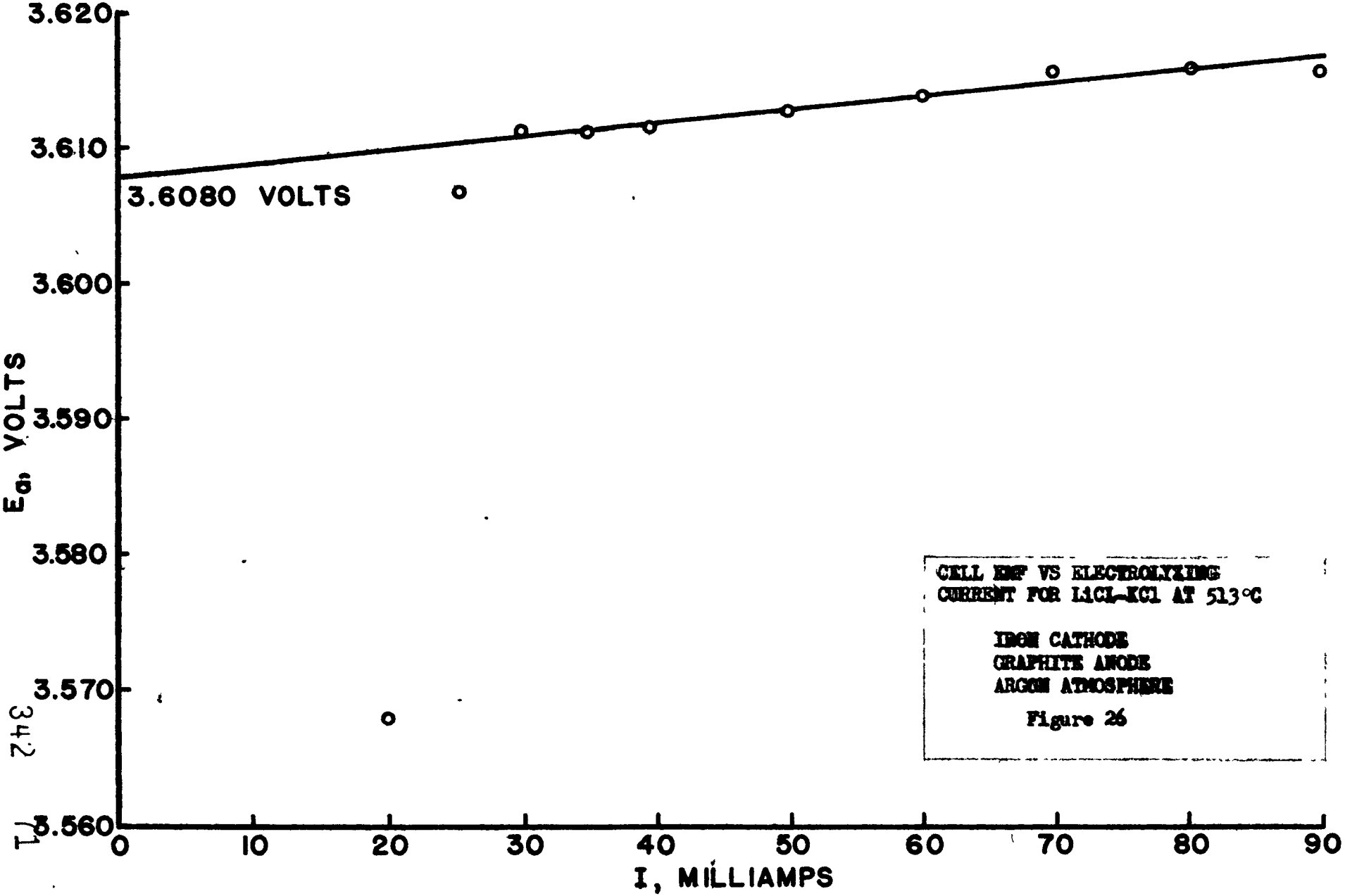


CELL EMF VS ELECTROLYZING CURRENT FOR LiCl-KCl AT 513°C

IRON CATHODE
GRAPHITE ANODE
ARGON ATMOSPHERE

Figure 26

342

-63-

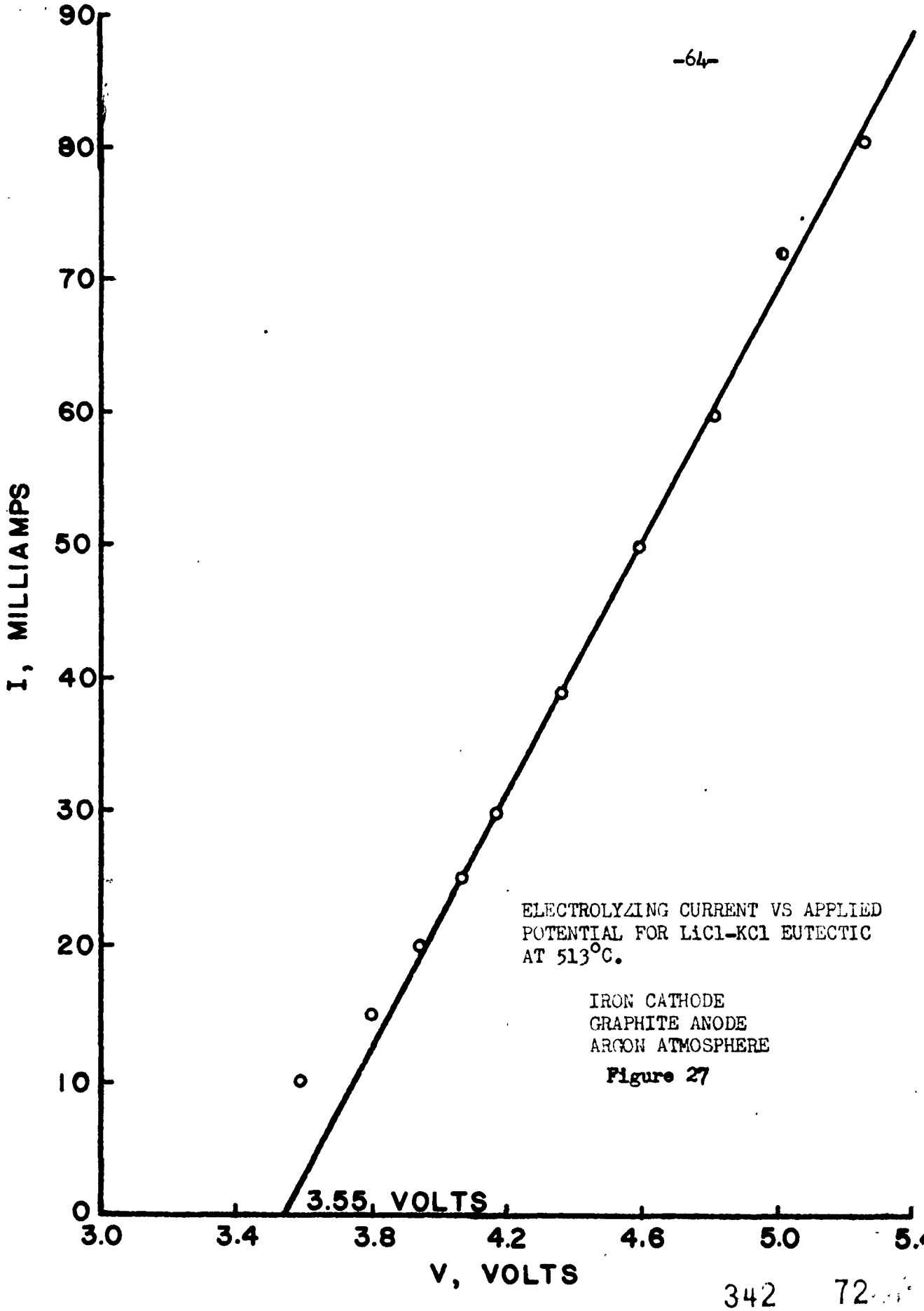


ELECTROLYZING CURRENT VS APPLIED POTENTIAL FOR LiCl-KCl EUTECTIC AT 513°C.

IRON CATHODE
GRAPHITE ANODE
ARGON ATMOSPHERE

**Figure 27**

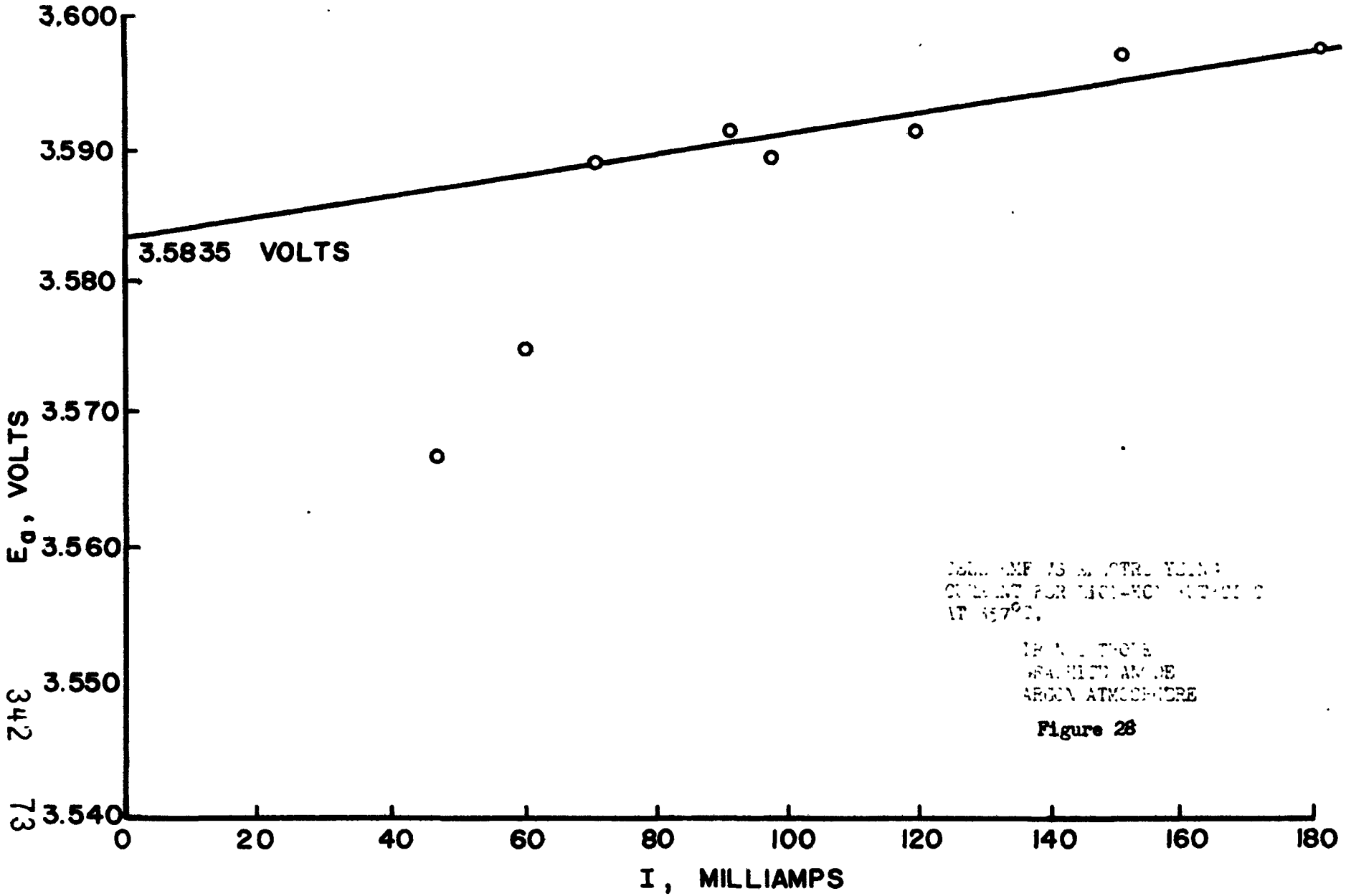
3.600
3.590
3.580
3.570
3.560
3.550
3.540
3.5835 VOLTS
$E_a$, VOLTS
0
20
40
60
80
100
120
140
160
180
I, MILLIAMPS

Figure 28

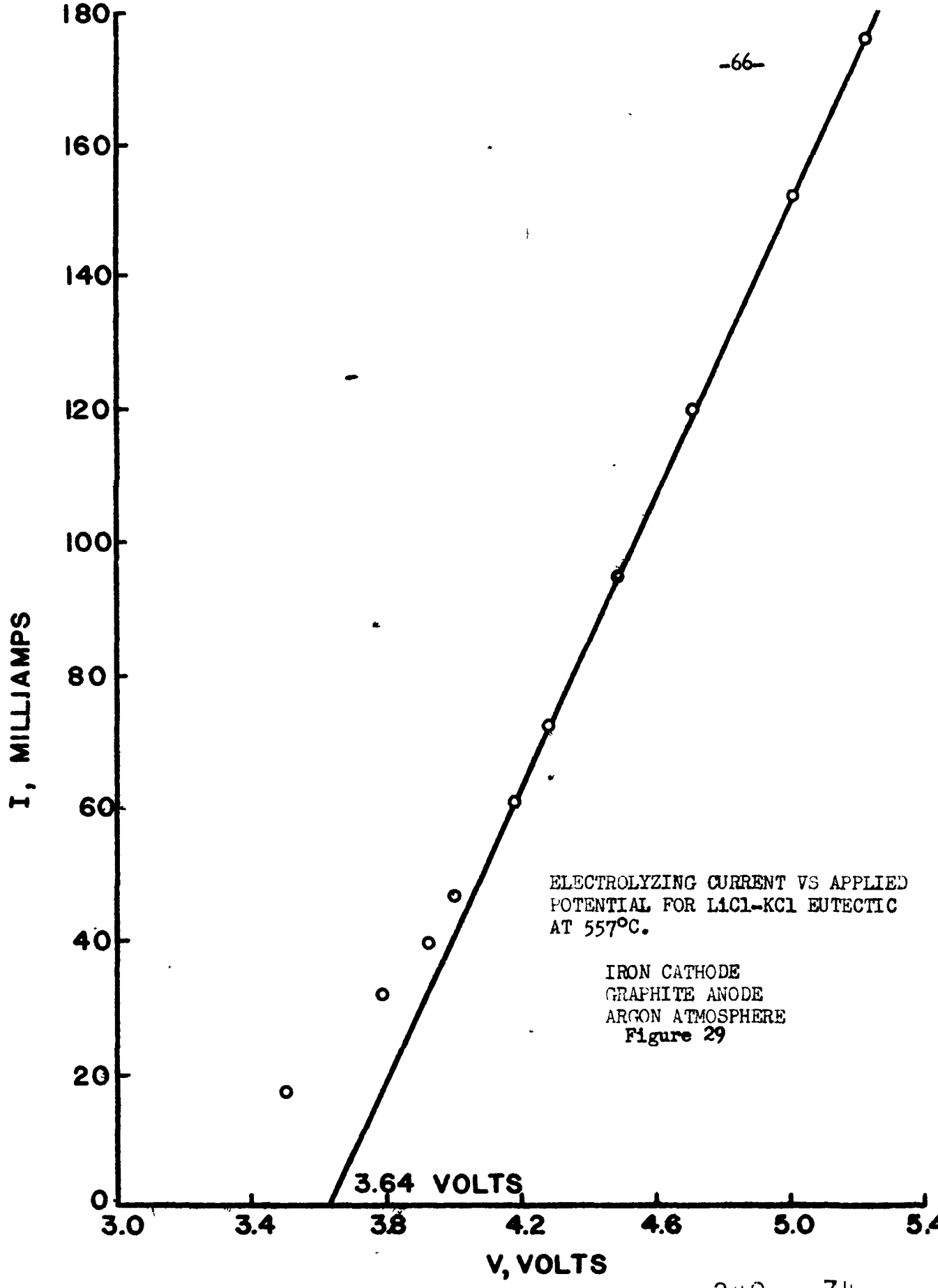


ELECTROLYZING CURRENT VS APPLIED POTENTIAL FOR LiCl-KCl EUTECTIC AT 557°C.

IRON CATHODE
GRAPHITE ANODE
ARGON ATMOSPHERE

**Figure 29**

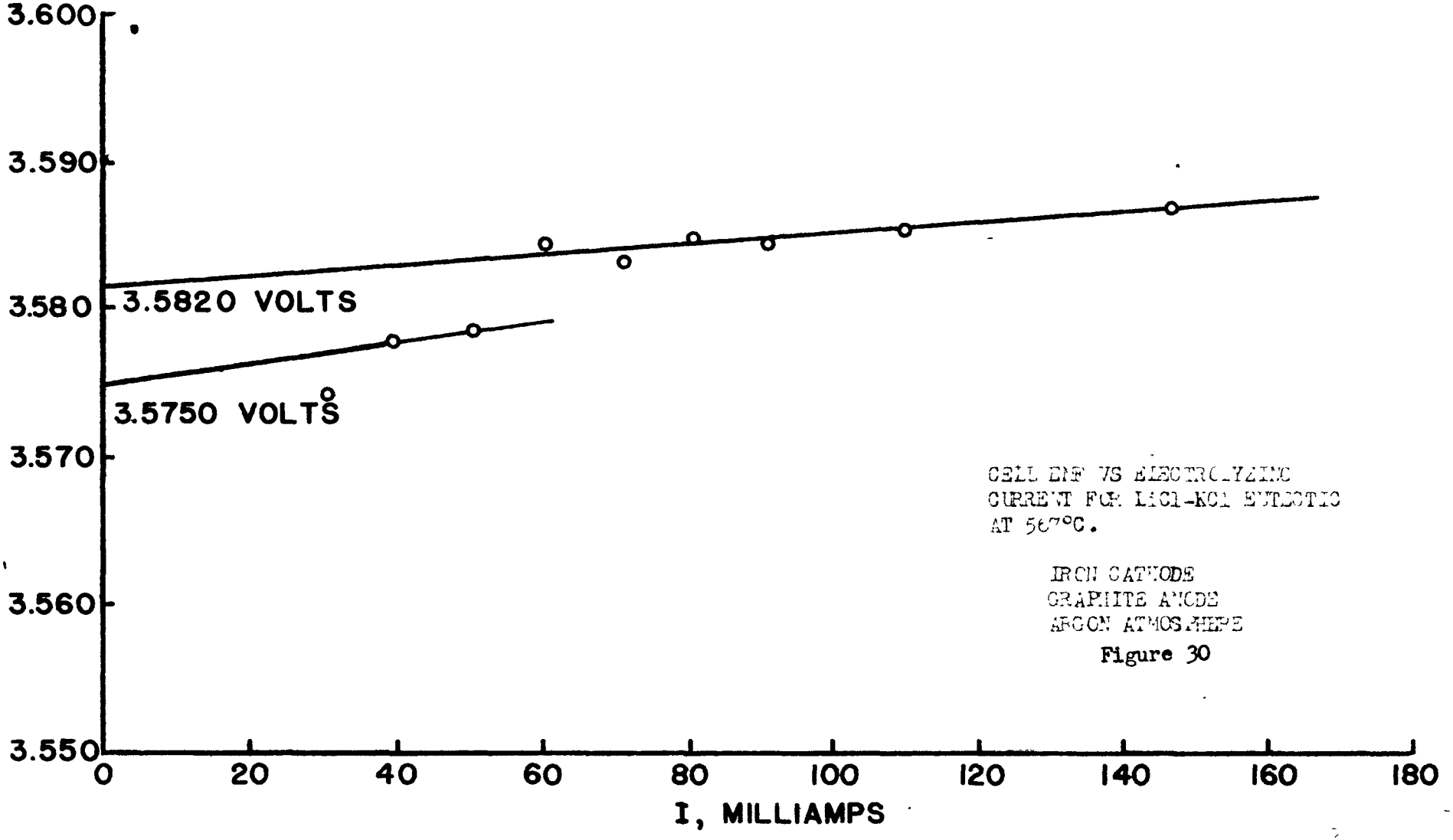


CELL EMF VS ELECTROLYZING CURRENT FOR LiCl-KCl EUTECTIC AT 567°C.

IRON CATHODE
GRAPHITE ANODE
ARGON ATMOSPHERE

**Figure 30**

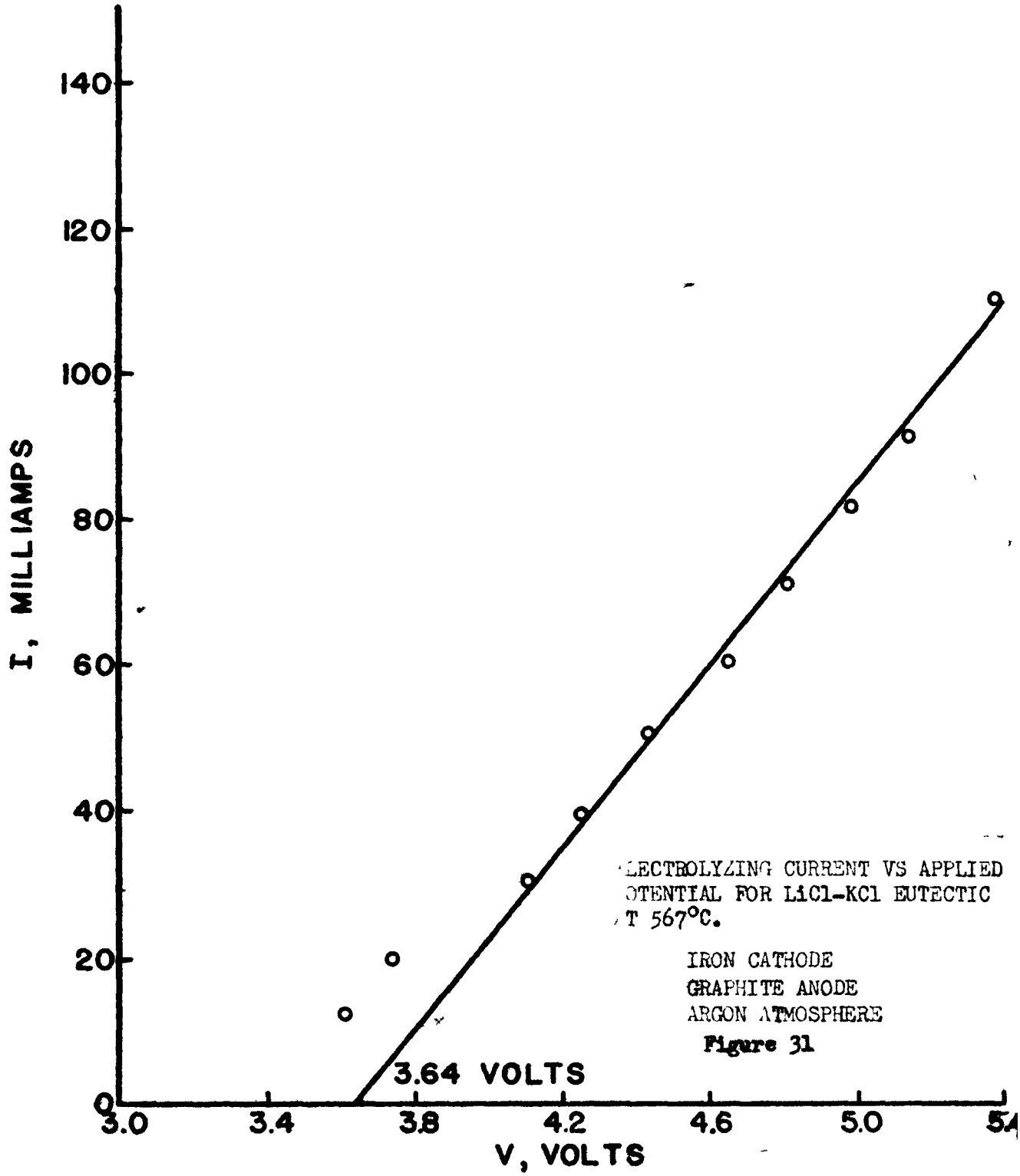


ELECTROLYZING CURRENT VS APPLIED POTENTIAL FOR LiCl-KCl EUTECTIC AT 567°C.

IRON CATHODE
GRAPHITE ANODE
ARGON ATMOSPHERE

**Figure 31**

of $NdCl_3$ which corresponds to 15 weight %. The thermodynamic emf ($E_{ao}$) is for the cell $Nd/NdCl_3$ in LiCl - KCl eutectic/$Cl_{2(g)}$. The results of this study are given as the decomposition potential and the thermodynamic emf ($E_{ao}$).

The decomposition potential curves for electrolysis at 513°C are given in figures 35, 39, while the curves for evaluating the thermodynamic emf are given in figures 34, 36, 38. The decomposition potential curves for the electrolysis at 586°C are given in figures 41, 43, 45, 47, and the curves for evaluating the thermodynamic emf are given in figures 42, 44, 46, 48.

The cell $Nd/NdCl_3$ in LiCl - KCl solvent/$Cl_2$ is produced by the electrolysis of the molten salt between inert graphite electrodes. In analyzing the curves of cell emf ($E_a$) versus electrolyzing current, the "breaks" corresponding to the decomposition of the LiCl and KCl are not found. Figure 37 shows the decay curves (cell emf's ($E_t$) versus the square root of time) for 0.002 mol fraction of $NdCl_3$, and the corresponding plot of $E_a$ versus I is given in figure 36. At the low current densities, the square root of time relationship for $E_t$ is well-obeyed. At the higher current densities where the applied voltage is greater than the decomposition potential of the eutectic constituents, the initial emf lies above that predicted by the $E_t$ versus $\sqrt{t}$ curve and very rapidly "tails into" this curve. A possible explanation of this behavior assumes two competing cathodic reactions which are:-

(1) - - - - - - - - $Nd^{+++} + 3e = Nd^{\circ}$

(2) - - - - - - - - $Li^{+} + e = Li^{\circ}$ ,

Since the "break" corresponding to the deposition of the Li is absent in the $E_a$ versus I curves (except at very low $NdCl_3$ concentrations),

the Li may react with the $NdCl_3$ in the molten salt according to

(3) - - - - - - - - - $3\ Li + NdCl_3 = Nd + 3\ LiCl$.

To explain the initial "tailing in" effect at the higher current densities, reaction 3 is assumed to be the initial rate controlling reaction and the initial discrepancy is due to the small amount of lithium initially present. The duration of this initial discrepancy is of the order of a few seconds.

If $E^o$ can be either measured directly or calculated from thermodynamic data, the activity and activity coefficients of $NdCl_3$ in LiCl - KCl eutectic (constant ratio of LiCl to KCl) can be obtained. $E^o$ was calculated since $NdCl_3$ is a solid at the temperatures of interest and hence $E^o$ could not be measured. The free energy data were taken from Quill (Chemistry and Metallurgy of Miscellaneous Materials: Thermodynamics) and correspond to the equations:

(4) - - - - - - - - - $Nd(s) + 3/2\ Cl_2(g) = NdCl_3(s)$

and

(5) - - - - - - - - - $NdCl_3(s) = NdCl_3(l)$

which give the overall reaction

(6) - - - - - - - - - $Nd(s) + Cl_2(g) = NdCl_3(l)$

The free energy of formation values are given by the relationship

(7) - - - - - - - - - $\frac{\Delta F_1 - \Delta H^o_{298}}{T} = \Delta S'$ where $\Delta S'$ is a function of

temperature only and empirically fits the equation:-

(8) - - - - - - - - - $\Delta S' = A + BT + CT^2$ .

The equation for $NdCl_3$ is:-

(9) - - - - - - - - - $\Delta S' = 57.7 - 0.61\left[\frac{T}{100}\right] + 0.014\left[\frac{T}{100}\right]^2$ ,

and placing (9) into equation (7) the free energy of formation of

$NdCl_3$ is given by:-

(10) - - - - $\Delta F_1 = -254{,}000 + 577C \frac{T}{100} - 61 \left[\frac{T}{100}\right]^2 + 1.4 \left[\frac{T}{100}\right]^3$ (± 1000).

The free energy change corresponding to the fusion of $NdCl_3$ is estimated by Quill to be:-

(11) - - - - - - - - $\Delta F_2 = 8000 - 8T$

and $\Delta F^\circ_T = \Delta F_1 + \Delta F_2$ for the reaction (6). Since $\Delta F^\circ_T = -nFE^\circ$, the value for $E^\circ$ at any temperature can be calculated. The calculated $E^\circ$ values for 513°C and 586°C are 3.044 volts and 2.999 volts respectively. Estimating the precision of the thermodynamic data, the theoretical values should be expressed as $E^\circ \pm 0.014$ volts.

The thermodyanic emf versus mol fraction is given in figure 32 and the same information is plotted in figure 33 as emf versus log N (mol fraction), which is a linear relationship. The values of n in the term $-2.3\ RT/nF$ calculated from the slope of the $E_{ac}$ versus log N curves are about 2.5. This value for n, while low, is in reasonable agreement with the expected value of 3. The slopes of these curves are very dependent upon the solute concentration. The values of concentration given here were computed from the known weights of the salts in the mixtures. Spot chemical analysis checks have shown that the computed concentrations of the $NdCl_3$ for the more dilute solutions are somewhat high. It is thought that this is due to depletion of $Nd^{+++}$ ions in the very dilute solutions studied. Therefore, if this correction is made, the slope of these curves will give a value of n in better agreement with the expected value of 3. As the temperature increases, the slope of the $E_{ac}$ versus log N curve should increase, but due to the lack of good analytical determinations of the concentration of the $NdCl_3$ this effect is not noted in the experimental results.

The results of the electrolysis study on the LiCl - KCl - $NdCl_3$ system can be summarized as follows:-

1) The experimental thermodynamic cell emf's are in reasonable agreement with calculated values.

2) The measured decomposition potentials show no correlation with thermodynamic cell emf's.

3) The thermodynamic emf's measured by the back-emf method exhibit a linear relationship of $E_{ao}$ versus log N.

4) The decay curve shows a linear relationship between the cell emf and the square root of the time ($E_t = E_a - bt^{1/2}$).

5) The initial deviation of the decay curve from the linear relationship of E versus $\sqrt{t}$ can be explained by a secondary reaction of the type $3Li + NdCl_3 = 3LiCl + Nd$. The Li remaining after the applied voltage is removed is completely reacted in a time interval of a few seconds. This also explains why the "break" in the $E_a$ versus I plot characteristic of the eutectic constituents is not usually found.

6) At the lower solute concentrations, the rate of reduction of $Nd^{+++}$ is greater than that of supply to the cathode compartment such that the amount of the deposited lithium on the cathode is sufficient for a break in the $E_a$ versus I curve characteristic of the eutectic constituents (figure 34).

7) Due to considerations arising from analysis of the decay curves of $E_t$ versus $\sqrt{t}$, it appears that the deposition of the neodymium occurs by two separate reactions:-

a) Direct electrolytic reduction, proceeding at all applied potentials above the decomposition potential of the $NdCl_3$.

TABLE III
Summary of the Electrolysis of $NdCl_3$ In
LiCl-KCl Eutectic

At 513°C $E^o = 3.044 \pm .014$ volts
At 586°C $E^o = 2.999 \pm .014$ volts

| Mol Fraction | $E_{ao}$ | Theo. emf | D.P. | $\alpha$ | Temp. °C |
|---|---|---|---|---|---|
| 0.0008 | 3.2400 | $3.204 \pm 0.014$ | 3.210 | .3 | 513 |
| 0.002 | 3.2100 | $3.183 \pm 0.014$ | --- | .3 | 513 |
| 0.008 | 3.1488 | $3.152 \pm 0.014$ | 3.165 | 1.2 | 513 |
| 0.003 | 3.1432 | $3.143 \pm 0.014$ | 3.260 | 1.0 | 586 |
| 0.008 | 3.1250 | $3.120 \pm .014$ | 3.200 | 0.8 | 586 |
| 0.016 | 3.0940 | $3.101 \pm .014$ | 3.095 | 1.4 | 586 |
| 0.028 | 3.0825 | $3.088 \pm .014$ | 3.090 | 1.2 | 586 |

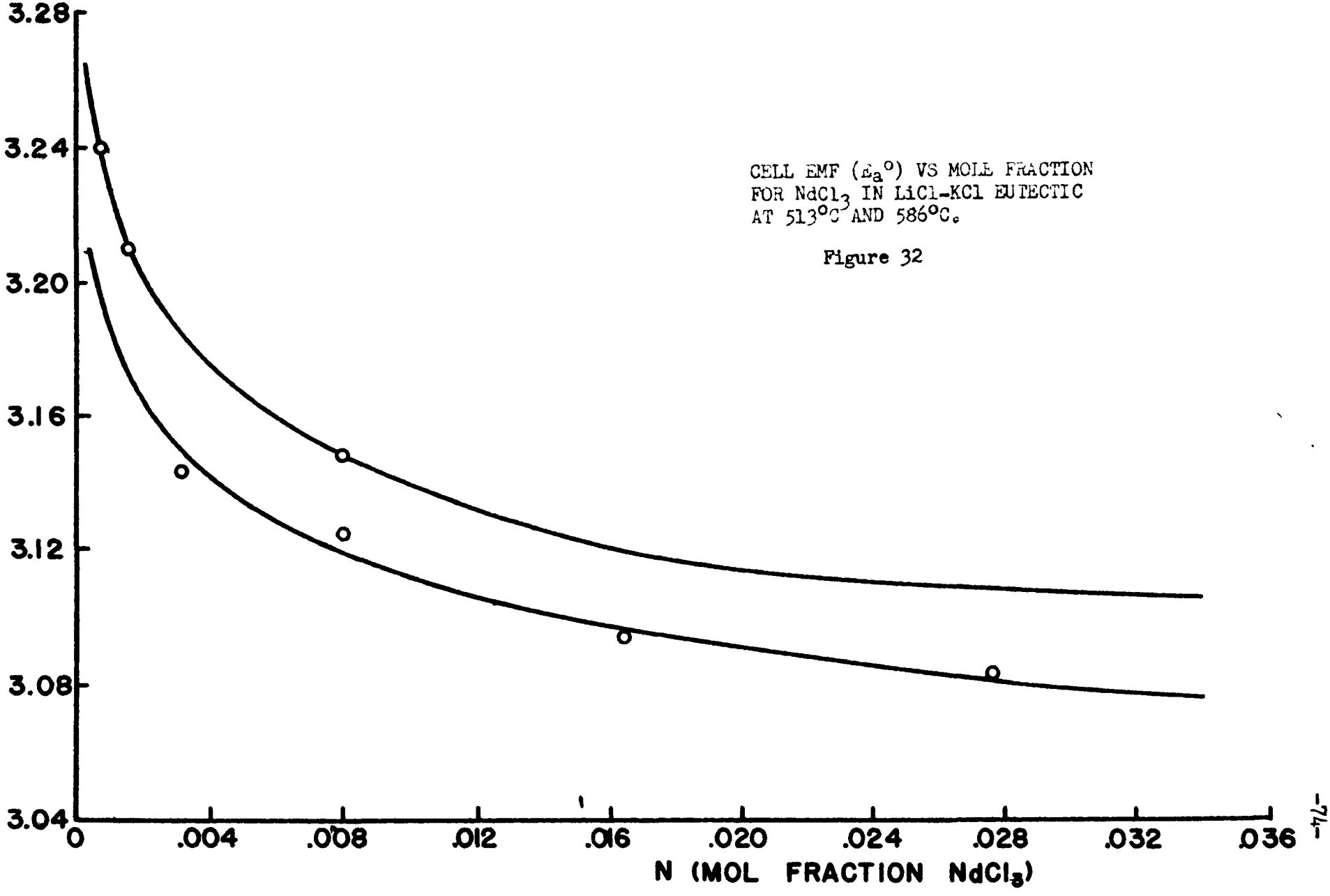


CELL EMF ($E_a^o$) VS MOLE FRACTION FOR $NdCl_3$ IN LiCl-KCl EUTECTIC AT 513°C AND 586°C.

Figure 32

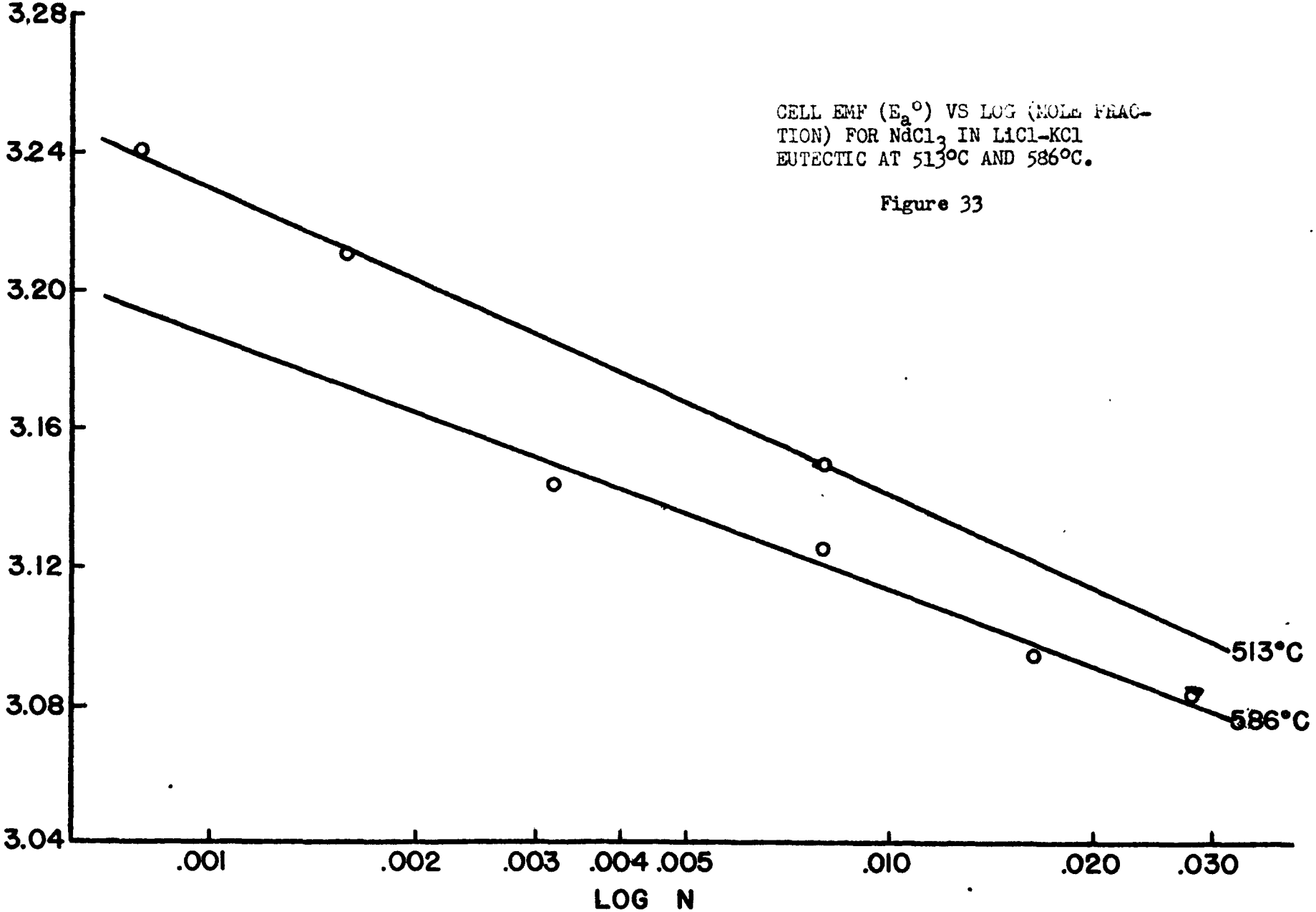


CELL EMF ($E_a^o$) VS LOG (MOLE FRACTION) FOR $NdCl_3$ IN LiCl-KCl EUTECTIC AT 513°C AND 586°C.

Figure 33

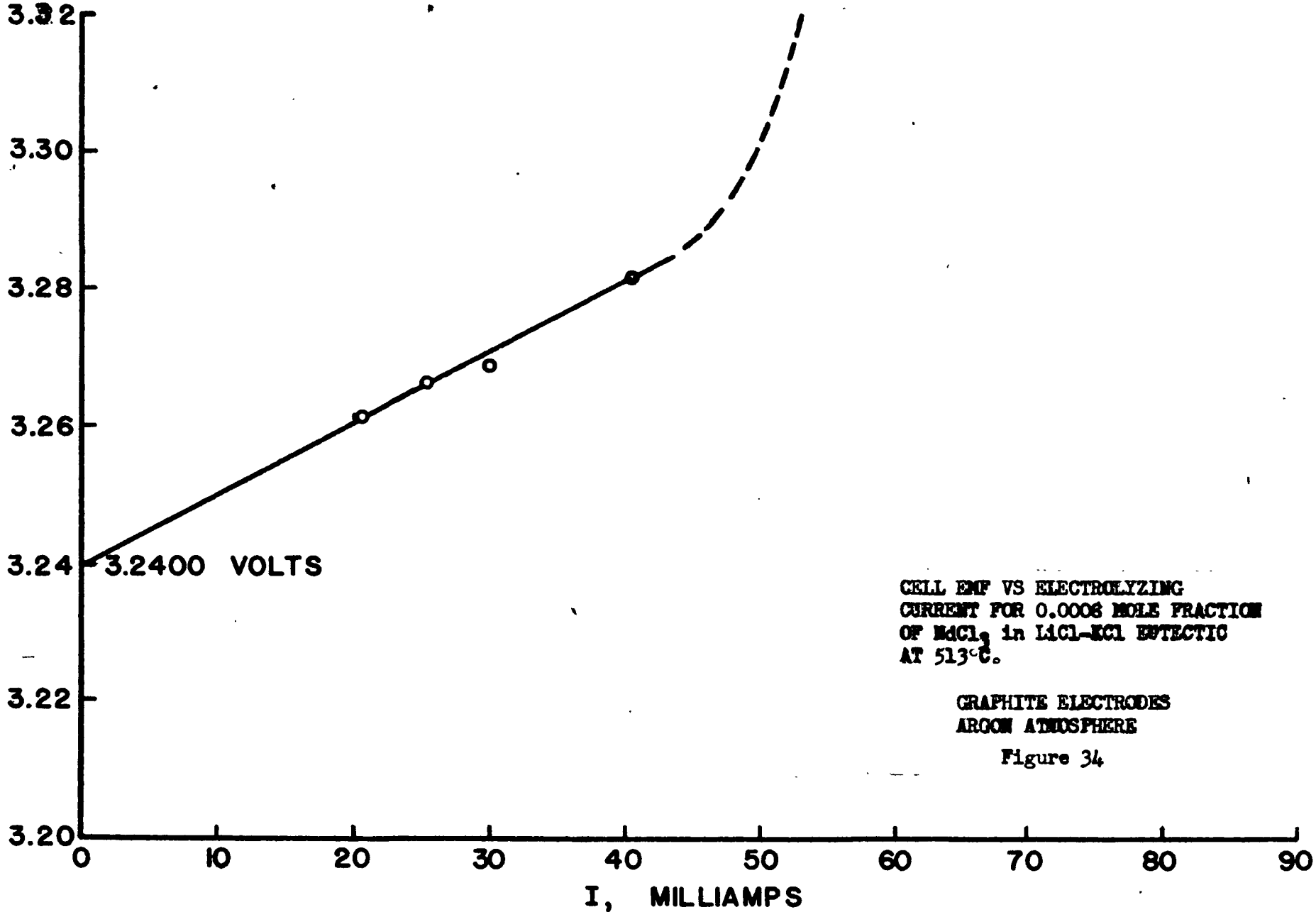


CELL EMF VS ELECTROLYZING CURRENT FOR 0.0006 MOLE FRACTION OF $MdCl_3$ in LiCl-KCl EUTECTIC AT 513°C.

GRAPHITE ELECTRODES
ARGON ATMOSPHERE

Figure 34

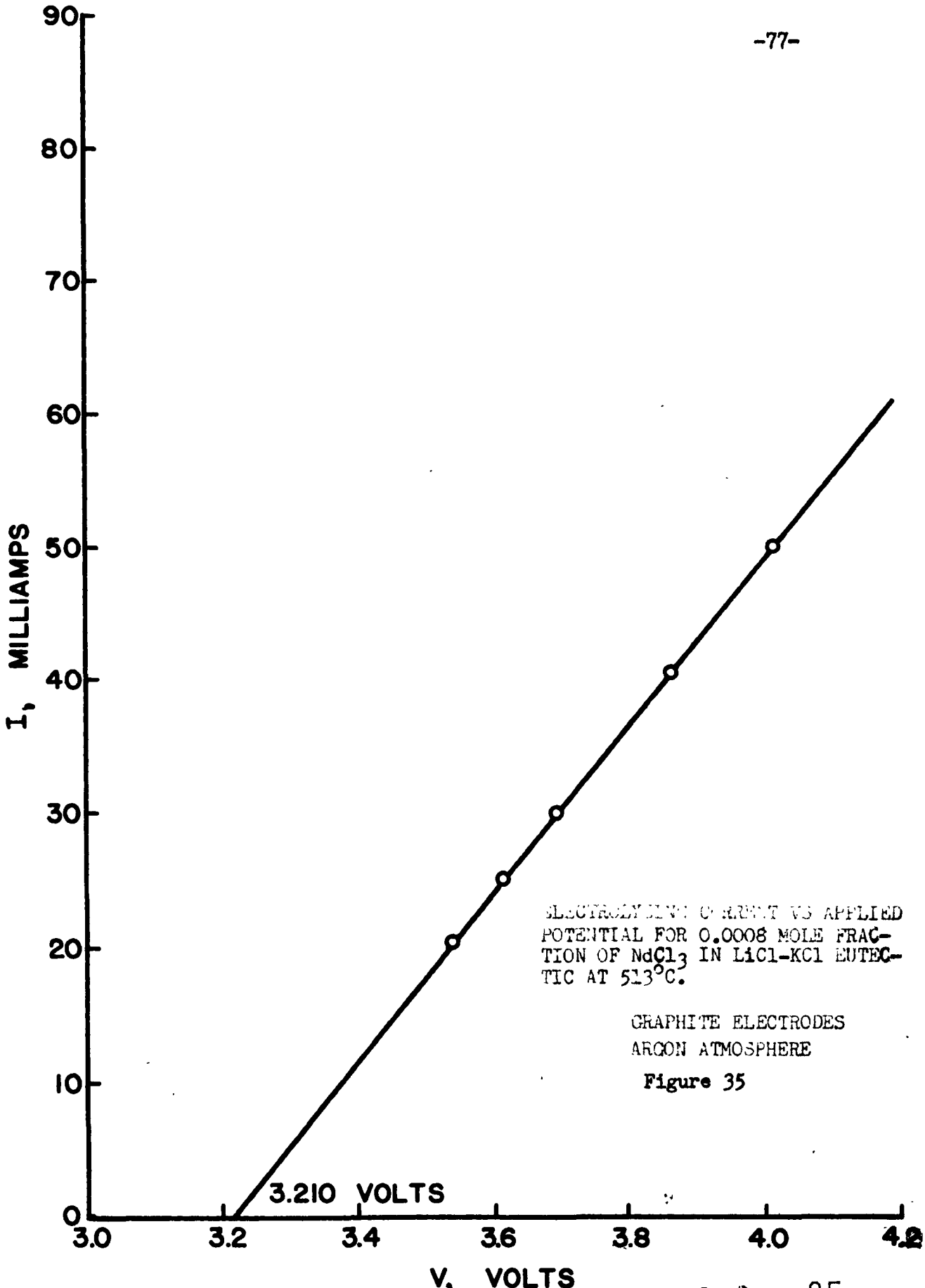


ELECTROLYSIS CURRENT VS APPLIED POTENTIAL FOR 0.0008 MOLE FRACTION OF $NdCl_3$ IN LiCl-KCl EUTECTIC AT 513°C.

GRAPHITE ELECTRODES
ARGON ATMOSPHERE

**Figure 35**

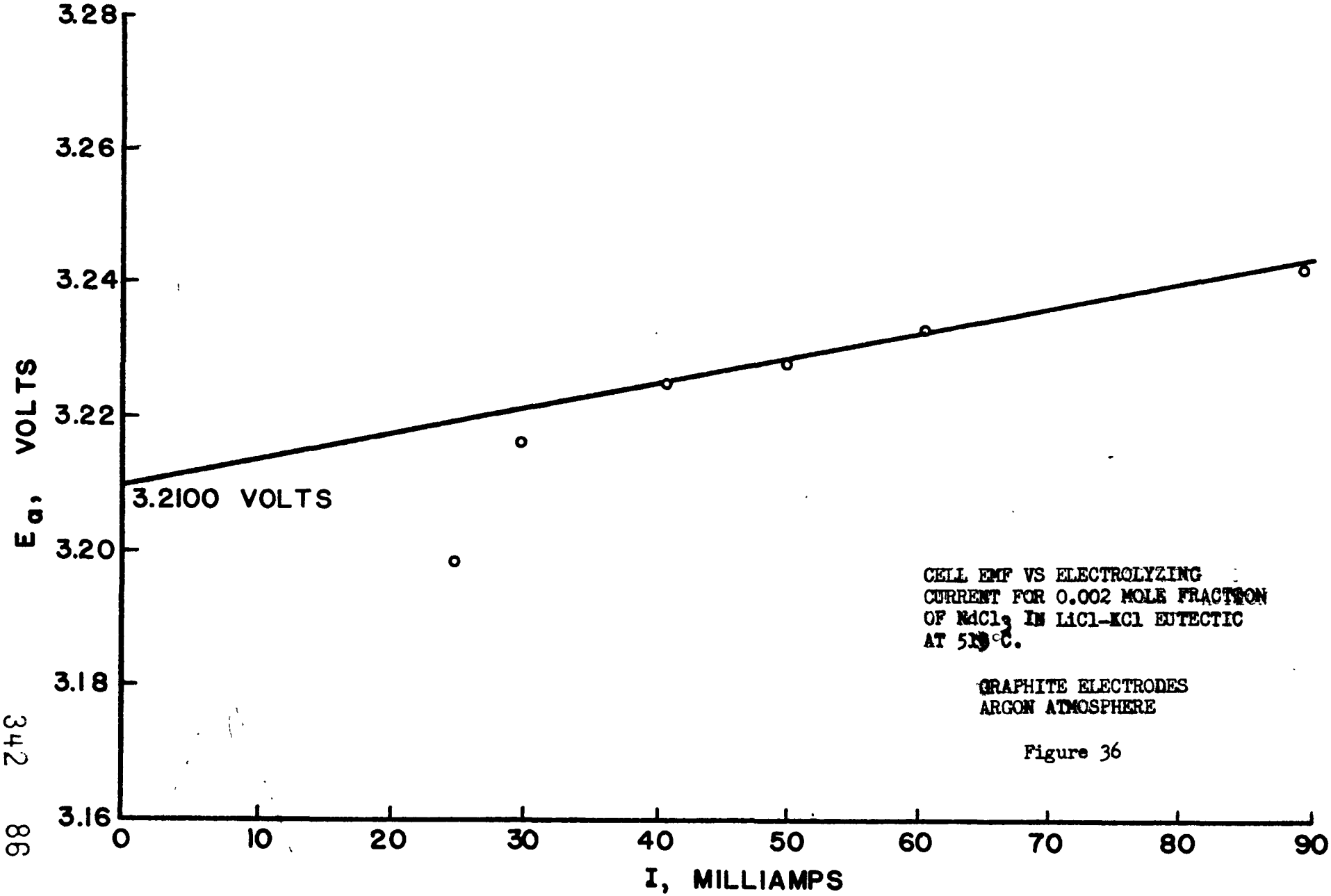


CELL EMF VS ELECTROLYZING CURRENT FOR 0.002 MOLE FRACTION OF $NdCl_3$ IN LiCl-KCl EUTECTIC AT 5[illegible]°C.

GRAPHITE ELECTRODES
ARGON ATMOSPHERE

Figure 36

CELL EMF VS SQUARE ROOT OF TIME FOR 0.002 MOL FRACTION OF $NdCl_3$ IN LiCl-KCl EUTECTIC AT 513°C

Figure 37

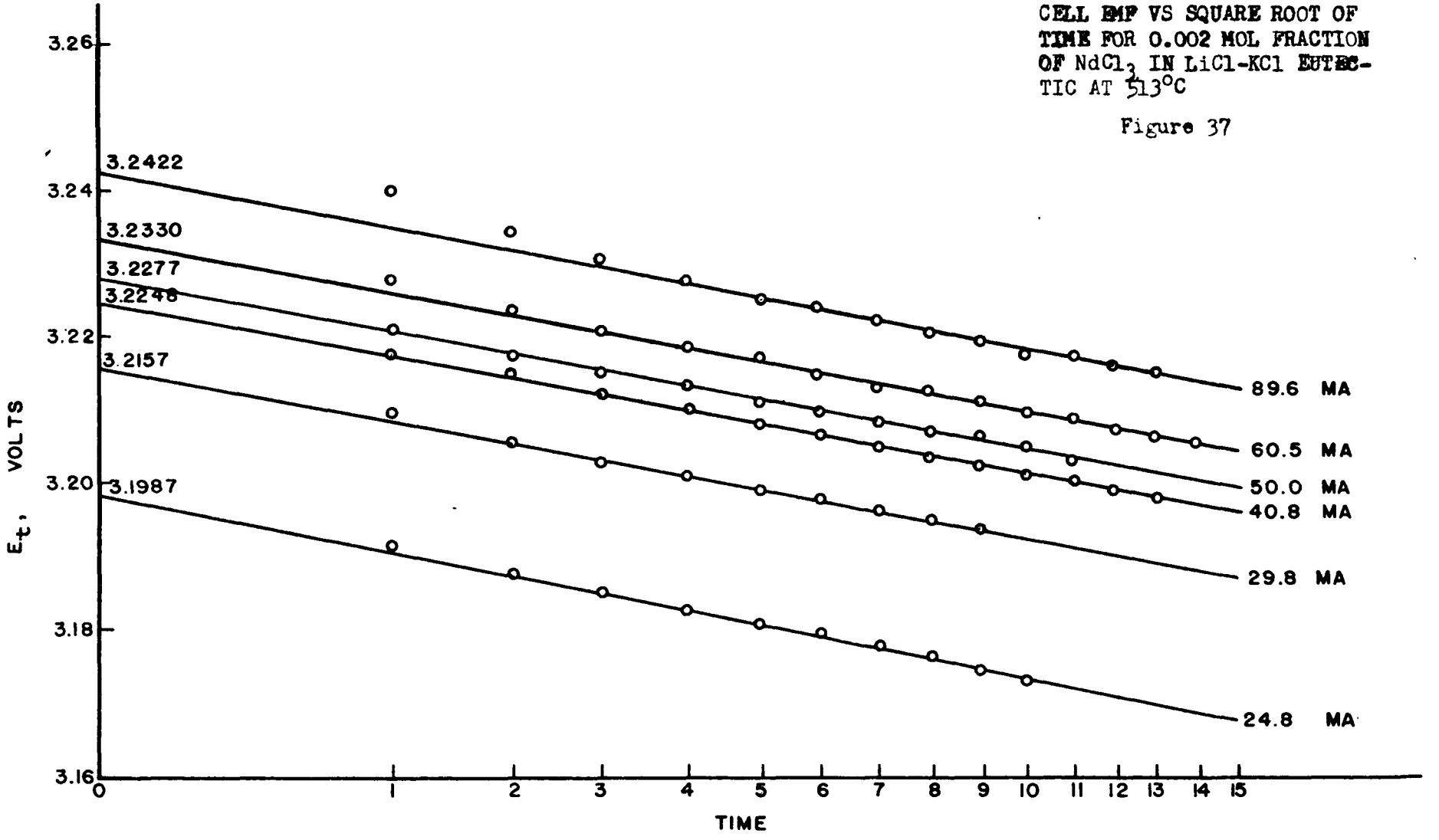

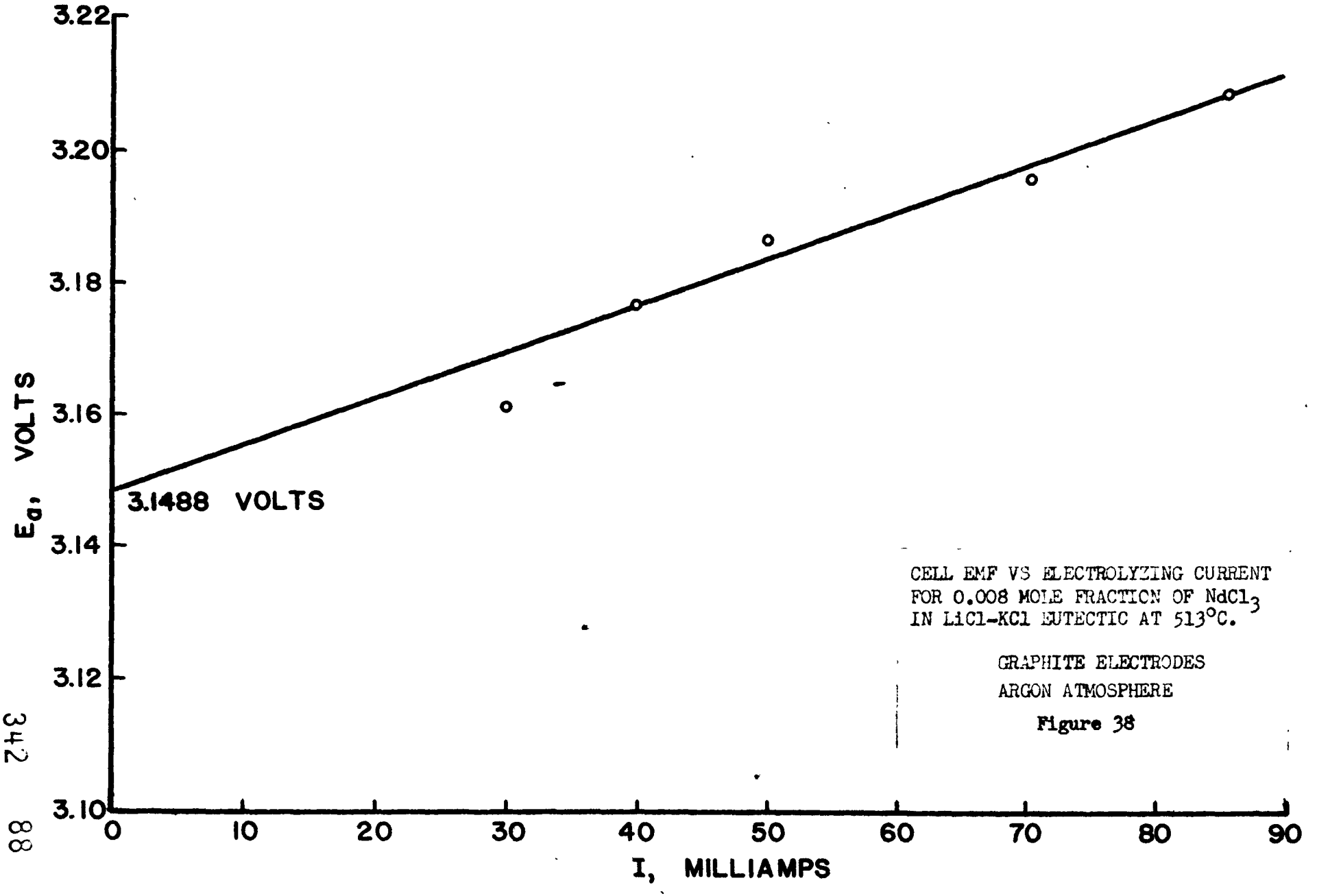


CELL EMF VS ELECTROLYZING CURRENT FOR 0.008 MOLE FRACTION OF $NdCl_3$ IN LiCl-KCl EUTECTIC AT 513°C.

GRAPHITE ELECTRODES

ARGON ATMOSPHERE

**Figure 38**

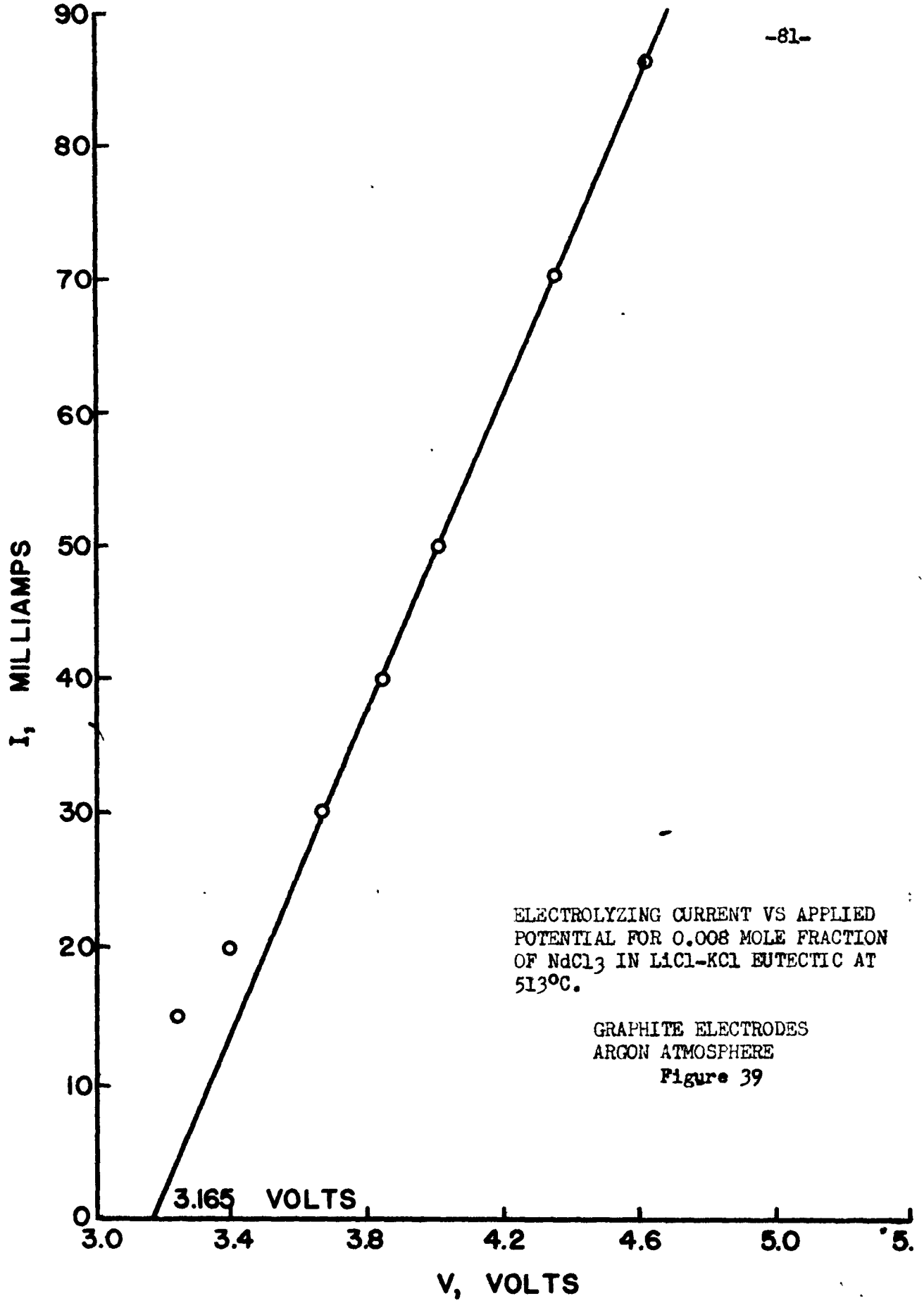


ELECTROLYZING CURRENT VS APPLIED POTENTIAL FOR 0.008 MOLE FRACTION OF $NdCl_3$ IN LiCl-KCl EUTECTIC AT 513°C.

GRAPHITE ELECTRODES
ARGON ATMOSPHERE

**Figure 39**

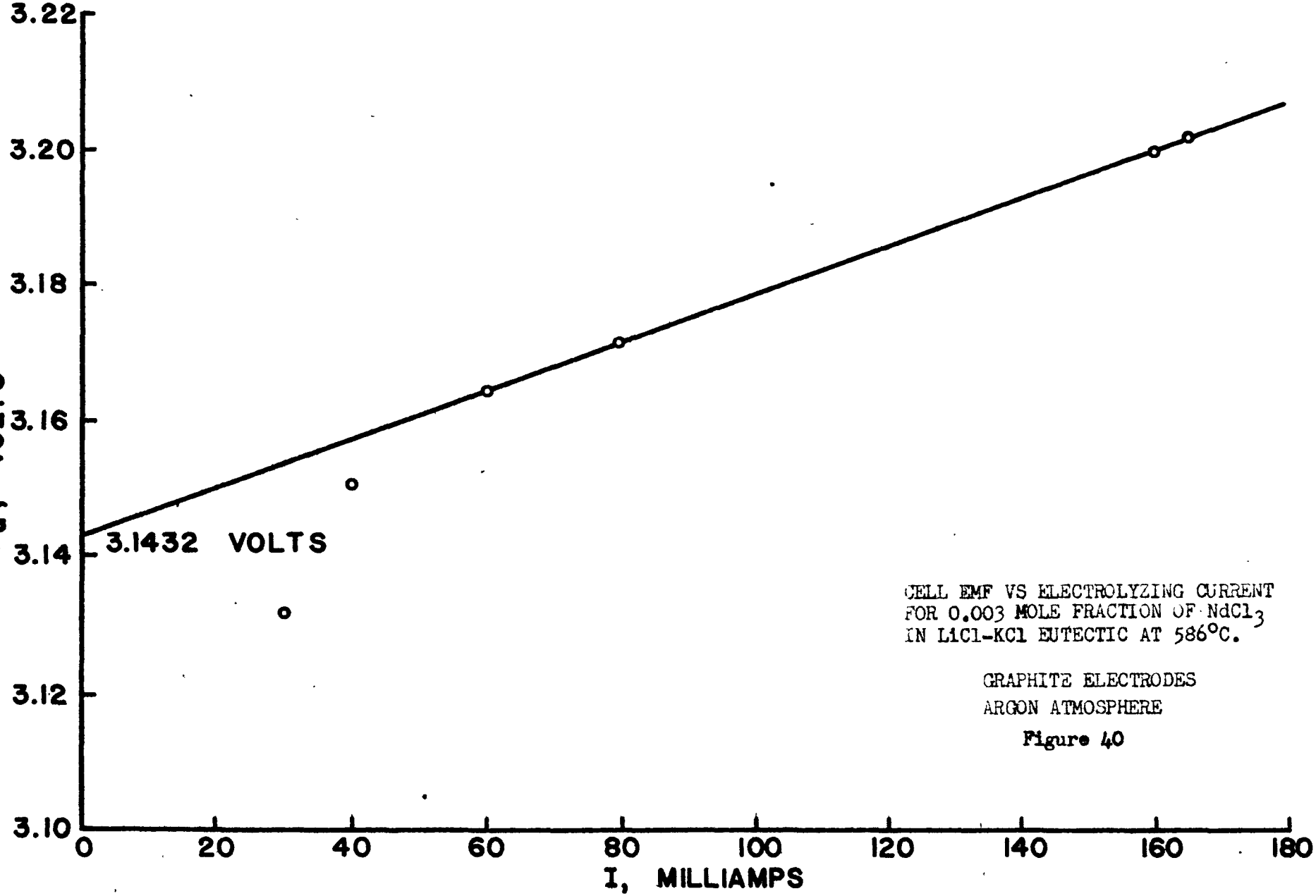


CELL EMF VS ELECTROLYZING CURRENT FOR 0.003 MOLE FRACTION OF $NdCl_3$ IN LiCl-KCl EUTECTIC AT 586°C.

GRAPHITE ELECTRODES
ARGON ATMOSPHERE

**Figure 40**

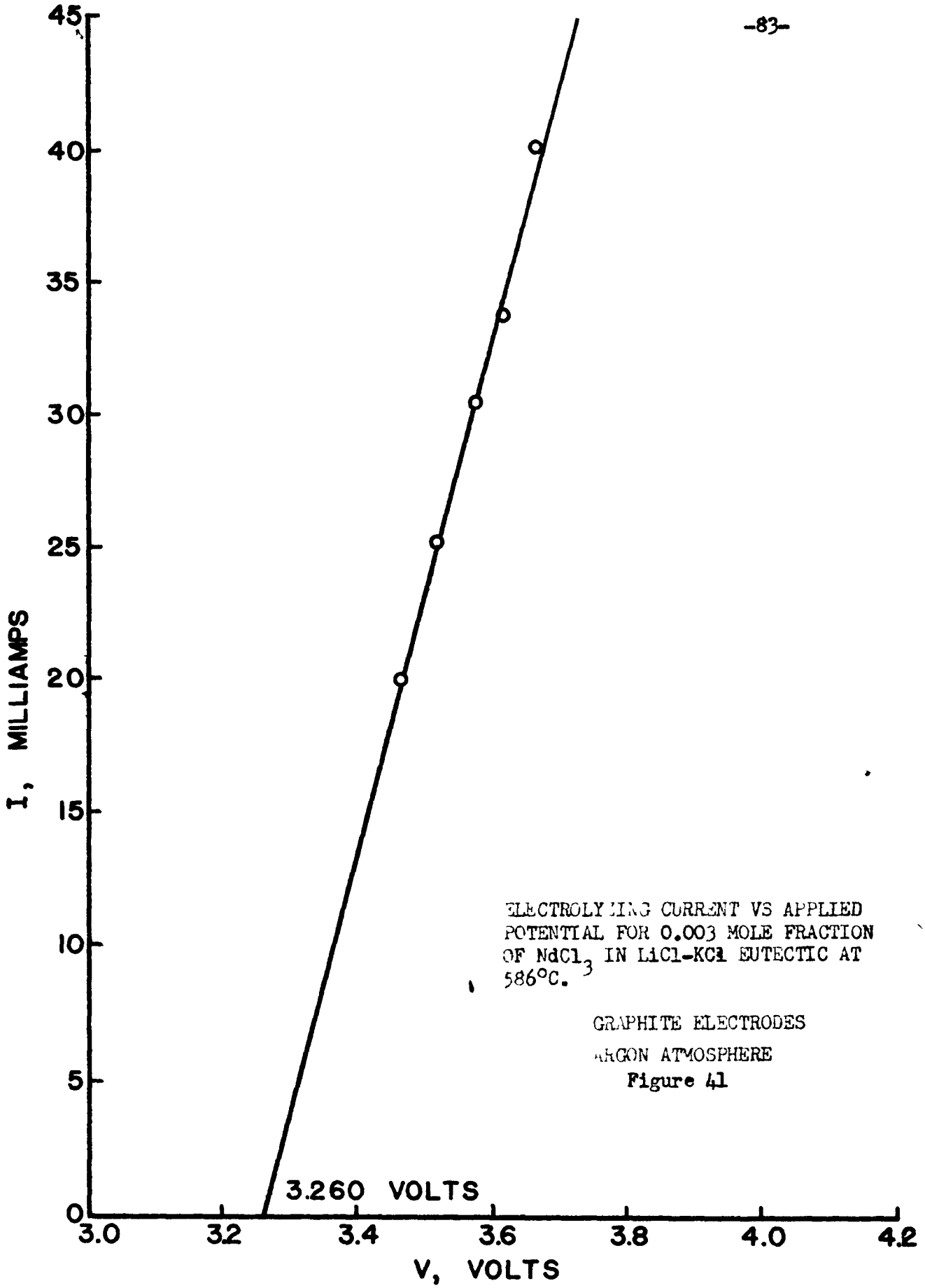


ELECTROLYZING CURRENT VS APPLIED POTENTIAL FOR 0.003 MOLE FRACTION OF $NdCl_3$ IN LiCl-KCl EUTECTIC AT 586°C.

GRAPHITE ELECTRODES

ARGON ATMOSPHERE

**Figure 41**

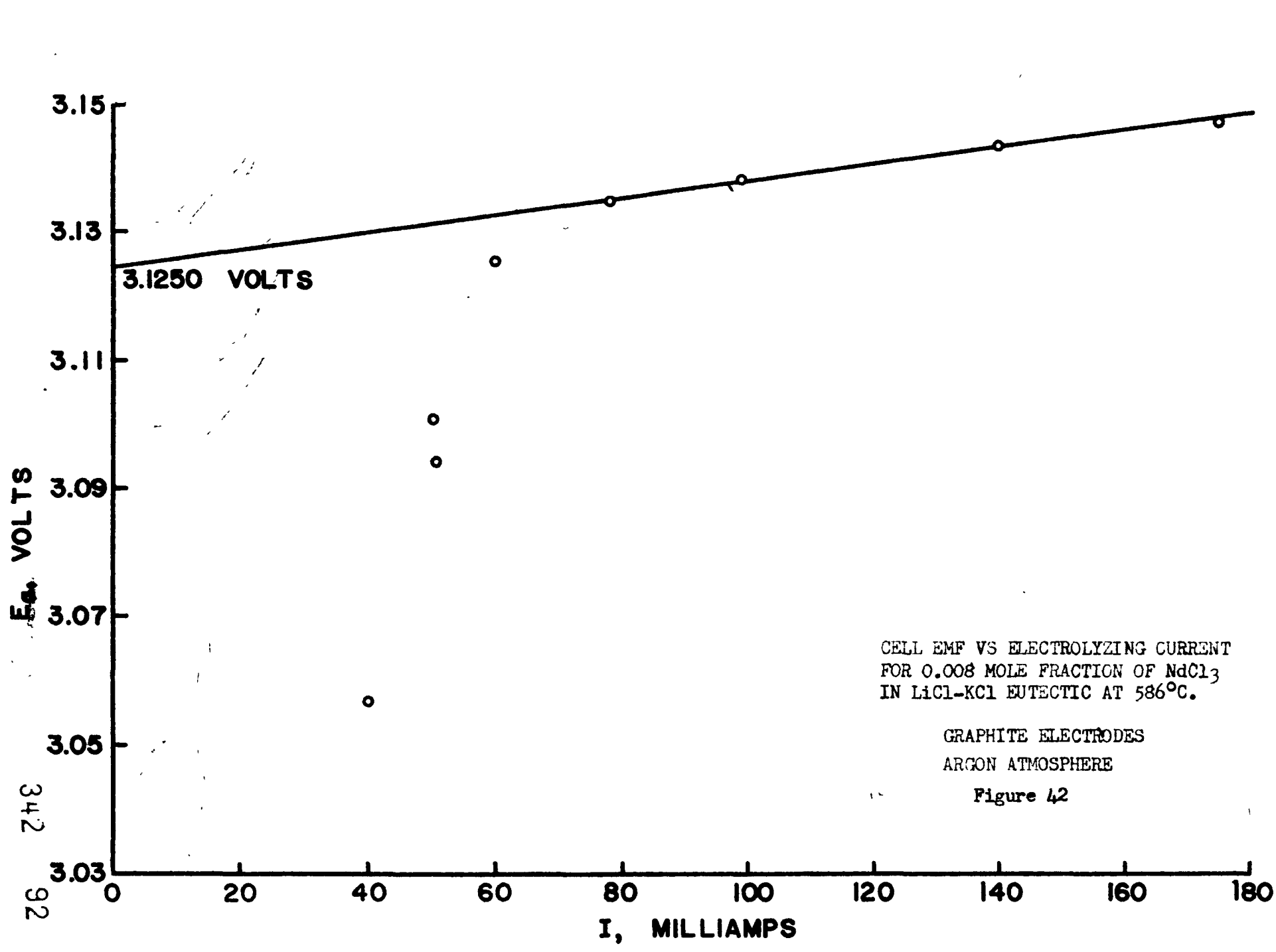


CELL EMF VS ELECTROLYZING CURRENT
FOR 0.008 MOLE FRACTION OF $NdCl_3$
IN LiCl-KCl EUTECTIC AT 586°C.

GRAPHITE ELECTRODES
ARGON ATMOSPHERE

Figure 42

342
92

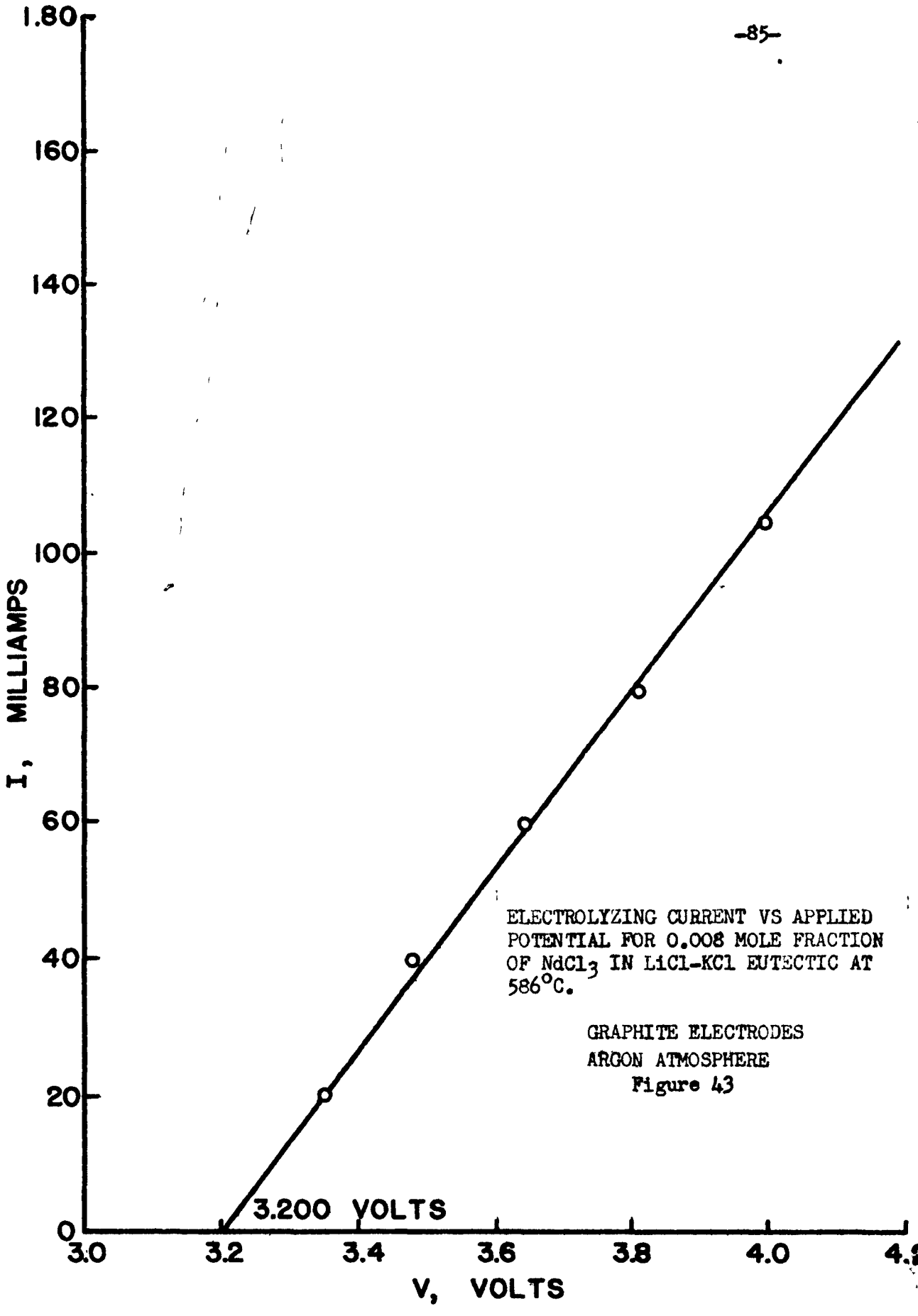


ELECTROLYZING CURRENT VS APPLIED POTENTIAL FOR 0.008 MOLE FRACTION OF $NdCl_3$ IN LiCl-KCl EUTECTIC AT 586°C.

GRAPHITE ELECTRODES
ARGON ATMOSPHERE
Figure 43

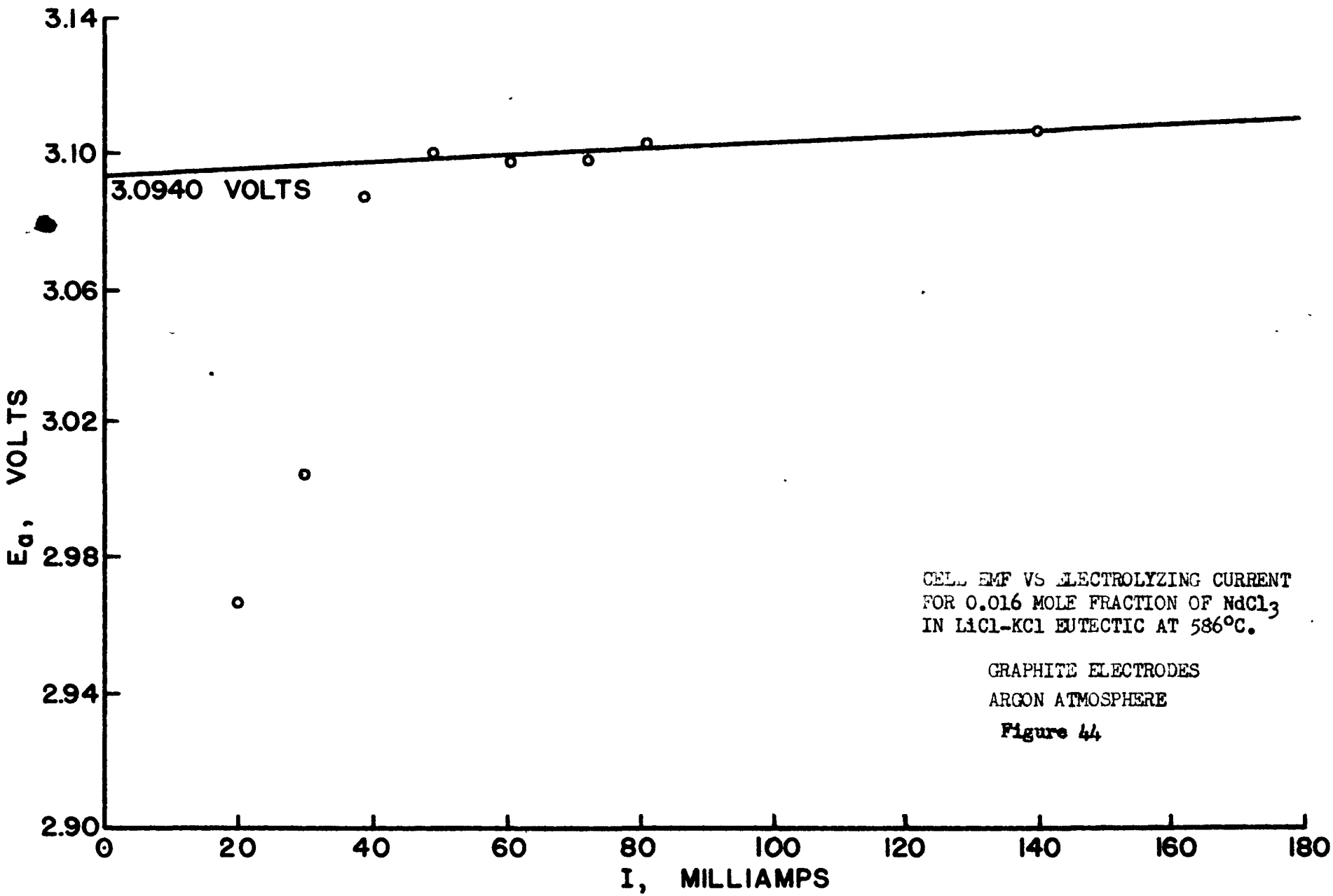


CELL EMF VS ELECTROLYZING CURRENT
FOR 0.016 MOLE FRACTION OF $NdCl_3$
IN LiCl-KCl EUTECTIC AT 586°C.

GRAPHITE ELECTRODES
ARGON ATMOSPHERE

**Figure 44**

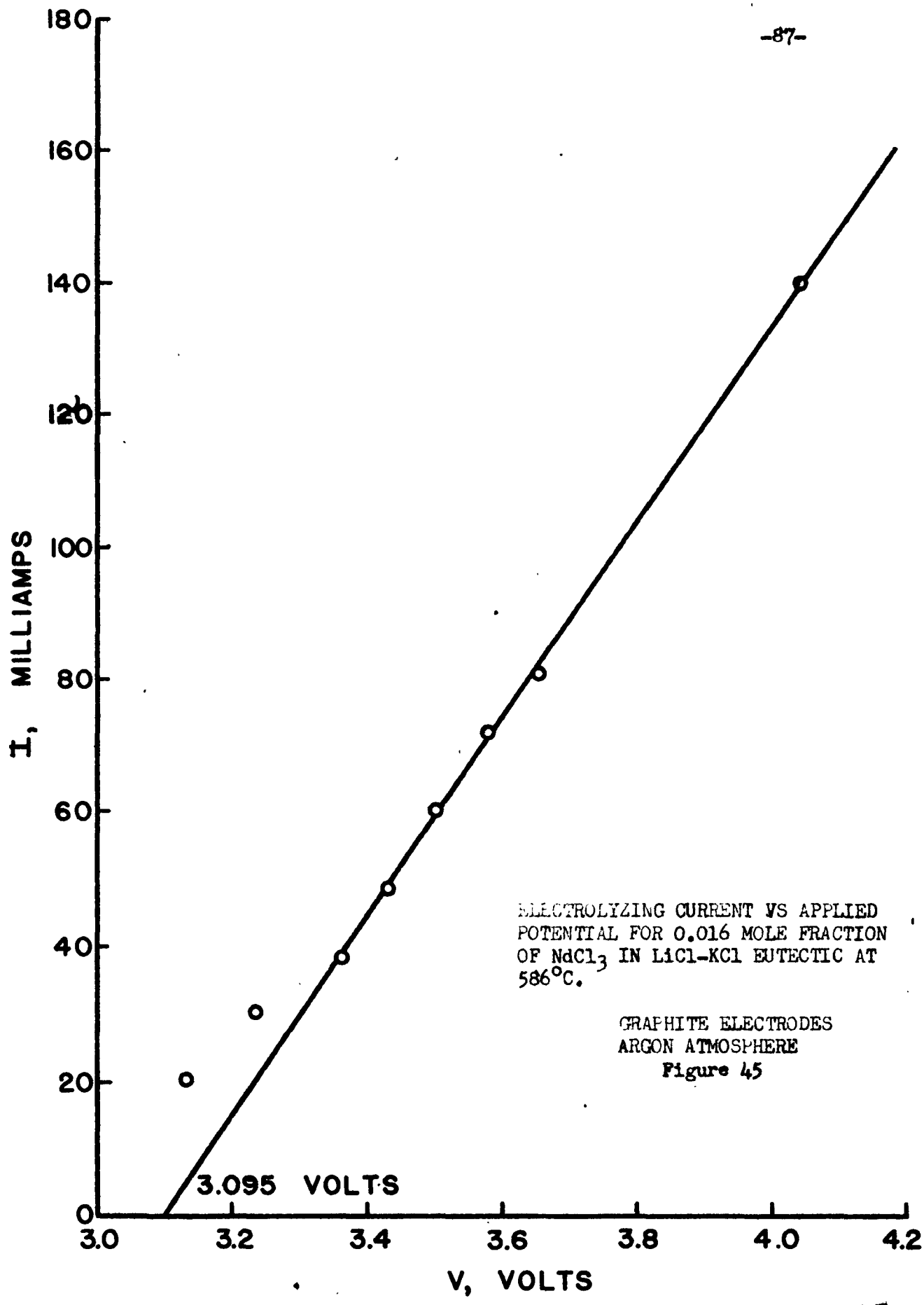


ELECTROLYZING CURRENT VS APPLIED POTENTIAL FOR 0.016 MOLE FRACTION OF $NdCl_3$ IN LiCl-KCl EUTECTIC AT 586°C.

GRAPHITE ELECTRODES
ARGON ATMOSPHERE
Figure 45

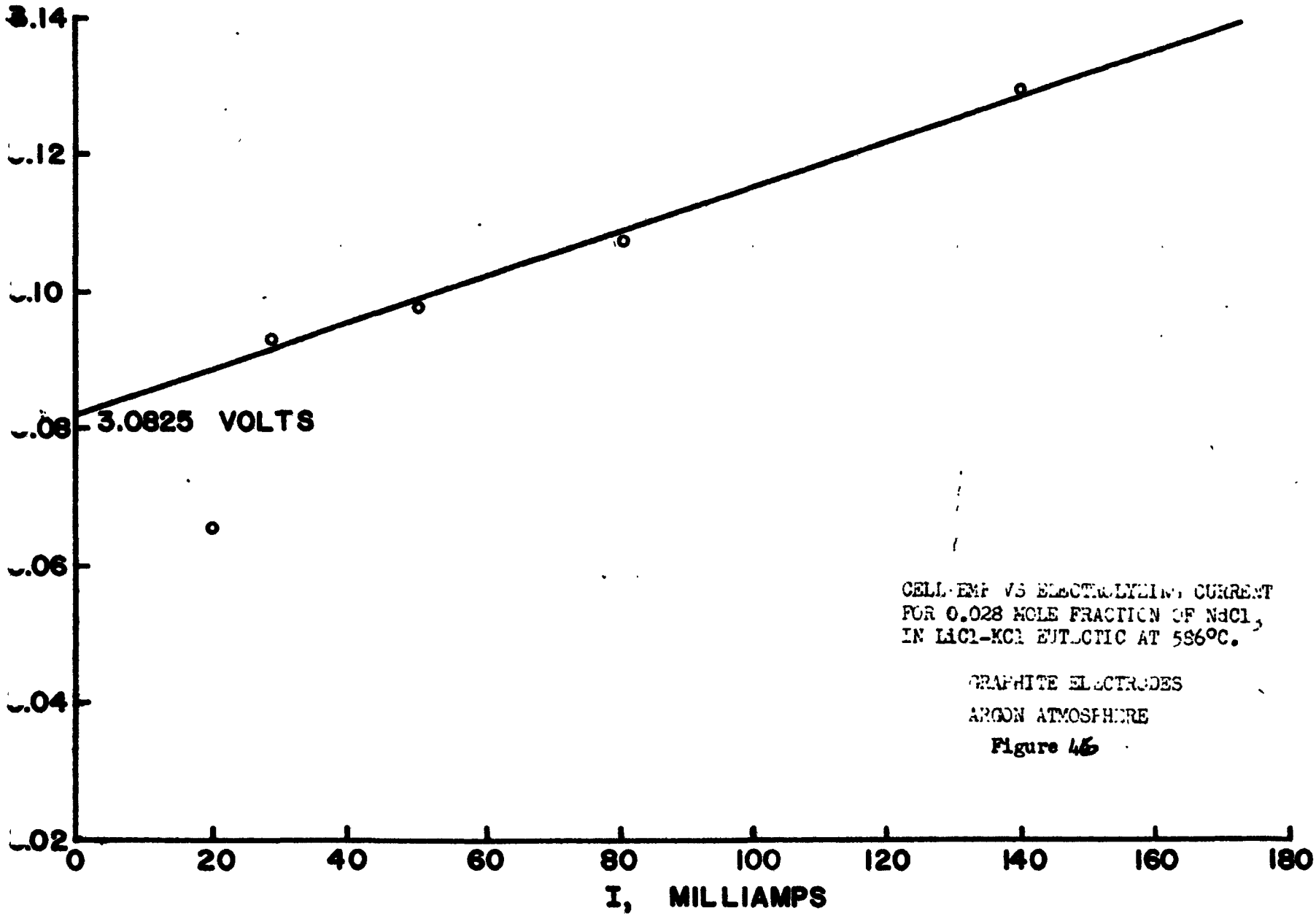


CELL EMF VS ELECTROLYTIC CURRENT FOR 0.028 MOLE FRACTION OF NdCl$_3$ IN LiCl-KCl EUTECTIC AT 586°C.

GRAPHITE ELECTRODES

ARGON ATMOSPHERE

**Figure 46**

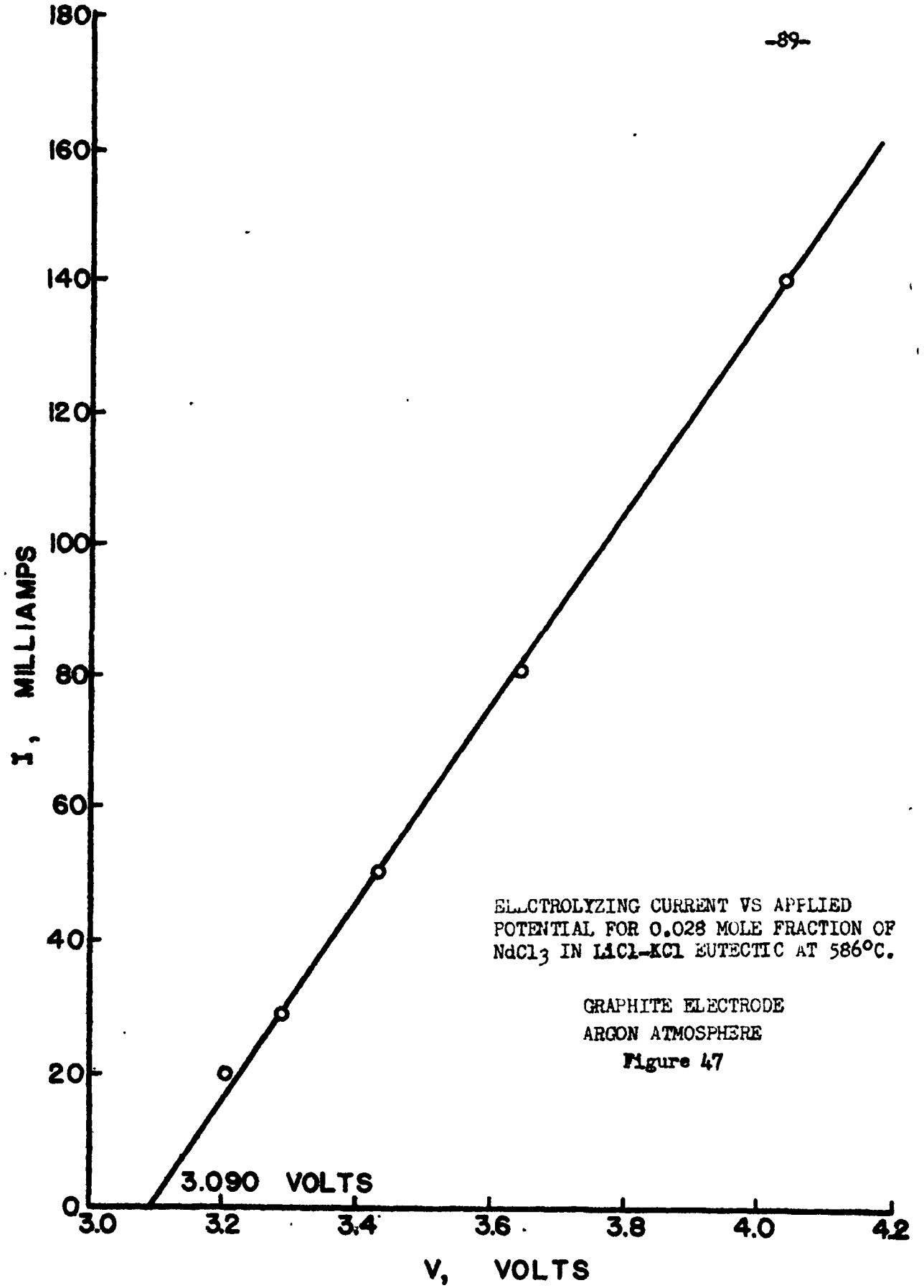


ELECTROLYZING CURRENT VS APPLIED POTENTIAL FOR 0.028 MOLE FRACTION OF $NdCl_3$ IN LiCl-KCl EUTECTIC AT 586°C.

GRAPHITE ELECTRODE
ARGON ATMOSPHERE

Figure 47

b) Secondary reduction according to the cathode reactions $Li^+ + e = Li$ and $3Li + NdCl_3 = Nd + 3LiCl$.

8) Since there are no depolarizing reactions occurring between the neodymium and the graphite, graphite electrodes are suitable for neodymium salt electrolysis

Electrolysis of Miscellaneous Systems

Some thermodynamic emf's and decomposition potentials will be given for the systems $MgCl_2 - LiCl - KCl$, $MgCl_2 - NaCl$, $PbCl_2 - LiCl - KCl$, $ZnCl_2 - LiCl - KCl$, $SnCl_2$, and KCl. The data are summarized in Table IV.

1) The decomposition potentials for all systems are in poor agreement with the measured and calculated thermodynamic emf's (which agree reasonably well).

2) For 0.40 mol fraction of $MgCl_2$ in NaCl the system tends toward ideal solution behavior as temperature increases

3) The thermodynamic emf for KCl at 800°C (Figure 53) indicates a depolarization of approximately 0.10 volts. It is believed that the deposited K was reacting with the cell materials at this high temperature

4) The experimental thermodynamic emf for pure $SnCl_2$ is about 1 volt below the calculated value for the reaction $SnCl_2 = Sn + Cl_2$.

If the $SnCl_2 - LiCl - KCl$ system is electrolyzed "breaks" are observed in the $E_a$ versus I curve at about 0.40 volts and also at about 1.4 volts. The latter value corresponds to the calculated thermodynamic emf for $SnCl_2$. The lower value may be that for the reaction $Sn^{++++} + 2e = Sn^{++}$ or for the reduction of a sub-halide.

5) Figure 57 shows the curve for $E_a$ versus I for 0.10 mol fraction of $ZnCl_2$ in LiCl — KCl. The two curves plotted here represent two separate electrolysis experiments. The values for $E_{ac}$ (the thermodynamic

TABLE IV

Summary of the Electrolysis Data for the Miscellaneous Systems

| Solute | Mol Frac. | Temp °C | Solvent | $E_{ac}$ | Theo emf* | D.P. |
|---|---|---|---|---|---|---|
| $MgCl_2$ | 0.10 | 500 | LiCl-KCl | 2.8240 | 2.722 ± .028 | 2.880 |
| $MgCl_2$ | 0.40 | 510 | NaCl | 2.7360 | 2.669 ± .028 | 3.000 |
| $MgCl_2$ | 0.40 | 710 | NaCl | 2.5709 | 2.569 ± .033 | 2.677 |
| $PbCl_2$ | 0.10 | 542 | LiCl-KCl | 1.3340 | 1.294 ± .065 | 1.290 |
| $ZnCl_2$ | 0.10 | 542 | LiCl-KCl | 1.7650 | 1.632 ± .109 | 1.760 |
| KCl | 1.0 | 800 | —— | 3.302 | 3.428 ± 065 | —— |
| $SnCl_2$ | 1.0 | 542 | —— | 0.346 | | —— |

* Assuming ideal solution behavior.

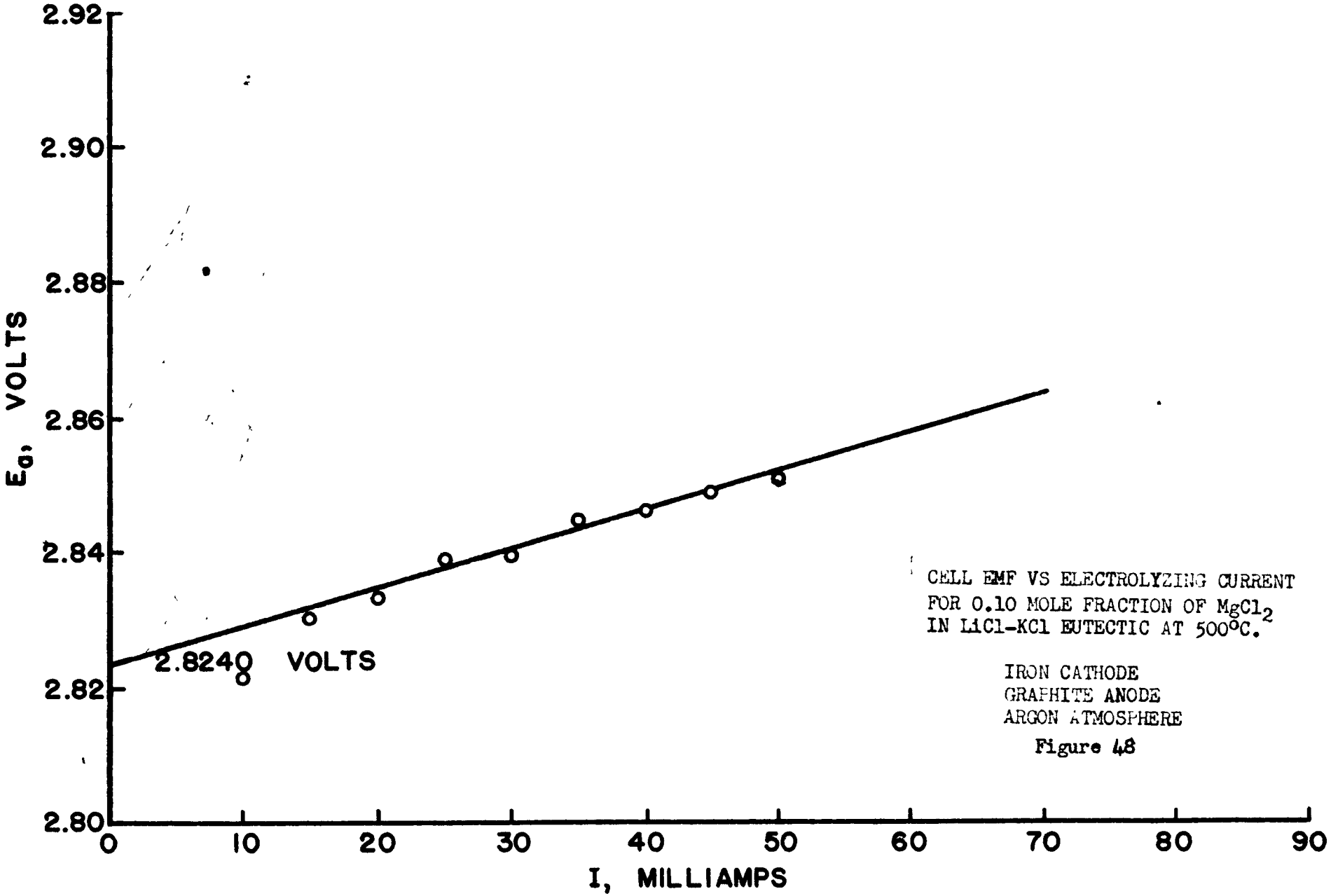


CELL EMF VS ELECTROLYZING CURRENT FOR 0.10 MOLE FRACTION OF $MgCl_2$ IN LiCl-KCl EUTECTIC AT 500°C.

IRON CATHODE
GRAPHITE ANODE
ARGON ATMOSPHERE

Figure 48

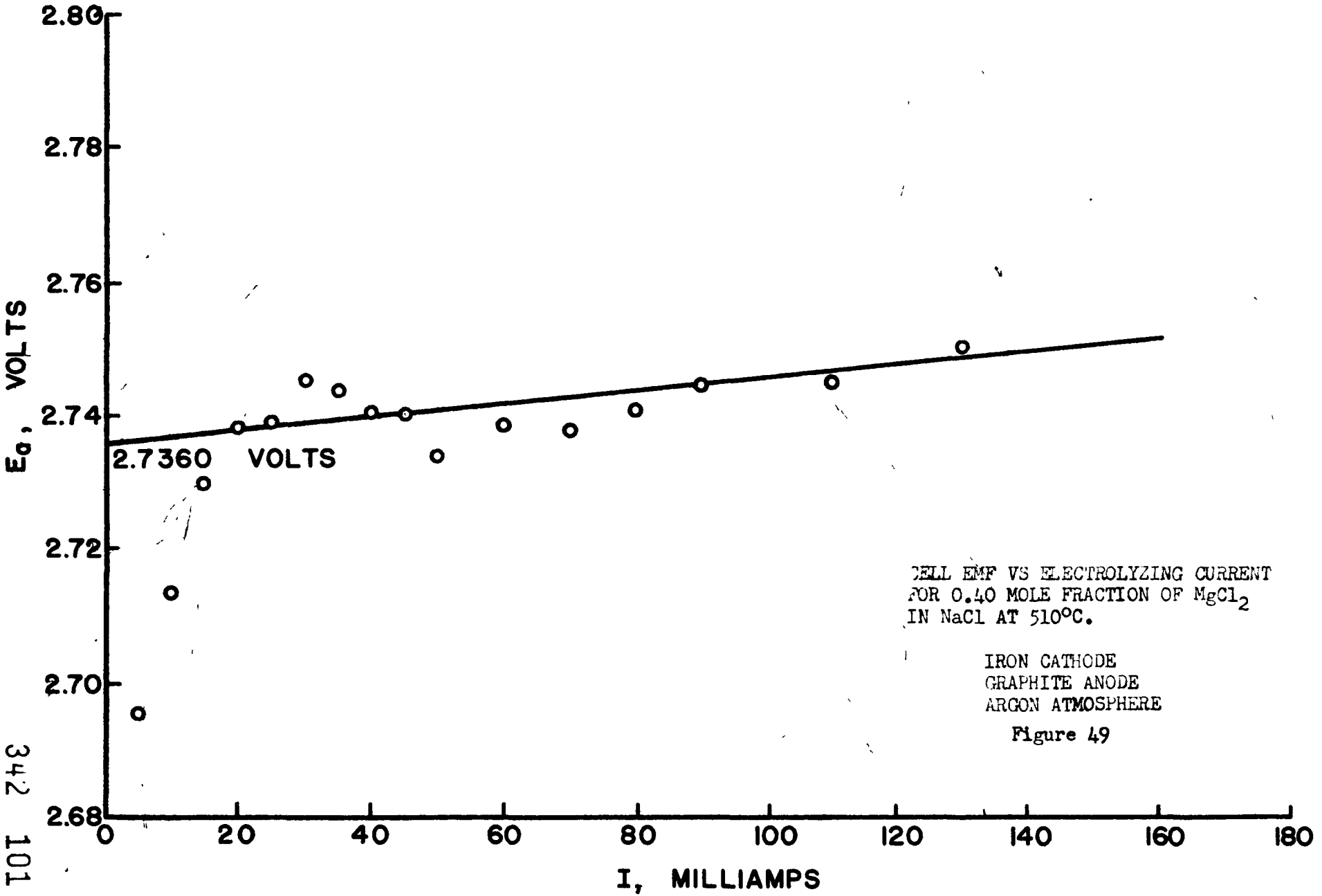


CELL EMF VS ELECTROLYZING CURRENT FOR 0.40 MOLE FRACTION OF $MgCl_2$ IN NaCl AT 510°C.

IRON CATHODE
GRAPHITE ANODE
ARGON ATMOSPHERE

Figure 49

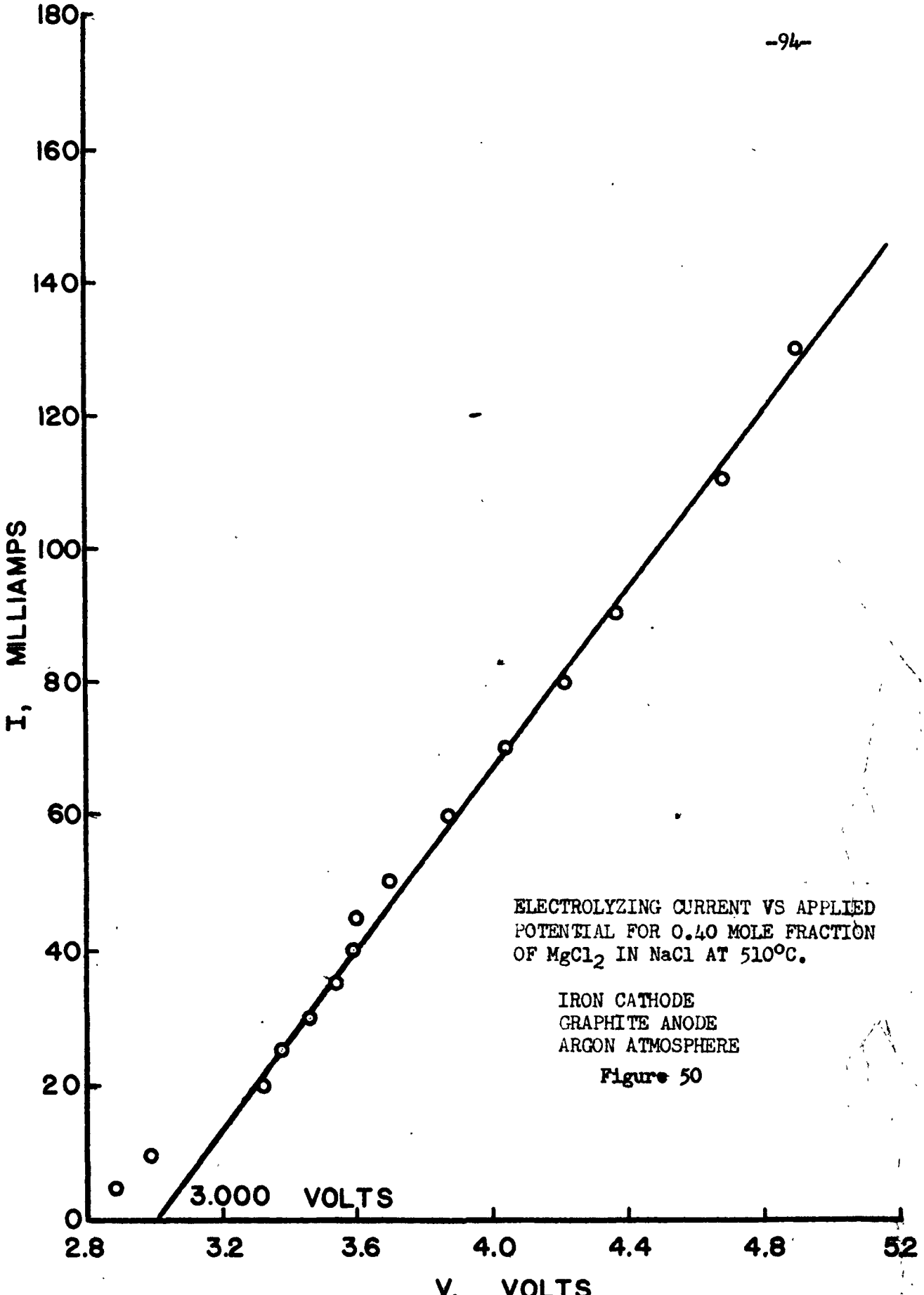


ELECTROLYZING CURRENT VS APPLIED POTENTIAL FOR 0.40 MOLE FRACTION OF $MgCl_2$ IN NaCl AT 510°C.

IRON CATHODE
GRAPHITE ANODE
ARGON ATMOSPHERE

Figure 50

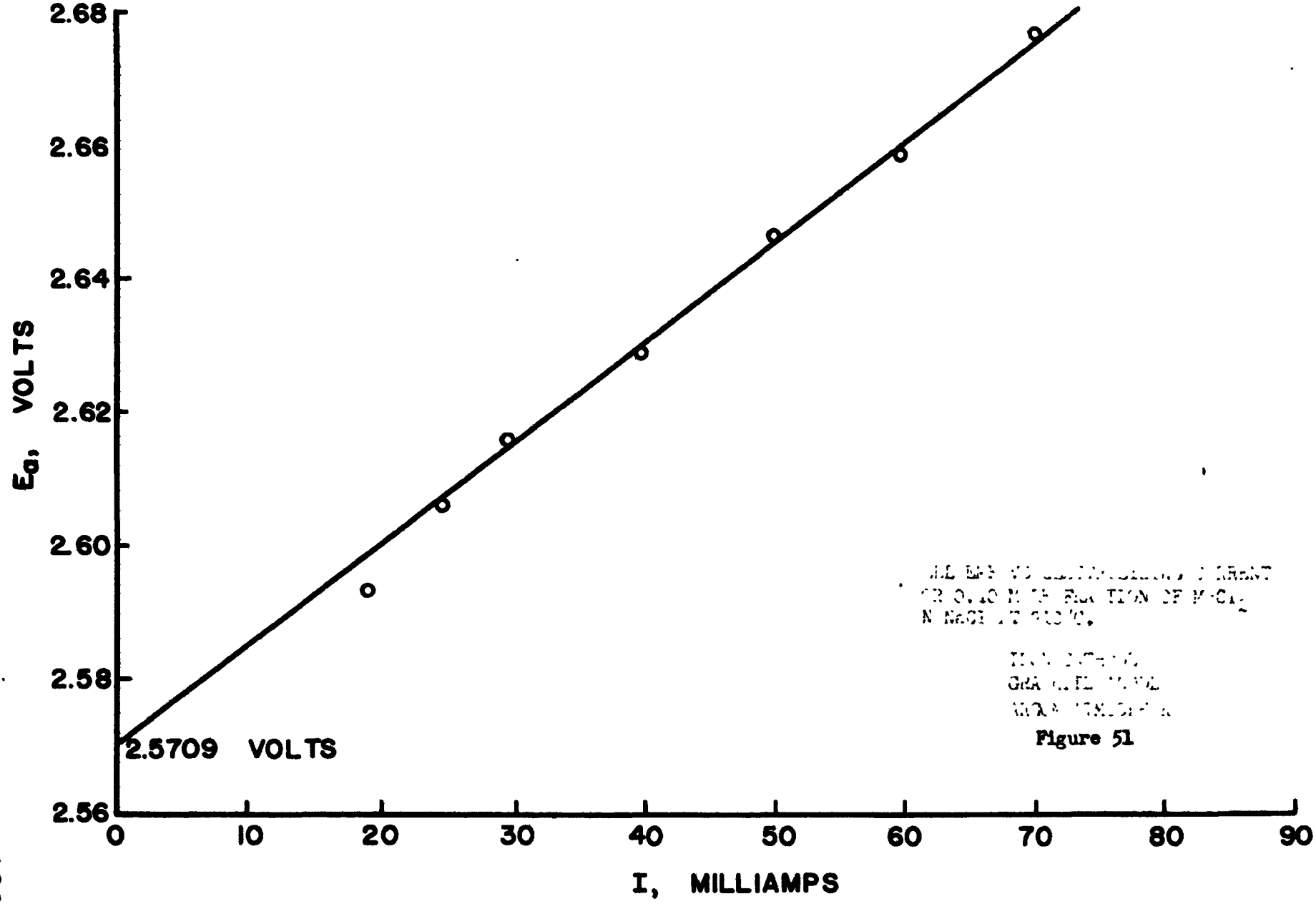


Figure 51

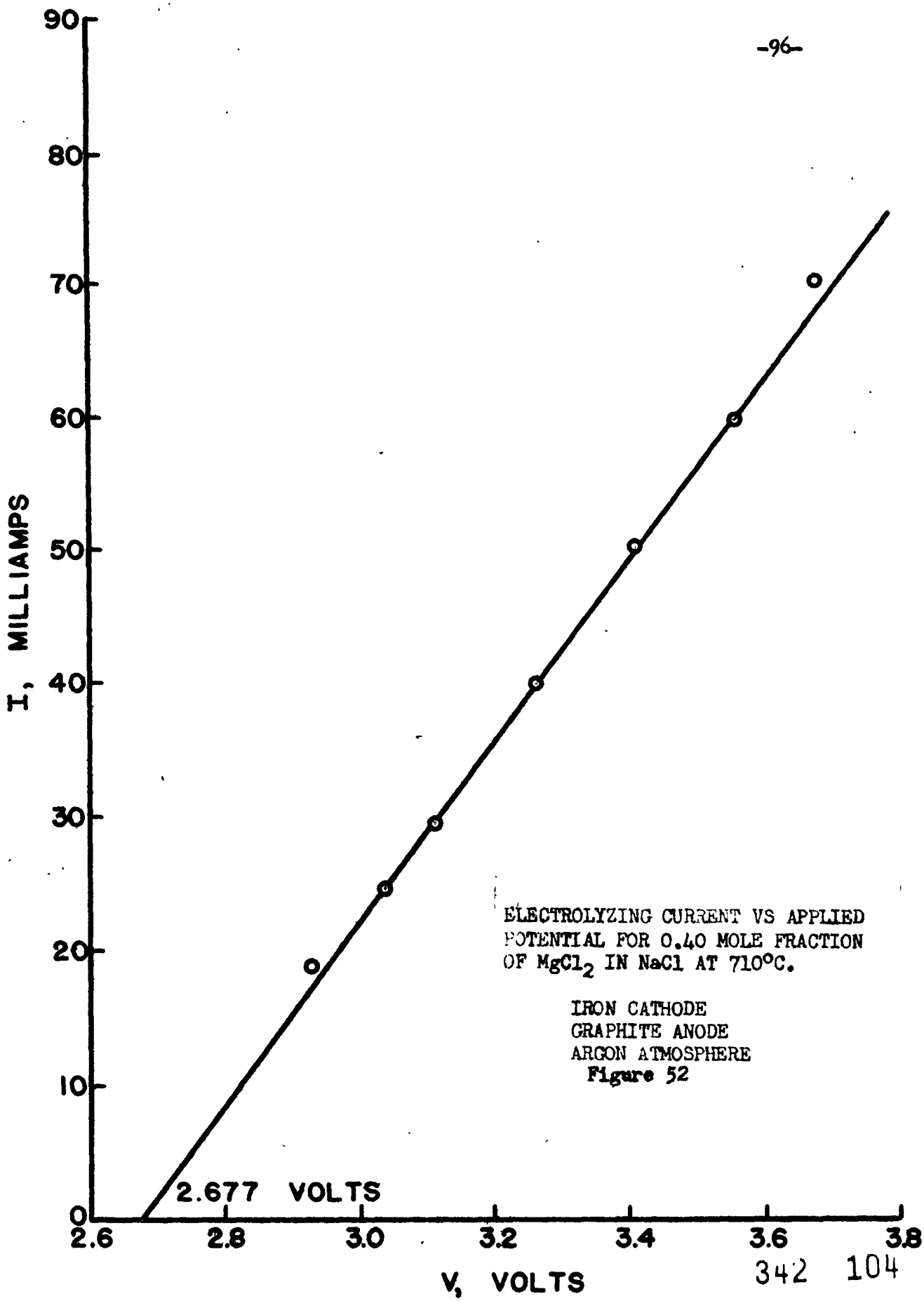


ELECTROLYZING CURRENT VS APPLIED POTENTIAL FOR 0.40 MOLE FRACTION OF $MgCl_2$ IN NaCl AT 710°C.

IRON CATHODE
GRAPHITE ANODE
ARGON ATMOSPHERE
**Figure 52**

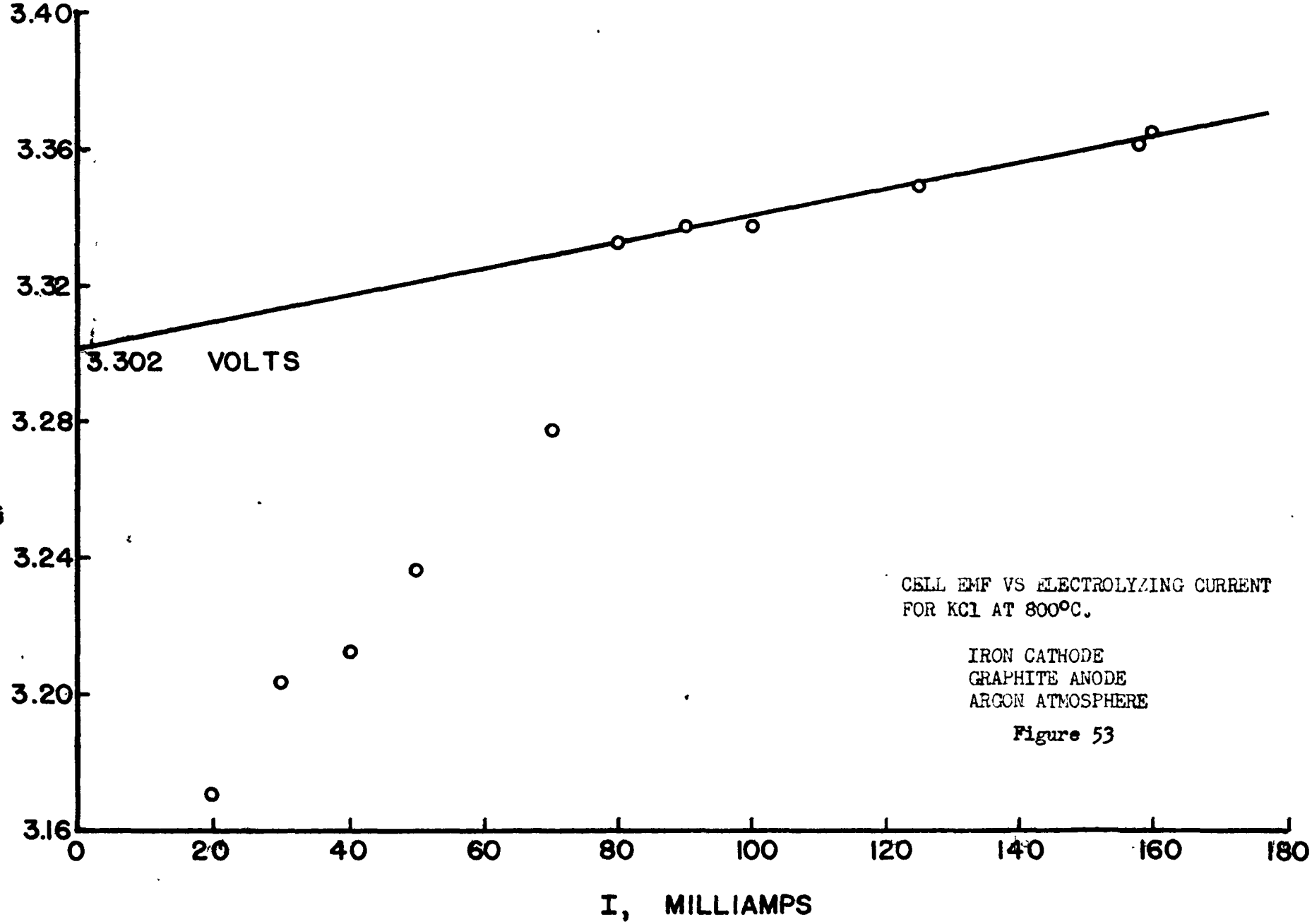


CELL EMF VS ELECTROLYZING CURRENT
FOR KCl AT 800°C.

IRON CATHODE
GRAPHITE ANODE
ARGON ATMOSPHERE

Figure 53

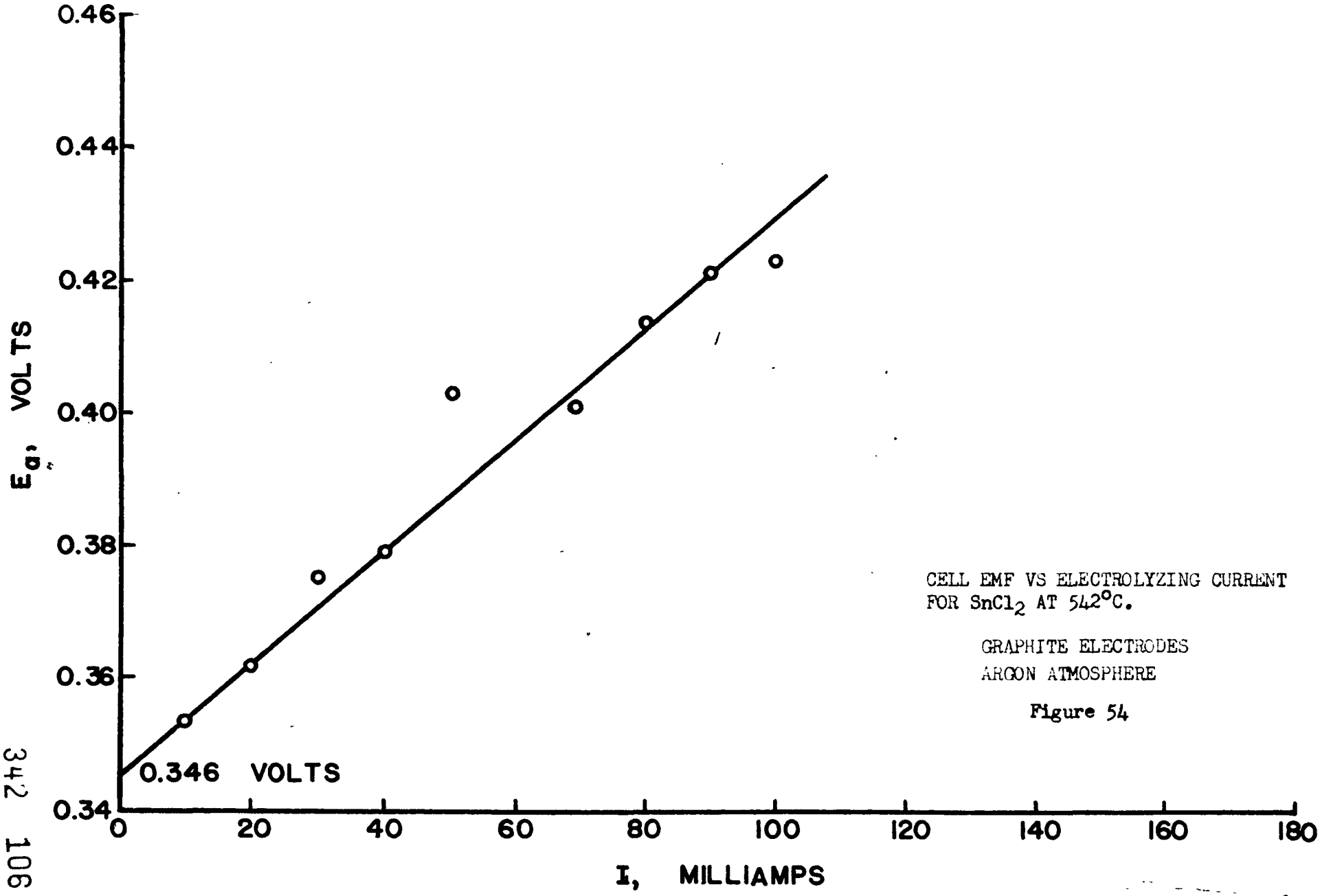


CELL EMF VS ELECTROLYZING CURRENT FOR $SnCl_2$ AT 542°C.

GRAPHITE ELECTRODES
ARGON ATMOSPHERE

Figure 54

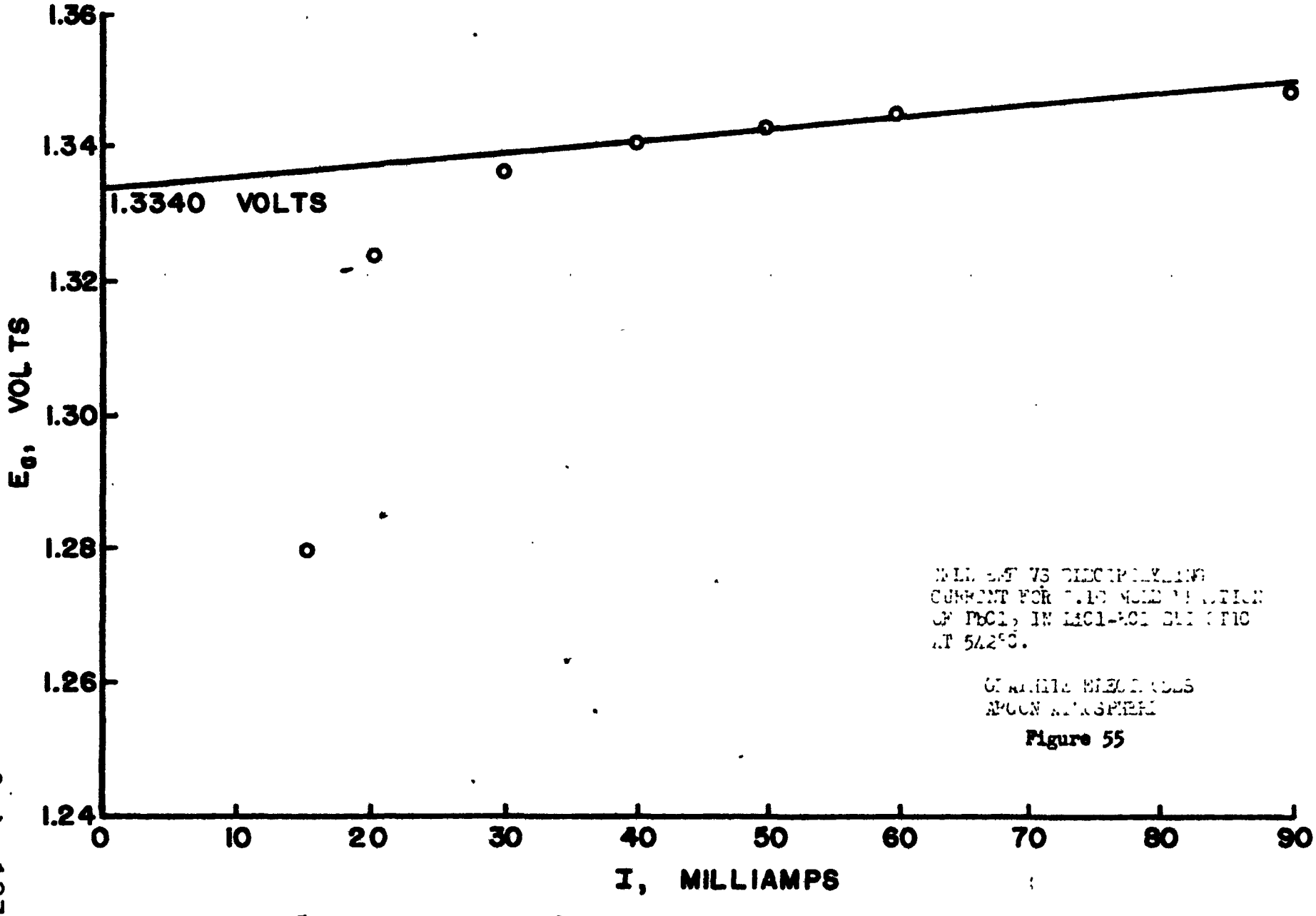


CELL EMF VS ELECTROLYZING CURRENT FOR 7.10 MOLE % SOLUTION OF $PbCl_2$ IN LiCl-KCl EUTECTIC AT 542°C.

CHLORINE ELECTRODES
ARGON ATMOSPHERE

**Figure 55**

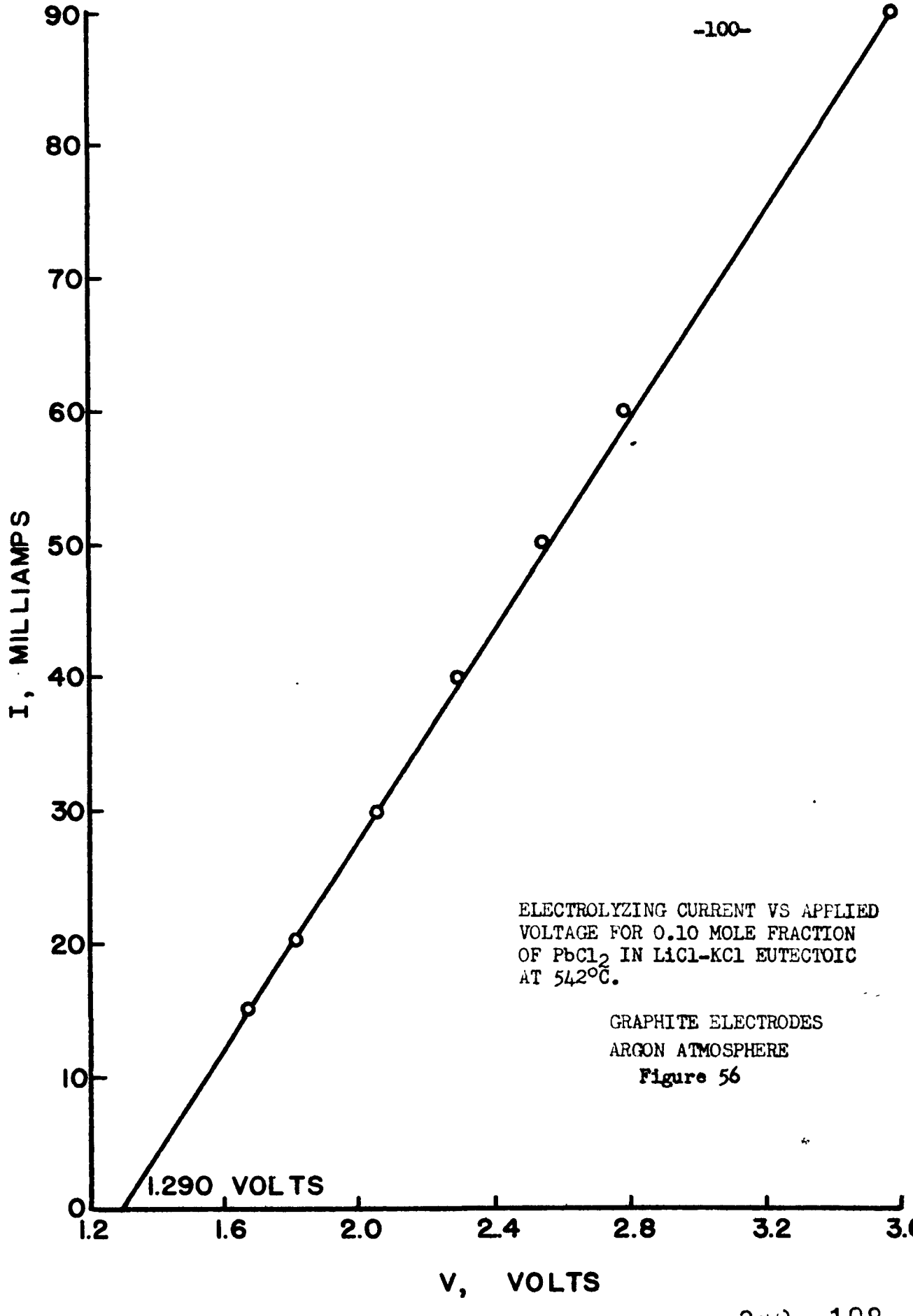


ELECTROLYZING CURRENT VS APPLIED VOLTAGE FOR 0.10 MOLE FRACTION OF $PbCl_2$ IN LiCl-KCl EUTECTOIC AT 542°C.

GRAPHITE ELECTRODES
ARGON ATMOSPHERE

**Figure 56**

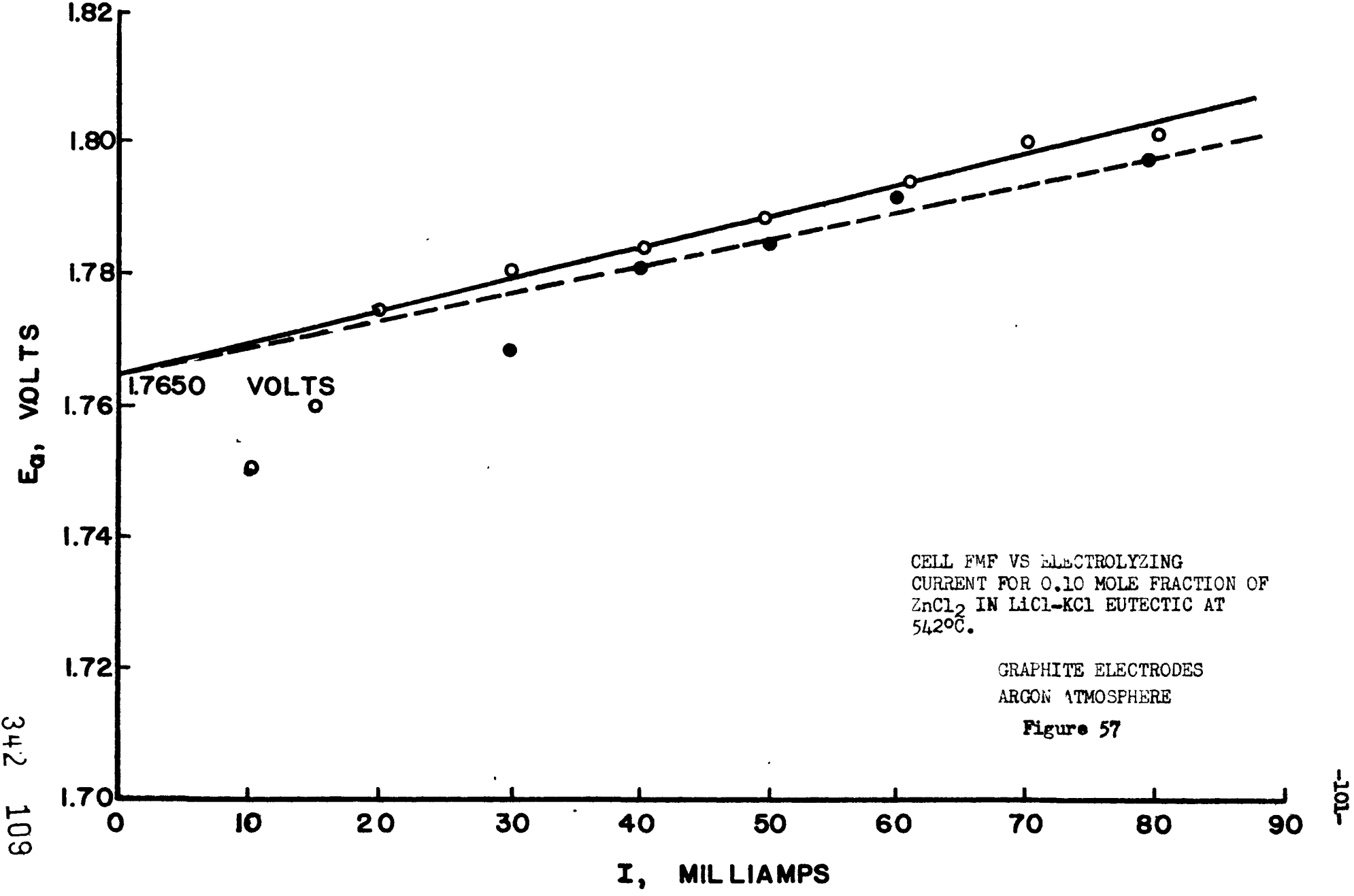


CELL FMF VS ELECTROLYZING CURRENT FOR 0.10 MOLE FRACTION OF $ZnCl_2$ IN LiCl-KCl EUTECTIC AT 542°C.

GRAPHITE ELECTRODES
ARGON ATMOSPHERE

**Figure 57**

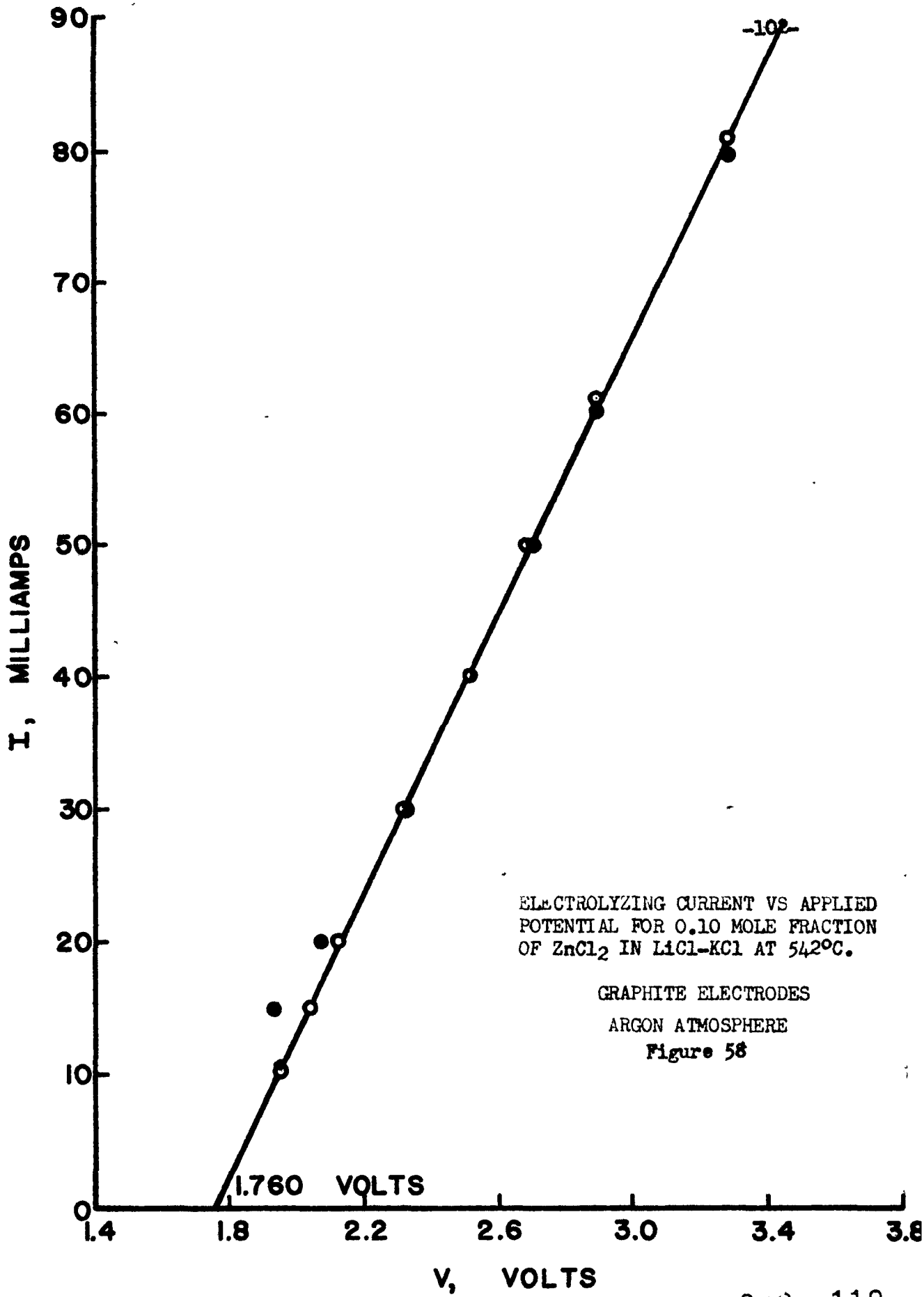


ELECTROLYZING CURRENT VS APPLIED POTENTIAL FOR 0.10 MOLE FRACTION OF $ZnCl_2$ IN LiCl-KCl AT 542°C.

GRAPHITE ELECTRODES

ARGON ATMOSPHERE

**Figure 58**

emf) are identical, showing good reproducibility.

6) The "break" for the decomposition of the solvent cation was again absent for the electrolysis of $MgCl_2$, $PbCl_2$, and $ZnCl_2$. The explanation here is that the deposited alkali metal reacts with the solute salt to give the solute metal.

Discrepancies Between $E_{ao}$ and Decomposition Potential Measurements

As discussed in the section on Measuring Methods, the experimental decomposition potential for the systems studied here should equal the thermodynamic emf ($E_{ao}$). But there is, in fact, no correlation between these two values.

In the measurement of thermodynamic emf's by the back-emf method, the $E_a$ values are determined with a fairly high precision. Also, the slope of the $E_a$ versus I curve is small, and thus the emf value at $I = 0$ ($E_{ao}$) may be accurately determined. On the other hand, the slope of the applied voltage versus electrolyzing current curve is much larger than the slope of the $E_a$ versus I curve, and a small error in determining this slope introduces a large error in the experimental decomposition potential. Further, the value for the applied voltage can be measured only to the nearest one hundredth of a volt, because of the somewhat erratic behavior of a cell on electrolysis.

Chemical Identification of Electrolysis Products

In general it is difficult to analyze quantitatively the cathode electrolysis products because of the small amount of the deposited metal. For the $PbCl_2$ and the $PbCl_2$ - $ZnCl_2$ mixtures, the constituents were quantitatively determined for several different mixtures. For pure $PbCl_2$, the metal was found to be 99+ % Pb. For one of the $PbCl_2$ - $ZnCl_2$ mixtures, the final cathode product analyzed 2% Zn.

For the LiCl - KCl mixture, the metal phase was lighter than the salt and flowed to the top. Thus, when the electrode was withdrawn no deposit was apparent. However, when the electrode was dipped into water, a violent gas evolution occurred indicating that the metals Li, K, or both were present on the electrode. As a further check, lithium and potassium metal were placed in a hollow iron tube, which was used as an electrode, and the value of $E_{ao}$ was identical with the result obtained when the cathode metal was made by electrolysis.

For $MgCl_2$ mixtures electrolyzed below the melting point of magnesium, the solid deposit was determined qualitatively to be Mg metal.

For the $NdCl_3$ electrolysis, the cathodic deposit was a powder, and not enough was deposited to permit chemical identification. However, when the electrode was dipped into water, a gas evolution occurred, but the reaction was not as vigorous as for the Li - K electrode. This electrode also had a distinctive odor which was lacking for the other metals.

The distinctive $Cl_2$ odor was noticable for the gas in the anode compartment, and when the gas came into contact with $NH_3 + H_2O$ vapors a white cloud was formed (indicating $NH_4Cl$ formation). Further, when $Cl_2$ is bubbled over the anode, the values for ($E_{ao}$) are identical with the results obtained when the gas electrode is produced by electrolytic deposition.

Electrolysis of Fluoride Melts

An attempt was made to study the electrolysis of fluoride melts in the range of 500°C to 600°C using pyrex glass as the cell material. The pyrex was slowly attacked by the fluorides. Both graphite and platinum anodes were tried and both showed a rapid deterioration.

The melt was the eutectic composition of the ternary NaF - KF - LiF systems. Qualitative analysis of the cathodes showed that a highly reactive metal had been deposited (i.e., Na, Li, K).

It is believed that fluoride electrolysis studies could be successfully completed if a suitable anode material could be found. The criterion here is that the standard free energy of formation for the fluoride compound of the anode material, e.g., $CF_4$, $PtF_2$, $AuF_2$, etc., be positive at the temperature of electrolysis. The free energy versus temperature data are practically non-existent for the possible electrode materials (e.g., carbon, platinum, and gold) in the temperature ranges close to $\Delta F^\circ = 0$ such that no estimate of the temperature at which $\Delta F^\circ = 0$ could be made. From the data available, it would appear that gold may be the best anode material in fluoride electrolysis (i e., it gives the lowest temperature for $\Delta F^\circ = 0$, possibly about 900°C).

$Al_2O_3$ showed no reaction with the NaF - KF - LiF eutectic at 800°C - 900°C and would be a suitable cell material for electrolysis experiments at temperatures up to 900°C. At still higher temperatures, it should be possible to use a graphite crucible and a $CaF_2$ saturated system in which the cell separators are of solid $CaF_2$.

In summary it can be said that the entire problem of fused fluoride electrolysis is one of finding an electode material which will not react with nascent fluorine. Fluoride melts containing oxides could be studied by the back-emf method if platinum anodes were used.

SUMMARY

A new method for measuring the thermodynamic emf's in molten salt cells of the type $M/MCl_2$ in molten salt solvent/$Cl_2$ is presented. Some thermodynamic emf's measured by this method are compared with calculated theoretical cell emf's and thermodynamic emf's measured by the classical method (where available) and show reasonable agreement in most cases. Within the precision of the thermochemical data used in the calculation of the theoretical emf's, the systems studied obey Raoult's law. It has been shown that the decomposition potential for these systems should equal the thermodynamic emf. However, due to the lack of precision in the applied voltage measurement and the inaccuracy in the voltage-current extrapolation, the measured decomposition potentials show no correlation with the thermodynamic emf's. The results for the systems studied are summarized in Tables I through IV and in figures 8, 25- 33.

The determination of thermodynamic emf by the back-emf method is comprised of three steps:-

1) For each steady-state electrolysis at current I, the decay of the cell emf after the applied voltage is removed is recorded as a function of the time.

2) The decay curve of step (1) is replotted as cell emf versus the square root of time, and the resulting linear relationship extrapolated to time equal to zero.

3) The value of cell emf at time equal to zero from step (2) is plotted as a function of the electrolyzing current I The resulting linear relationship is extrapolated to zero current, and this emf,

designated as $E_{ao}$, is the thermodynamic emf.

The results of the electrolysis study of the molten $PbCl_2 - ZnCl_2$ system are:-

1) The experimental decomposition potentials show no agreement with measured or calculated thermodynamic cell emf's.

2) The experimental thermodynamic emf's show excellent agreement with the values Wachter and Hildebrand[20] obtained by the classical method.

3) An emf value corresponding to the decomposition of $ZnCl_2$ is observed. This emf value is much lower than that calculated, due to the alloying of Zn with Pb.

4) The decay curves exhibit a linear relationship between the cell emf ($E_t$) and the square root of the time.

The results of the electrolysis of the LiCl - KCl system are:-

1) The values for the thermodynamic emf agree well with the calculated values of theoretical cell emf between 500°C to 600°C.

2) Since the theoretical cell potentials for LiCl and KCl are very close together, the double "break" in the $E_a$ versus I curve was not observed in all cases.

3) The decay curves exhibit a linear relationship between cell emf ($E_t$) and the square root of time.

4) The metal and gas electrodes behave reversibly, and the emf values are reproducible.

5) Since the decomposition potential for the molten eutectic is large, this system makes a good molten salt solvent.

The results of the electrolysis of the system $NdCl_3 - LiCl - KCl$ are:-

1) The measured thermodynamic emf's are in agreement with the calculated theoretical potentials to within the accuracy of the thermochemical data.

2) The measured decomposition potentials show no agreement with the thermodynamic emf's.

3) The thermodynamic emf exhibits a linear relationship with ln concentration up to 0.03 mol fraction of $NdCl_3$ for 513°C and 586°C. The value of n calculated from the slope of this plot has a value of about 2.5, in reasonable agreement with the value for Nd equal to 3.

4) The "break" in the $E_a$ versus I curve for the decomposition of LiCl and KCl were absent except for low $NdCl_3$ concentration where the limiting current density for the reduction of $Nd^{+++}$ was reached.

5) At the higher current densities, where the applied potential exceeds the decomposition potential of the eutectic, the decay curves depart initially from the linear $E_t$ versus $\sqrt{t}$ relationship. This initial deviation is due to the presence of Li on the cathode.

6) The reduction of $NdCl_3$ proceeds in two ways:-

a) Direct electrolytic reduction below the decomposition potential of the eutectic.

b) Direct reduction and reduction by Li above the eutectic decomposition potential.

Exploratory studies were made on the following systems:-

$MgCl_2$ - NaCl,

$MgCl_2$ - LiCl - KCl,

KCl,

$PbCl_2$ - KCl - KCl,

$ZnCl_2$ - LiCl - KCl,

Pure $SnCl_2$, and $SnCl_2$ - LiCl - KCl.

The back-emf method for evaluating the thermodynamic emf for molten salt cells has the following advantages:-

1) It is an experimentally easier method than the classical method because:-

a) The molten salt is readily purified by a pre-electrolysis stage.

b) The chlorine electrode is produced by electrodeposition and methods of chlorine purification are not necessary.

c) The electrodeposited metal cathodes are free of oxide films. For some of the more electropositive metals, this may be the only successful method for producing reversible metal cathodes.

2) Analysis of the decay curves yields information on possible electrode reactions and also values of over-potentials present.

REFERENCES


1. Kortüm, G. and J. O'M. Bockris: Text Book of Electrochemistry. Elsevier Publishing Co., Houston, Texas, 1951.

2. Drossbach, P.: Elektrochemie geschmolzener Salze. Edwards Brothers, Inc., Ann Arbor, Michigan, 1943.

3. Conway, B. E.: Electrochemical Data. Elsevier Publishing Co., Houston, Texas, 1952.

4. Quill: Chemistry and Metallurgy of Miscellaneous Materials: Thermodynamics. McGraw-Hill Book Co., Inc., New York, 1950.

5. Kubaschewski and Evans: Metallurgical Thermochemistry. Butterworth-Springer LTD., London, 1951.

6. Hall, F. P., and H. Insley: Phase Diagrams for Ceramists. J. Am. Ceram. Soc., part II, Nov. 1947.

7. Parkes: Meller's Modern Inorganic Chemistry. Longmans, Green & Co. Inc., New York, 1951.

8. National Bureau of Standards: Selected Values of Chemical Thermodynamic Properties (1947 and subsequently).

9. Bichowsky, F. R., and F. D. Rossini: The Thermochemistry of the Chemical Substances. Reinhold Pub. Corp., New York, 1936.

10. Kelly, K. K.: Contributions to the Data on Theoretical Metallurgy. U. S. Bureau of Mines Bulletions.

11. Glasstone, S.: Thermodynamics for Chemists. D. Van Nostrand Co., Inc., New York, 1947.

12. Kellogg, H. H.: Trans. AIME 188, 1951.

13. Cubiciotti, D.: Trans. AIME 197, 1106 (1953).

14. Peterson, G. F.: Free Energies of Some Metal Oxides and Fluorides. Carbide and Carbon Chemicals Co., ANP Experimental Engineering, 1953.

15. Bockris, J. O'M and J. W. Tomlinson: Constitution of Melts. Research 2, 362 (1949).

16. Tsuchiya: J. Electrochem. Soc. Japan, 17, 76(1949).

17. Salstrom, E. J., J. Am. Chem. Soc., 56, 1272 (1934).

18. Salstrom, E. J., and J. H. Hildebrand: J. Am. Chem. Soc., 52, 4641 (1930).

19. Salstrom, E. J., and J. H. Hildebrand: J. Am. Chem. Soc., 52, 4050(1930)

20. Wachter, A., and J. H. Hildebrand: J. Am. Chem. Soc., 52, 4655(1930)

21. Lee, E. K., and E. P. Peterson: Trans. Electrochem. Soc., 88, 171(1945)

22. Walden, P.: Z. physik Chem., A157, 389(1931)

23. Voight, A., and W. Blitz: Z anorg. Chem., 133, 277(1924)

24. Fuseya, G., and K. Ouchi: J. Electrochem. Soc., Japan 17, 254 (1949)

25. Lorenz, R., and H. Velde: Z. anorg. Chem., 183, 81(1929)

26. Platenev, S.E., and T. Rozov: Acta Physicochim. U.R.S.S., 1, 341(1937)

27. Grube, G., and E.A. Rau:,Z. Electrochem., 40, 352(1934)

28. Oppenheimer, F.: Z. anorg. Chem., 189, 297(1930)

29. Rose, B.A., G.J. Davis, and H.J.T. Ellingham: Disc. Faraday Soc. No. 4, 154(1948)

30. Banergie, T.: J. Scien. Ind. Res. 12, 457(1953)

31. Senderoff, S. and A. Brenner: J. Electrochem. Soc., 101, 16(1954)

32. Steinberg, M.A., M.E. Sibert, and E. Wainer: J. Electrochem. Soc., 101, 63(1954)

33. Iron Age, 173, 166(1954)

34. Steel, 134, 146(1954)

35. Ralston, O.C.: National Bur. Cir. 529, 37(1953)

36. Chem. Proc. Eng. 35, 89(1954)

37. Hock, A.L., Magnesium Review and Abstracts, 9, 1-30(1953)

38. Palguev, S.F., and M.V. Zmirnov: Zhurnal Prikladnoi Khimii, 26, 1166(1953)

39. Van Lancken, M.: Allumino 23, 40(1954)

40. Spedding, F.H., and A.H. Doane: J. of Metals 6, 504(1954)

41. Metals Industry 84, 468(1954)

42. Gruzensky, P.M., and W.S. Crawford: U. S. Bur. Mined I. C. 7681, May 1954

43. Morriss, K.B., D.Z. Douglass, and C. B. Vaughn:
J. Electrochem. Soc. 101, 343(1954)

44. Kanton, S.K., M. Shreenivasan, and G. S. Tendolkar:
Nuclear Engineering, A I.ChE.

45. Baker, P.S., G. f. Wells, and W. R. Rathkamp
J. of Chem Education, 31. 515(1954)

46. Lorenz, [illegible] Z. für Elektrochem., 58, 912 (1954).

47. Cuthbertson, J.W.; Chemistry and Industry Nov. 29, [illegible])1952

48. Marden, J.W.: J. Electrochem. Soc, 100, 37c(1953)

49. Oldham, G.: Mining Journal(London) Annual Review, May 1953, p 93-97

50. Steinberg, M, [illegible] Sibert, and E. Wainer:
Zirconium and Zirconium Alloys
ASM, Cleveland, Ohio, 1953

51. Kroll, W.J.: Metal Industry, 83, 81(1953)

52. Chuk Ching Ma: Ind. and Eng. Chemistry, 44, 342(1952)

53. Jacobs, J.H., P.E. Churchwood, T.E. Hill, W.H. Curry, E.C. Perkins, and O.Q. Leone: Mining Journal, 237, 523(1951)

54. Hellmuth, Hartmann, and W. Massing:
Z. für anorg. und allgem Chemie, 266, 98(1951)

55. Cordner, and Worner: Australian J. of Applied Science 2, 358(1951)

56. Gray: Bulletin of the Institution of Mining and Metallurgy 61, 141(1952)

57. Moschel: Angewandte Chemie 63, 385(1951)

58. Drossbach: Zeitschrift für Elektrochemie Berichte der Bunsengesellschaft fur Physikalische Chemie 56 23(1952)

59. Drossbach: ibid 56, 31(1952)

60. Eger, G.: Zeitschrift für Erzbergbau und Metallhuttenwesen 5, 270(1952)

61. Dodero, M.: Journal de Chimie Physique et de physico-Chimie Biologique 49, c11(1952)

62. Kellogg, H.H.: J. of Metals 191, 137(1951)

63. Chizhikov, Untinski: Zhurnal Prikladnoi [illegible] 22, 1306(1949)

64. Muller, F.: Chimia 3, 285(1949)

ibid 4, 1(1950)

65. Grothe, H.: Zeitschrift für Erzbergbau und Metallhuttenwesen 3, 213(1950)

66. Cubiocciotti: U. S. Atomic Energy Commission MDDC-1053 (1946)

67. Rogers and Viens: Canadien Mining and Metallurgical Bulletion 41, 625(1948)

68. Seyboldt and Burke: Proceedure in Experimental Metallurgy. John Wiley and Sons, Inc. New York, 1953)